



LUND UNIVERSITY

Ligand-Binding Affinity Estimates Supported by Quantum-Mechanical Methods

Ryde, Ulf; Söderhjelm, Pär

Published in:
Chemical Reviews

DOI:
[10.1021/acs.chemrev.5b00630](https://doi.org/10.1021/acs.chemrev.5b00630)

2016

Document Version:
Publisher's PDF, also known as Version of record

[Link to publication](#)

Citation for published version (APA):
Ryde, U., & Söderhjelm, P. (2016). Ligand-Binding Affinity Estimates Supported by Quantum-Mechanical Methods. *Chemical Reviews*, 116(9), 5520-5566. <https://doi.org/10.1021/acs.chemrev.5b00630>

Total number of authors:
2

General rights

Unless other specific re-use rights are stated the following general rights apply:
Copyright and moral rights for the publications made accessible in the public portal are retained by the authors and/or other copyright owners and it is a condition of accessing publications that users recognise and abide by the legal requirements associated with these rights.

- Users may download and print one copy of any publication from the public portal for the purpose of private study or research.
- You may not further distribute the material or use it for any profit-making activity or commercial gain
- You may freely distribute the URL identifying the publication in the public portal

Read more about Creative commons licenses: <https://creativecommons.org/licenses/>

Take down policy

If you believe that this document breaches copyright please contact us providing details, and we will remove access to the work immediately and investigate your claim.

LUND UNIVERSITY

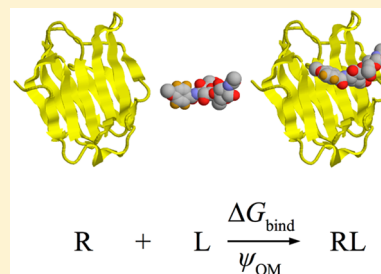
PO Box 117
221 00 Lund
+46 46-222 00 00

Ligand-Binding Affinity Estimates Supported by Quantum-Mechanical Methods

Ulf Ryde^{*,†} and Pär Söderhjelm[‡]

[†]Department of Theoretical Chemistry and [‡]Department of Biophysical Chemistry, Lund University, Chemical Centre, P.O. Box 124, SE-221 00 Lund, Sweden

ABSTRACT: One of the largest challenges of computational chemistry is calculation of accurate free energies for the binding of a small molecule to a biological macromolecule, which has immense implications in drug development. It is well-known that standard molecular-mechanics force fields used in most such calculations have a limited accuracy. Therefore, there has been a great interest in improving the estimates using quantum-mechanical (QM) methods. We review here approaches involving explicit QM energies to calculate binding affinities, with an emphasis on the methods, rather than on specific applications. Many different QM methods have been employed, ranging from semiempirical QM calculations, via density-functional theory, to strict coupled-cluster calculations. Dispersion and other empirical corrections are mandatory for the approximate methods, as well as large basis sets for the stricter methods. QM has been used for the ligand, for a few crucial groups around the ligand, for all the closest atoms (200–1000 atoms), or for the full receptor–ligand complex, but it is likely that with a proper embedding it might be enough to include all groups within ~6 Å of the ligand. Approaches involving minimized structures, simulations of the end states of the binding reaction, or full free-energy simulations have been tested.



CONTENTS

1. Introduction	5520
2. Methods	5522
2.1. Energy Functions	5522
2.2. QM-Cluster, QM/MM, and Continuum-Solvation Methods	5524
2.3. Calibration Studies	5526
2.4. Importance of Sampling	5526
2.5. MM/PBSA, LIE, and FES Methods	5527
2.6. Quality Measures	5528
3. Single-Structure Approaches	5528
3.1. QM-Cluster Calculations	5528
3.2. Host–Guest Systems	5532
3.3. QM/MM Calculations	5533
3.4. Fragmentation Calculations	5539
3.4.1. PA and Similar Approaches	5539
3.4.2. MFCC and Similar Approaches	5540
3.4.3. FMO	5541
3.5. Linear-Scaling Calculations	5543
4. End-Point Approaches	5545
4.1. MM/PBSA Approaches	5545
4.2. LIE-Type Approaches	5550
4.3. Other Approaches	5551
5. Free-Energy Simulations	5552
5.1. FES Simulations	5552
5.2. Reference-Potential Methods	5552
6. Concluding Remarks	5553
Author Information	5555
Corresponding Author	5555
Notes	5555

Biographies	5555
Acknowledgments	5555
Abbreviations	5555
References	5556

1. INTRODUCTION

One of the most important types of chemical reactions that are governed by noncovalent interactions is the binding of a small molecule to a biological macromolecule, e.g., a protein or a nucleic acid, i.e., the reaction



where R is the macromolecule (the receptor), L is the small molecule (the ligand), and RL is their complex. The free energy of this reaction, ΔG_{bind} , is the binding affinity, and it is related to the binding constant K_{bind} by

$$K_{bind} = e^{-\Delta G_{bind}/RT} \quad (2)$$

where R is the gas constant and T is the absolute temperature. (Strictly speaking, the binding free energy should have a standard-state symbol. In practice, few papers discuss or specify the standard state, although binding affinities calculated with 1 bar or 1 M standard states differ by 8 kJ/mol at ambient temperature, arising from the volume term in the translational

Special Issue: Noncovalent Interactions

Received: October 23, 2015

Published: April 14, 2016

entropy; to avoid possible confusion, we have dropped the standard-state symbol throughout this paper.)

Binding reactions are ubiquitous in biology. For example, any substrate needs to bind to its enzyme to be converted to the product, and it can be argued that the activation energy is the difference in binding energy of the substrate and the rate-limiting transition state. However, the arguably most important type of binding reaction is the association of a drug candidate to its target receptor. It is the prime aim of drug development to find a small molecule that binds strongly to a certain biomacromolecule. Moreover, it is also important that the drug candidate does not bind to other, often similar, macromolecules, so that it does not interfere with other key functions in the body, and that it has proper transport, metabolism, and excretion properties, which often are governed by the binding to other biomacromolecules, e.g., transporters and metabolic enzymes. Therefore, the study of binding affinities is of immense interest in pharmaceutical chemistry, and the development of a new drug typically involves the synthesis and test of the binding of thousands of drug candidates. Naturally, it would be of great gain if binding affinities could be estimated fast and accurately by computational methods.

Consequently, numerous methods have been developed with this aim.¹ Most computational methods are based on some sort of energy function. It can be developed either by a statistical analysis of experimentally characterized ligand–receptor complexes or from a physical description of the interactions. Statistical energy functions can come from an analysis of atom–atom distances, converted to an empirical potential of mean force (knowledge-based scoring functions), or from a regression analysis of binding affinities and a collection of terms that are believed to be important for the binding affinity, e.g., hydrogen bonds, ionic interactions, metal bonding, desolvation, hydrophobic effects, stacking, etc. (empirical scoring functions). Physics-based energy functions are typically in the form of a molecular-mechanics (MM) force field that contains terms for the stretching of bonds, bending of angles, rotation of torsion angles, Coulombic interaction between atomic partial charges, and van der Waals attraction (dispersion) and exchange repulsion.

Likewise, many approaches have been used to predict the structure of the ligand–receptor complex and estimate the binding affinity using these energy functions. The most commonly used one is to change the structure until a minimum energy is obtained, i.e., a geometry optimization. This is a formidable task for a biomacromolecule, because the potential-energy surface is extremely complicated with essentially an infinite number of local minima. This is often solved by keeping the macromolecule fixed, excluding the solvent molecules, running many calculations from different starting points, or employing special algorithms (e.g., genetic algorithms) that try to find the global minimum. In their simplest form, such docking calculations can estimate the binding affinity within seconds, often using knowledge-based or empirical scoring functions. They can often predict structures close to the experimentally determined geometry of the complex, but they have problems distinguishing them from other poses and predicting accurate binding affinities for a diverse set of targets.^{2,3}

Alternatively, binding affinities can be estimated as averages of interaction energies over molecular dynamics (MD) or Monte Carlo (MC) simulations. Such calculations reduce the local-minimum problem, but they are also much more time-consuming. Many variants have been suggested, but the two

most used are the linear interaction energy (LIE) and the MM/PBSA or MM/GBSA (MM combined with Poisson–Boltzmann or generalized Born and surface area) approaches.^{4,5}

However, a more strict statistical mechanical way to obtain binding free energies is by free-energy simulation (FES) techniques.^{6,7} These also involve MD or MC sampling, but also the conversion of the ligand to either another ligand (giving the difference in ΔG_{bind} between the two ligands) or a noninteracting ligand (giving the absolute ΔG_{bind}). Such conversions need to be performed in many small steps to give a proper convergence, so the FES approaches are computationally expensive.

A problem with these calculations is that the estimated binding affinities need to be very accurate. Equation 2 shows that a difference in binding constants of 1 order of magnitude translates to a difference of only 6 kJ/mol in ΔG_{bind} . Thus, the accuracy of a computational method needs to be better than this to be useful in drug development. Unfortunately, very few computational methods have such an accuracy, especially not MM methods, with their lacking description of polarization, charge transfer, many-body effects, etc. Therefore, there has lately been quite some interest in improving ligand-binding estimates by using quantum-mechanical (QM) methods. They can in principle include all contributions to the receptor–ligand interaction energy and therefore provide an ideal energy function. However, in practice, QM calculations are also approximate, and depending on the level of theory used, sometimes the approximations may deteriorate the results below the level obtained by MM methods, e.g., because you cannot afford a proper sampling of the phase space. Moreover, often only a part of the receptor–ligand complex is used in the QM calculation. Therefore, it is not certain that QM calculations will automatically improve calculated binding affinities.

In this paper, we review the use of QM methods for the calculation of ligand-binding affinities. Several reviews have been published on related subjects.^{8–26} It is not trivial to delimit the subject, because essentially all MM force fields are partly based on QM parameters and nearly all computational studies of ligand binding involve some QM calculations, e.g., to obtain the atomic charges of the ligand. Therefore, we have restricted the review to studies that present estimates of ΔG_{bind} involving explicit QM components, i.e., excluding papers only devoted to the structure of the RL complex²⁷ or involving QM only to obtain parameters in the MM force field (e.g., quantum-polarized ligand docking²⁸ and other methods to obtain system-specific QM charges^{17,29–35}). We also omit ligand-based (3D) quantitative structure–activity relationship (QSAR) methods,^{36–40} QM studies of drug metabolism,⁴¹ or approaches to study enzyme mechanisms and reaction energies.^{9,42–45} Moreover, the review is focused on method developments, i.e., papers with at least a partial focus on the methods. Pure applications that employ QM methods are sometimes mentioned, but are not exhaustively reviewed, and we do not discuss the implications of the calculated affinities on specific biological systems.

We have chosen to organize the review according to how the free energies are estimated. Thus, methods based on single structures, on MD sampling of only the end points (complex and possibly free ligand and free receptor), or on FES are discussed in separate sections. There are several other equally reasonable ways to structure the material, e.g., by the QM method used or the part of the system treated by QM. To help the less experienced reader, we give in the first section a short review of

different QM methods and different methods to estimate binding affinities. The review ends with some concluding remarks.

2. METHODS

In this section, we will give a brief introduction to most of the QM methods used when calculating binding affinities. For a more detailed account of the methods, the interested reader is referred to textbooks in computational chemistry.^{46,47}

2.1. Energy Functions

QM methods are based on the solution of the Schrödinger equation

$$\hat{H}\psi = E\psi \quad (3)$$

where E is the total energy and \hat{H} is the Hamilton operator, which defines the system (the particles involved, i.e., electrons and nuclei, and their interactions). From the wave function, ψ , all measurable properties of the system can be calculated. Unfortunately, the Schrödinger equation can be solved analytically only for the simplest one-electron systems; for all other systems, only approximate solutions can be found. Therefore, numerous approximate QM methods have been developed.

In the Hartree–Fock (HF) method,^{48,49} it is assumed that each electron interacts with the average field of all the other electrons. This is a quite crude approximation, because the correlated movement of electrons is omitted. The simplest way to correct this shortcoming is by many-body perturbation theory to the second order (MP2).⁵⁰ This is also the simplest theoretical method that explicitly treats dispersion interactions. More accurate results are obtained with an exponential ansatz, the coupled-cluster approach. Currently, the gold-standard QM method is such an approach, including single, double, and (perturbatively treated) triple excitations, CCSD(T),⁵¹ which typically gives an accuracy of about 4 kJ/mol.

On the other hand, HF calculations can be sped up (by a factor of ~1000) by ignoring some terms and replacing others by empirical parameters, the semiempirical QM (SEQM) methods.⁵² Many such methods have been suggested, including AM1,⁵³ RM1,⁵⁴ PM3,⁵⁵ PDDG/PM3,⁵⁶ PM6,⁵⁷ and OM2.⁵⁸ SEQM methods typically give quite poor energies for large structures, owing to the missing dispersion interactions, but also to a poor description of hydrogen and halogen bonds, all of which are fundamental to obtain proper binding energies. Therefore, several groups have developed corrections to the SEQM energies and gradients, e.g., the DH,⁵⁹ D2H,⁶⁰ DH2X,⁶¹ and D3H4⁶² corrections.

Density-functional theory (DFT) is not based on the Schrödinger equation.^{63,64} Instead, it concentrates on the electron density, which is a function of three Cartesian coordinates (the wave function is a much more complicated function of the three coordinates for each electron in the system). Still there is a one-to-one relationship between the wave function and the electron density, but it is not known exactly what equation to solve to find the electron density for a system. Therefore, a great number of DFT methods have been suggested, e.g., BP86,^{65,66} PBE,⁶⁷ TPSS,⁶⁸ M06-L,⁶⁹ and mPWLYP.⁷⁰ Some of them include a fraction of HF exchange, called hybrid functionals, e.g., B3LYP,^{71,72} BH&HLYP,⁷³ PW6B95,⁷⁴ and M06-2X.⁶⁹ In general, DFT methods are both faster and more accurate than the MP2 method. Lately, it has been pointed out that the results of HF and DFT methods can be improved by including a simple empirical correction for the missing dispersion interaction.^{75,76} The most applied corrections are the DFT-D2

and DFT-D3 approaches by Grimme and co-workers,^{77–79} but other approaches give similar results.^{80–82} A semiempirical variant of DFT is the density-functional-based tight binding method, for which there are several variants, e.g., DFTB,⁸³ SCC-DFTB⁸⁴ (self-consistent charges), and SCC-DFTB3.⁸⁵ Dispersion corrections have been developed also for these methods.^{86,87}

Nearly all QM methods solve the Schrödinger equation by expanding the wave function in a series of known functions, the basis set. Naturally, the quality of the solution improves as the basis set is enhanced. Typically, reasonable geometries can be obtained with two basis functions for each valence electron, one for the core electrons, and an extra set of functions with one degree of angular momentum higher than the valence electrons, called an SVP basis set, e.g., 6-31G*, def2-SV(P), or cc-pVDZ.^{88–90} However, energies are far from converged at that level; instead, three or four functions are needed for the valence electrons, TZP, e.g., 6-311G(2df,2p), def2-TZVP, and cc-pVTZ, or QZP, e.g., def2-QZVP or cc-pVQZ.^{89–91} For anionic systems and for an accurate account of dispersion, diffuse functions are also needed, e.g., 6-31+G*, def2-TZVPD, or aug-cc-pVTZ.^{90,92} In a few studies, minimal basis sets with only one basis function for each valence electron have been used (SZ and SZP without and with polarizing functions, respectively). For the SEQM methods, the (minimal) basis set is defined by the method and therefore not explicitly specified.

One of the prime problems with too small basis sets is that an atom may employ basis functions from nearby atoms. This is a major problem when calculating interaction energies, because these basis functions exist only in the complex and therefore will overestimate the binding energy. This is called the basis-set superposition error (BSSE), and it is typically cured by performing calculations for the separated moieties with the basis set (but not the nuclei) from the complex, the counterpoise (CP) correction.⁹³ However, there are indications that this overcompensates for the BSSE and that it may be favorable to use only half of the CP correction.^{80,94–99}

The curse of the QM methods is that the time consumption for solving the Schrödinger equation increases steeply with the size of the system. For example, DFT, HF, MP2, and CCSD(T) show an exponential dependence on the number of basis functions with exponents of 3, 4, 5, and 7, although this can be somewhat reduced by prescreening methods. In practice, single-point energy calculations can today be performed by SEQM, DFT, and CCSD(T) methods for systems with around 10000, 2000, and 30 atoms. Further reduction in the time consumption can be obtained by localizing the wave function, so-called local methods, e.g., LCCSD(T0).^{100,101} With the latest domain-based local-pair natural-orbital methods, DLPNO-CCSD(T) calculations with up to 200 atoms are possible.¹⁰²

Another way to speed up QM calculations is to replace a large QM calculation with several smaller ones, by dividing the molecule into several fragments. Energies are typically calculated by the series expansion

$$E = \sum_i^n E_i + \sum_{i<j}^n \Delta E_{ij} + \sum_{i<j<k}^n \Delta E_{ijk} + \dots \quad (4)$$

where E_i are the energies of each fragment (monomer), ΔE_{ij} are the interaction energies of all possible pairs of fragments (dimers), ΔE_{ijk} are the interaction energies of all possible triplets of fragments (trimers), and so on. In all practical applications, the expansion is truncated at the dimer level. Two types of methods

have been used for binding-energy calculations. Methods of the first type use the full expansion in eq 4 and aim at producing a total energy for the full system, corresponding to the energy one would obtain in a normal QM calculation of the full system. Then any relative energies can be computed by simple subtraction. On the other hand, they involve the calculation of numerous monomer and dimer energies that have very little influence on the binding energy. The second class only aims at calculating interaction energies. Then it is enough to include dimers that involve the ligand and one fragment of the receptor, i.e., much fewer calculations.

Among the methods of the first class, the fragment molecular orbital (FMO) method^{103,104} is the most widely used. In this method, the wave function of each monomer is computed iteratively in the exact or approximate electrostatic potential generated by the other fragments. Next, the energy of each pair of fragments (dimer) is computed, using the final electrostatic potential from the other fragments as external potential. FMO formulations for many QM methods have been developed, including HF, MP2–MP4, and CCSD(T).¹⁰³ Recently, the FMO method has been interfaced with two implicit solvent models, the polarized continuum model (PCM)¹⁰⁵ and Poisson–Boltzmann (PB) solvation,¹⁰⁶ and with the accurate EFP (effective fragment potential) force field.¹⁰⁷ FMO has been extensively used to calculate ligand-binding energies, especially at the MP2 level, but two theoretical problems hamper such applications: Due to the neglect of Pauli effects in the external potential, the method does not work well with large and diffuse basis sets,¹⁰⁸ which are needed for a quantitative account of dispersion. Moreover, no rigorous correction for the BSSE has been presented.

The simplest fragmentation methods of the other class are based on the approximate pairwise additivity (PA) of interaction energies. They could involve simple attempts to estimate residue components of binding affinities by pairwise QM calculations of the ligand and each interacting group, without addressing that the groups may be overlapping or that the groups are connected in the biomacromolecule. However, it is more common to use the molecular fractionation with conjugate caps (MFCC) method, in which the interaction energy is computed as a sum of interactions between the ligand and capped fragments, correcting for the caps by subtracting the interaction energies involving conjugate caps,¹⁰⁹ i.e., joined neighboring caps (Figure 1).

Such pairwise approaches neglect many-body interactions between the ligand and several fragments. This has been addressed in several ways. The simplest approach is to include a point-charge model of the other fragments in each calculation, the electrostatically embedded pairwise additive (EE-PA) model¹¹⁰ or the electrostatically embedded generalized MFCC (EE-GMFCC) approach.¹¹¹ Appreciably more sophisticated is the polarizable multipole interaction with supermolecular pairs (PMISP) method,¹¹² which combines QM calculations of individual fragment–ligand interactions with a polarizable multipole description of the many-body effects (the same idea was later used in the EFMO method¹¹³). The relations between the various fragmentation methods are schematically illustrated in Figure 2.

Linear-scaling methods also take advantage of the locality of QM but attempt to explicitly calculate the electron density for the full system.¹¹⁴ They have been developed especially for SEQM and DFT methods, allowing for calculations on entire proteins.

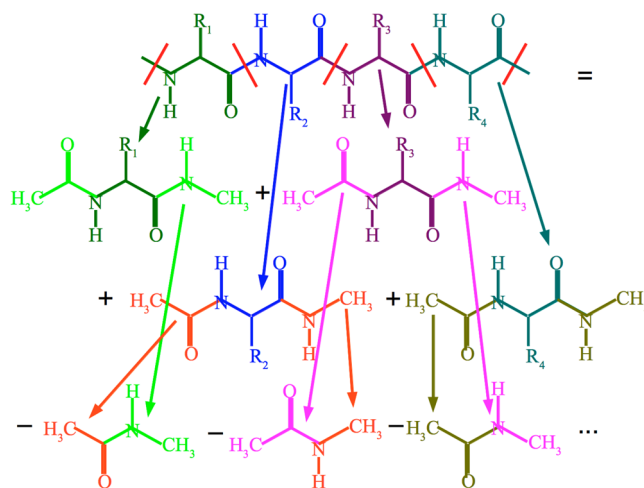


Figure 1. MFCC partitioning of a protein backbone, exemplified by a tetrapeptide segment, which is divided into four capped amino acids and four conjugate caps (joined caps), which are subtracted.

Some of these methods, e.g., the divide-and-conquer approaches, also use fragmentation as part of their solution.¹¹⁵

If SEQM or fragmentation methods still are too expensive, the next level of approximation is the use of molecular-mechanics (MM) methods. These methods do not try to solve the Schrödinger equation, and electrons are ignored. Instead, a molecule is considered as a collection of balls connected by springs. The interaction between the atoms is determined by an empirical energy function, a force field, i.e., a mathematical function of the coordinates of all atoms that gives the total energy of the system (in the same way as the Schrödinger equation). Numerous different force fields have been suggested at various levels of approximation. However, for biomacromolecules, the most commonly used force fields contain harmonic terms for the bonds and angles, a trigonometric term for dihedrals, a Coulombic energy term for the electrostatic interaction, and a Lennard-Jones term for the van der Waals interactions:

$$\begin{aligned}
 E = & \sum_{\text{bonds}} k_b (b - b_0)^2 + \sum_{\text{angles}} k_a (a - a_0)^2 \\
 & + \sum_{\text{dihedrals}} \sum_{n=1}^{n=6} k_n (\cos(n\varphi + \delta_n) + 1) \\
 & + \sum_{\text{atom pairs}} \left(\frac{q_i q_j}{4\pi\epsilon_0 r_{ij}} + \frac{A_{ij}}{r_{ij}^6} + \frac{B_{ij}}{r_{ij}^{12}} \right) \quad (5)
 \end{aligned}$$

where b , a , φ , and r_{ij} are the bond lengths, angles, dihedral angles, and atom distances, k_b , k_a , and k_n are force constants, a_0 and b_0 are ideal bond distances and angles, δ_n is a phase factor, q_i and q_j are partial charges on the atoms, and A_{ij} and B_{ij} are pairwise Lennard-Jones constants. Such an energy function can rapidly be calculated for essentially any biomolecule. However, it omits several important interactions, in particular electronic polarization, but also charge transfer, charge penetration, and the coupling between the various terms. More advanced force fields exist that include some of these terms, e.g., SIBFA (sum of interactions between fragments ab initio computed), EFP, and NEMO,^{116–119} but they are rather expensive and tedious to parametrize. QM calculations, on the other hand, automatically include all such effects.

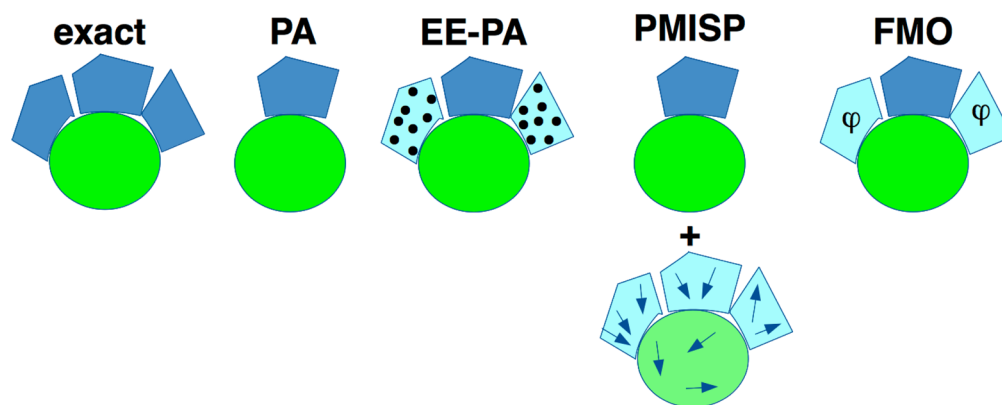


Figure 2. Schematic view of various fragmentation approaches. The ligand is the green oval, whereas the surroundings are shown as the three polygons. In the exact QM calculations, all four fragments are present at the same time. In PA, only the ligand and one fragment are present in each calculation and the other two fragments are ignored (for this and for the other four fragmentation methods, only one of these three dimer calculations is illustrated). MFCC uses the same approach as in PA, but with a more systematic way of obtaining fragments for a covalently bound receptor. In EE-PA, the other fragments are included by a point-charge model. In FMO, the other fragments are modeled by the exact or approximate electrostatic potential. In PMISP, the QM calculations are performed as in PA, but in addition, a polarized multipole MM calculation is performed of the full system to account for the interactions between all the fragments.

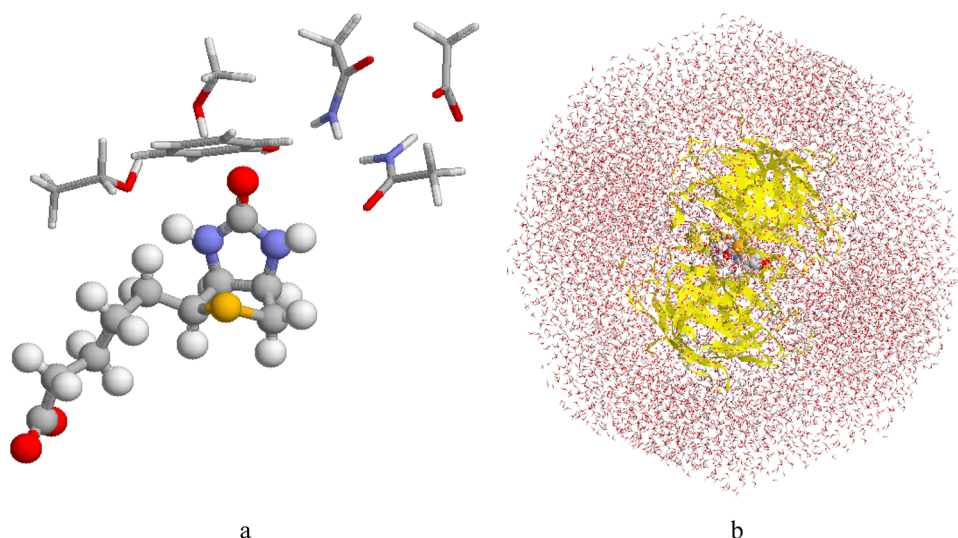


Figure 3. QM-cluster (a) and QM/MM (b) calculations, exemplified by biotin binding to avidin. In the first case, only six important hydrogen-bonding residues are included.¹⁹⁸ In the QM/MM calculation, the QM residues are shown as balls and sticks, the protein as ribbons, and the solvent as wireframes.

2.2. QM-Cluster, QM/MM, and Continuum-Solvation Methods

There are two approaches to calculate QM energies of proteins. In the QM-cluster approach, a small model (20–200 atoms) of the most important residues is cut from the active site and is studied isolated in vacuum or in a continuum solvent by QM methods (Figure 3a).^{42,43} The advantages of this approach are that you can easily control the conformations of all groups (i.e., that they belong to the same local minima) and that there are well-defined methods to estimate the zero-point energy, enthalpy, and entropy by an ideal-gas rigid-rotor harmonic-oscillator approximation, based on vibrational frequencies (i.e., normal-mode analysis, NMA).^{46,47} To avoid the fact that residues move during the geometry optimization in a way that is not possible in the full receptor, some atoms are often fixed, but then no entropies can be estimated.⁴² The main disadvantages are that important residues may have been missed in the selection of the QM system and that the effect of the surroundings may be

modeled in an inaccurate way.^{120,121} It has also been suggested that the use of fixed atoms during the geometry optimization is problematic.^{122,123}

The second approach is QM/MM calculations, in which the ligand and sometimes a small, but important part of the receptor is treated by QM, whereas the remainder of it and typically also a number of explicit solvent molecules are treated by MM methods (Figure 3b).^{44,45} The size of the QM system can be only the ligand, the ligand and a few nearby residues, or the ligand and all residues within a certain distance, typically 3–6 Å (Figure 4a–c). In principle, the QM and MM energies can simply be added, ensuring that no term is double counted. Still, there are many variants on how this is performed in practice. One common scheme is used in the ONIOM approach, which also allows for an arbitrary number of layers, treated either by QM or by MM.¹²⁴ In particular, the treatment of the electrostatic interactions between the QM and MM systems is crucial. It can be performed at the MM level, using QM-derived charges for the QM system. In this mechanical embedding (ME) approach, the QM and MM

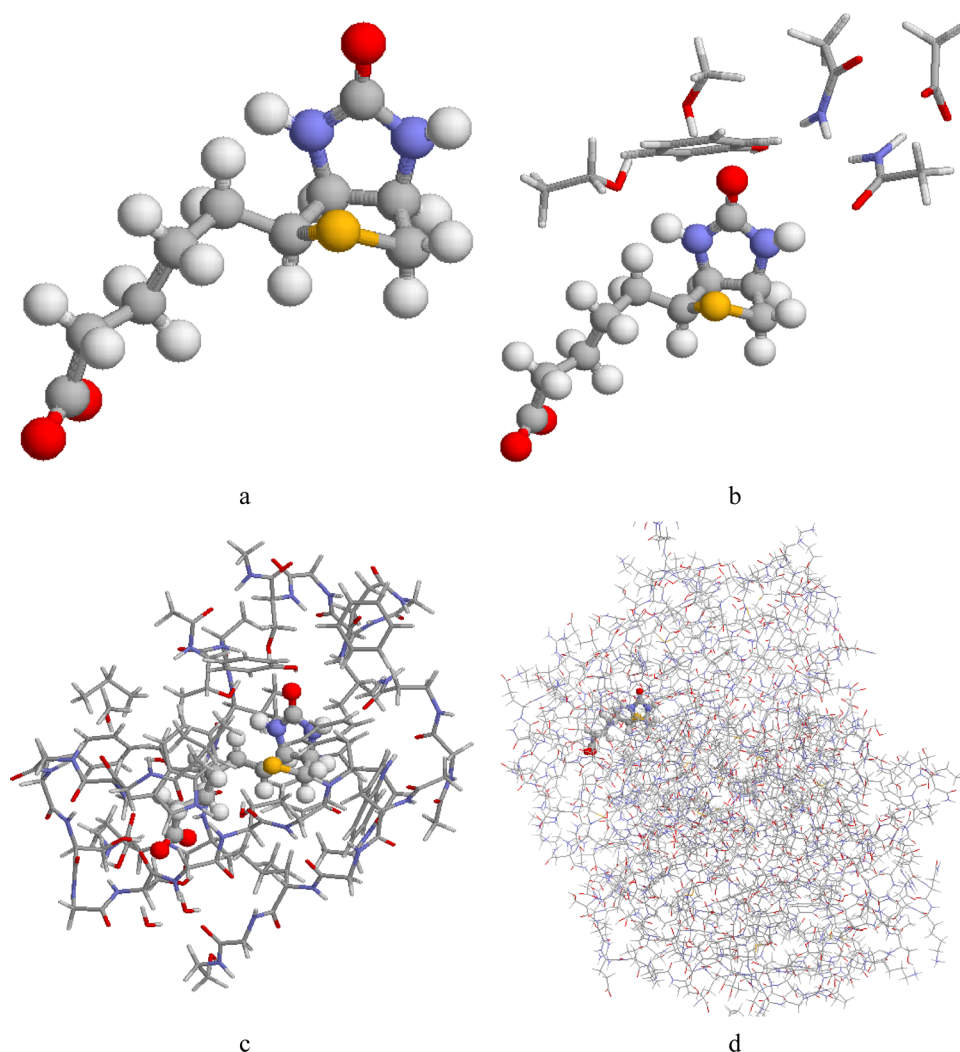


Figure 4. Four sizes of QM systems used in different calculations, involving (a) only the ligand, (b) the ligand and a few selected interacting groups, (c) the ligand and all residues within 6 Å, and (d) the whole protein–ligand complex. In all cases, the same avidin–biotin system is shown, with biotin in a ball-and-stick model.

systems are not polarized by each other. Alternatively, the MM system may be represented by the MM point charges in the QM calculation, leading to a polarization of the QM system. This is called electrostatic embedding (EE), and it is the most commonly used approach. However, it may lead to overpolarization of the QM system, and it involves an inconsistent treatment of the QM and MM systems.¹²⁵ The ideal way is the use of polarized embedding (PE), in which both the QM and MM systems polarize each other self-consistently within the QM calculation.^{126,127} However, this requires special QM software and a polarizable MM force field. QM/MM calculations may also differ in the treatment of bonds between the QM and MM systems, although the great majority of ligand-binding studies have simply truncated the QM system by hydrogen atoms.⁴⁴ The main disadvantage of QM/MM is that it is strongly affected by the local-minimum problem, which can be partly solved by performing several calculations starting from different MD snapshots or by estimating free energies.^{44,128,129} The selection of the QM system may also strongly affect the results,¹²⁵ and it has lately been suggested that single-point calculations with very large QM systems (600–1000 atoms) should be employed to obtain stable energies.^{130,131}

A third alternative is the inclusion of the whole receptor–ligand complex in the QM calculations (Figure 4d). It avoids all the technical problems of QM/MM and the potentially biased choice of the QM system. However, the large size of the QM system introduces limitations in the QM method and basis set that can be employed, which may affect the results; it must be remembered that the binding-affinity calculations require an extremely high accuracy in the results (~ 6 kJ/mol) and the binding typically involves significant London dispersive interactions, which require correlated methods and large basis sets to be accurately estimated.

All biochemical reactions take place in water solution, and it is well-known that this environment can strongly affect the reaction energies. Therefore, it is important to model such effects. In MD and MC simulations, the solvent is typically modeled by explicit water molecules. However, a cheaper alternative is to treat the surroundings as a featureless dielectric continuum, characterized by a dielectric constant. There are many variants of such continuum-solvation methods.¹³² For QM methods, the polarizable continuum model (PCM)^{132–134} and the related conductor-like solvent model (COSMO)¹³⁵ are normally used. For MM methods, it is more common to use the generalized Born (GB) method^{136,137} or to solve the Poisson–Boltzmann

(PB) equation.^{138,139} Common to all these methods is that they depend on an atomic radius for each atom, which is a fitted parameter. Moreover, they give only the polar solvation free energy (the average electrostatic interactions of the solute with the solvent). To obtain a total solvation free energy, which can be compared to experiment, a nonpolar part needs to be added, estimating the cost of forming a cavity in the solvent, as well as the dispersion and repulsion interactions between the solute and solvent. For PB and GB methods, it is typically obtained as a linear relation to the solvent-accessible surface area (SASA). For PCM, separate terms for the cavitation, dispersion, and repulsion energies^{133,140,141} or the parametrized SMD model¹⁴² is employed, whereas the COSMO-RS (real solvent) approach is used for COSMO.^{143,144}

2.3. Calibration Studies

Many groups have studied how various QM methods perform for small model complexes of noncovalent interactions, typically based on CCSD(T)/CBS (i.e., extrapolations to a complete basis set) reference calculations.^{145–147} Here we mention a few applications with direct relation to ligand binding. Merz et al. have investigated the accuracy of various QM methods for ligand-binding interaction energies by dividing the complex between indinavir and HIV protease into 21 small fragments (20–30 atoms), consisting of one part of the ligand and one or two residue models of the protein.¹⁴⁸ For each fragment, CCSD(T)/CBS reference energies were calculated and compared to energies calculated with more approximate MM and QM methods. They obtained the best results with MP2/aug-cc-pVQZ calculations, although B97-D/TZVP and M06-L/aug-cc-pVQZ also gave good results. The long-term aim was to identify systematic errors in the approximate methods for certain types of interactions, which can then be subtracted as corrections.

Grimme et al. used the same complexes to test the DFT-D3 method.⁹⁸ The calculations showed that most DFT-D3 methods could reproduce the reference calculations with mean absolute deviations (MADs) of 2–18 kJ/mol with the def2-TZVP basis set and slightly better ones for the def2-QZVP basis set. The SEQM methods PM6-DH2 and DFTB gave MADs of 21 and 15 kJ/mol. Even at the TZVP level, the BSSE is sizable, 11–64 kJ/mol. A similar study was also performed on typical pairwise interactions in a folded protein, giving further statistics.¹⁴⁹

Yilmazer and Korth have made an interesting comparison of MM, SEQM, and DFT methods, with and without solvation, to calculate protein–ligand interaction energies, using increasingly larger models (including all protein atoms within a radius of 3, 5, 7, or 10 Å from the ligand).¹⁵⁰ With the lack of experimental or accurate QM data, they simply studied the correlation and differences of ranking between the various methods. They showed that there are only small differences between various DFT methods or basis sets, but a clear difference between MM, SEQM, and DFT. These three types of methods also give significantly different solvation effects. In terms of MAD, all differences are large, e.g., 13 kJ/mol between PBE and BP86 and 59 kJ/mol between PM6-DH+ and BP86-D2/TZVP. They also used the 10 smallest models of the 3 Å set to perform a benchmark study of various theoretical methods, employing LPNO-pCCSD/def2-TZVPP-corrected MP2-F12/aug-cc-pVDZ calculations with CP corrections.¹⁵¹ They recommend SCS-MP2 and B2PLYP-D3 as reference methods, TPSS-D3/def-TZVPP as the most accurate DFT method, and PM6-DH+ as the best SEQM method.

Grimme has developed a series of methods, based on HF or DFT, that can be used with small basis sets, but still give accurate results.^{87,152–155} They are intended as alternatives to SEQM methods for large molecules, to perform extensive conformational searches, or to calculate vibrational frequencies. For example, the HF-3c method gave an MAD of 26 kJ/mol for 12 supramolecular binding free energies.¹⁵⁴

2.4. Importance of Sampling

The advantage of using an accurate QM method has to be balanced against the computational cost of each energy evaluation, which in practice limits the amount of conformational sampling that can be afforded. In this section, we will outline the statistical-mechanical basis for this balance and discuss the general aspects of combining expensive and cheap energy evaluations (e.g., QM and MM). In the following sections, we will discuss particular statistical-mechanical methods and how they can be used together with QM calculations.

In general, a closed atomistic system in thermal equilibrium can be represented by an ensemble of structures that satisfy some external constraints (e.g., constant temperature and volume). According to statistical mechanics, the potential energy of the structures follows a Boltzmann distribution; i.e., the probability of the system being in a certain microstate i is given by

$$p(i) = \frac{1}{Q} e^{-E_{\text{pot}}(i)/RT} \quad (6)$$

where E_{pot} is the potential energy of the microstate and Q is a normalization constant, usually called the partition function. The microstates can be grouped into conformations, corresponding to well-defined energy basins in the potential-energy landscape. According to the Boltzmann distribution, only conformations with low energy (within a few RT from the global minimum) have significant probability and thus contribute to observed quantities such as the binding free energy.

Simple systems have only one or a few dominant conformations. On the other hand, solvated systems tend to have many equally contributing conformations, because the water molecules can adopt a multitude of positions and orientations. Biological macromolecules and druglike molecules typically have many internal conformations, as well as many possible orientations (binding poses), all adding to the complexity of the ensemble for a solvated protein–ligand system. This distinction between simple and complex systems has important consequences for the optimal balance between sampling and energy evaluation and thus for the choice of QM method. There have been many successful computations of gas-phase interaction free energies using a single dimer structure, but the same does not hold for binding free energies. In fact, it has long been recognized that a rigorous calculation of the binding free energy requires an extensive sampling of conformations and often millions of energy evaluations.^{6,7} This holds regardless of the type of energy function, and thus, QM calculations of binding free energies may become prohibitively expensive.

When using QM calculations, one always has to think in terms of multiple energy functions. In fact, most QM ligand-binding methods also involve calculations at the MM level (e.g., for the crystallographic refinement or for sampling). To understand the consequences of this duality, we assume that the energy landscape determining the binding free energy can be described by (anharmonic) vibrations around a set of dominant conformations. Figure 5 illustrates the principal ways in which two different potential-energy functions may differ under this

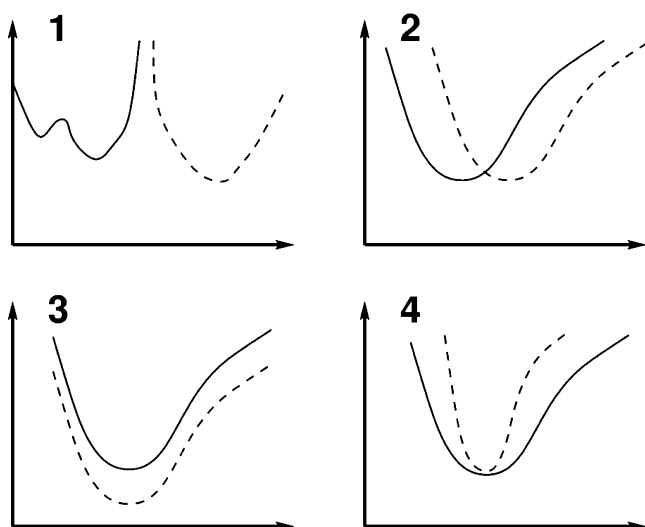


Figure 5. Four principle ways in which two potential-energy functions (solid and dashed lines, e.g., corresponding to QM and MM) may differ, as discussed in the context of how well a computational method combining QM and MM might be expected to perform. The x axis represents some collective coordinate, such as the protein–ligand distance, whereas the y axis represents the potential energy.

assumption (of course, all effects can be combined): (i) They can have different sets of dominant conformations. (ii) For a given conformation, the central (energy-minimized) structure can be different. (iii) For a given conformation, the depth of the energy well can be different. (iv) For a given conformation, the shape of the energy well can be different.

The choice of how to combine the QM and MM calculations depends on how large an importance one ascribes to the various effects. In particular, methods that use single-point QM calculations on snapshots from an MD simulation typically assume that only the third effect is important, and will give wrong results if the position or shape of the energy well differs significantly, primarily because the selected ensemble of snapshots is not Boltzmann-weighted with respect to the QM energy; i.e., the snapshots do not necessarily correspond to geometries with low potential energy. In addition, the entropic effect estimated from the MM calculations can be inaccurate when the shape of the potential-energy surface differs. On the other hand, methods that employ energy minimization at the QM level are less sensitive to the second and fourth effects, but typically assume a harmonic shape of the energy well and neglect the contributions from other conformations. Both approaches, and most other methods, assume that the first effect is insignificant, so that a set of relevant conformations can be obtained from MD sampling or from crystallographic refinement, but some methods employ a conformational search at the QM level.^{156,157}

2.5. MM/PBSA, LIE, and FES Methods

Three methods have been much used to estimate binding affinities with computational methods, MM/PBSA, LIE, and FES. They will be shortly introduced in this section, because several attempts have been made to extend these approaches with QM methods.

In 1994, Åqvist et al. suggested the linear interaction-energy (LIE) method.^{4,158} It is based on two MD simulations, one of the receptor–ligand complex (RL) and one of the free ligand in water (L). The binding free energy is estimated from the

difference in the average electrostatic and van der Waals interaction energies between the ligand and the surroundings ($E_{\text{el}}^{\text{L-S}}$ and $E_{\text{vdW}}^{\text{L-S}}$) in the two simulations:

$$\Delta G_{\text{bind}} = \alpha(\langle E_{\text{vdW}}^{\text{L-S}} \rangle_{\text{RL}} - \langle E_{\text{vdW}}^{\text{L-S}} \rangle_{\text{L}}) + \beta(\langle E_{\text{el}}^{\text{L-S}} \rangle_{\text{RL}} - \langle E_{\text{el}}^{\text{L-S}} \rangle_{\text{L}}) \quad (7)$$

The two terms are scaled by empirical constants, α and β . β should be 0.5 according to the linear-response approximation, but it often is assigned values of 0.3–0.5 depending on the chemical nature of the ligand.^{159,160} The other parameter is truly empirical. The Åqvist group has claimed that a value of 0.18 can be used for most systems,¹⁶¹ although most other research groups treat it as a fitting parameter.¹⁶² Sometimes additional terms are added, e.g., a term depending on the change in the SASA and a constant term,^{163,164} and with many terms, it approaches the QSAR methods. A variant with minimized structures and continuum-solvation methods has also been suggested.¹⁶⁵ When comparing the results of LIE with those of other methods, it should be remembered that fitting of a number of parameters always improves the performance of the method, but reduces its predictive ability (unless the parameters are transferable).

In 1998, Kollman and co-workers suggested the MM/PBSA approach (MM combined with PB and SASA continuum solvation).^{5,166,167} It suggests that the free energy of a molecule can be estimated from the sum of six terms:

$$G = E_{\text{int}} + E_{\text{el}} + E_{\text{vdW}} + G_{\text{pol}} + G_{\text{np}} - TS \quad (8)$$

The first three terms are the internal (bonds, angles, and dihedral energies), electrostatic, and van der Waals terms from a standard MM force field of the molecule in vacuum. The fourth term is the polar (electrostatic) solvation energy, which is obtained with the PB or GB (giving an MM/GBSA method) continuum-solvation methods. The fifth term is the nonpolar continuum-solvation energy, estimated by a linear relation to the SASA. The last term is the entropy, which is estimated from an NMA of vibrational frequencies calculated at the MM level. For ligand-binding affinities, typically the receptor–ligand complex is simulated by MD, sampling ~1000 snapshots, from which average energies are calculated after the water molecules are stripped off. The binding affinity is then obtained as

$$\Delta G_{\text{bind}} = \langle G_{\text{RL}} - G_{\text{R}} - G_{\text{L}} \rangle_{\text{RL}} \quad (9)$$

in which the structures of the receptor and the free ligand are obtained from the RL structures by simply removing the ligand or the receptor. Of course, this is an approximation that ignores the deformation of the receptor and the ligand in the complex, but it strongly improves the convergence of the energies and leads to an exact cancellation of the E_{int} term.¹⁶⁷

Both MM/PBSA and LIE are approximate methods, based on sampling of the receptor–ligand complex, and possibly also the free ligand and the receptor, i.e., the end states of the reaction in eq 1. The strict way to obtain binding free energies is by free-energy simulations (FESs), typically using the thermodynamic cycle in Figure 6. The free-energy difference between two states, A and B, can be calculated by

$$\Delta G_{\text{A} \rightarrow \text{B}} = -RT \ln \left\langle \exp \left(\frac{-(E_{\text{B}} - E_{\text{A}})}{RT} \right) \right\rangle_{\text{A}} \quad (10)$$

where E_{A} and E_{B} are the energies of the two states, respectively, and the angular brackets represent an ensemble average over the

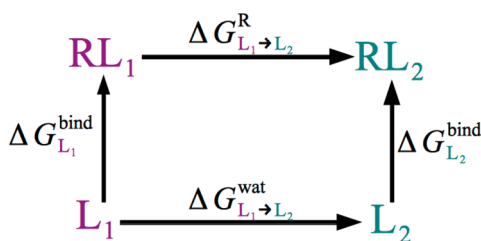


Figure 6. Thermodynamic cycle for the calculation of relative binding free energies by FES calculations. It is hard to directly estimate $\Delta G_{L_1}^{\text{bind}}$ and $\Delta G_{L_2}^{\text{bind}}$ because they involve a very large change (deleting the full receptor). Therefore, the relative free energy of binding is instead estimated by $\Delta G_{L_1 \rightarrow L_2}^{\text{bind}} = \Delta G_{L_2}^{\text{bind}} - \Delta G_{L_1}^{\text{bind}} = \Delta G_{L_1 \rightarrow L_2}^{\text{R}} - \Delta G_{L_1 \rightarrow L_2}^{\text{wat}}$, because it involves only the smaller change of transforming L_1 to L_2 .

A state. This approach is called exponential averaging (EA) or free-energy perturbation.¹⁶⁸ This exponential average converges only if the difference between the two states is small, and in most cases, the calculations need to be done for many (alchemical) intermediate states, e.g., obtained by a mixed energy function of the type

$$E_\lambda = (1 - \lambda)E_A + \lambda E_B \quad (11)$$

where λ is a coupling parameter that transfers the system from A ($\lambda = 0$) to B ($\lambda = 1$). At the MM level, such a mixed energy can be obtained at a low cost, but at the QM level, it requires two QM calculations, one of each state.

There are many alternatives to eq 10 for the calculation of the free energies, e.g., thermodynamic integration (TI),¹⁶⁹ the Bennett acceptance ratio (BAR),^{170,171} or the multistate BAR (MBAR) methods.¹⁷² Modern simulation packages typically provide the energies needed to calculate free energies with all these methods. Test calculations indicate that BAR and MBAR give free energies with the best statistical properties.¹⁷¹

If the two states A and B are two (similar) ligand molecules, eq 10 will give the relative free energy of binding. However, the calculations have to be done both for the ligands bonded to the receptor and for the free ligands in water solution, according to the thermodynamic cycle in Figure 6, illustrating that differences in hydration energies are as important as interactions with the receptor for the net binding affinity. Alternatively, state B may be a noninteracting ligand, in which all electrostatics and Lennard-Jones interactions with the surroundings have been turned off. Then absolute binding energies will be obtained, but this requires the use of restraints to keep the molecule in the binding site and to allow the definition of a proper standard state.^{173,174} The convergence is typically slower, because the change is larger and it may take a long time for water molecules to diffuse into the binding site, replacing the ligand.

2.6. Quality Measures

In the paper, we often use R^2 to give an impression of the performance of the various methods (especially in the tables). This measure was selected not because we consider it as the best measure, but because it is most often reported in papers and it can also easily be calculated from reported affinities. However, it should be kept in mind that it is a very forgiving measure, which may give good results even if the calculated affinities are grossly overestimated (as they often are with computational methods, especially if solvation or entropy is omitted). In our view, it should always be combined with a measure of how close the calculated and experimental affinities are in energy terms, e.g., the

mean absolute deviation (MAD) or the root-mean-squared deviation (RMSD), possibly after removal of the mean signed deviation (MSD, i.e., the systematic error), giving MADtr. Additional quality measures can be added to give a more nuanced picture of the performance, e.g., the predictive index (PI)¹⁷⁵ or Kendall's rank correlation, based on all data (τ) or only on statistically significant pairs (τ_{90}).¹⁷⁶

3. SINGLE-STRUCTURE APPROACHES

The simplest, but also most approximate, approach to include QM calculations in binding-affinity calculations is the employment of single structures, e.g., obtained from a crystal structure, from docking, or by an energy minimization. The advantage of such an approach is of course the speed; no expensive conformational sampling is performed. On the other hand, such an approach will be strongly affected by the local-minimum problem: An energy minimization will end up in one of an almost infinite number of possible local minima of the receptor–ligand complex, and it is far from certain that this structure is the most important for the binding. As we will discuss below, it is often observed that individual binding affinities estimated by snapshots from MD simulations differ by ~ 80 kJ/mol even after minimization.^{29,177,178} On the other hand, MM studies by Gilson and co-workers on host–guest systems have shown that only a few low-lying conformers contribute to the binding free energy,^{179,180} but it is not clear whether this applies to the much more complicated biomacromolecules. Moreover, energies estimated from minimized structures are enthalpies, not the free energies that govern the binding. This is a more serious problem for binding-affinity calculations than, e.g., for enzyme reactions, because the former always involve major entropy terms, owing to the loss of translational and rotational freedom of the ligand, which at least in the gas phase amount to ~ 60 kJ/mol at ambient temperature.¹⁸¹ In fact, it is often observed that similar molecules, e.g., enantiomers, have significantly different binding entropies, and there is often a strong inverse correlation between binding enthalpies and entropies of analogous ligands, the much discussed enthalpy–entropy compensation.^{182–185}

A natural approach would be to perform of single-point QM energy calculations directly on crystallographic structures, but it is well-known that systematic errors in both the crystallography and the QM calculations would make such energies almost useless, with errors of hundreds of kilojoules per mole.¹⁸⁶ The use of docked structures is usually better, because the docking involves a conformational search for the ligand inside the protein. However, it is still restricted to a single or a few structures, and no valid Boltzmann averaging of the structures is made.

In the following, we will discuss QM binding-affinity calculations with QM-cluster, QM/MM, and whole-system calculations with either fragmentation or linear-scaling approaches in separate subsections. A subsection is also devoted to calculations on host–guest systems.

3.1. QM-Cluster Calculations

QM-cluster calculations (cf. section 2.2) of binding affinities are rather uncommon. There are several reasons for this. First, binding-affinity calculations with MM methods have never used such an approach, so there is no natural extension from such methods. Second, if all groups close to a typical drug candidate should be included in the calculations, this gives a quite large QM system (200–1000 atoms), which has been problematic to treat with accurate QM methods until recently. Third, it is hard to include all important free-energy terms in such calculations, and

Table 1. Summary of QM-Cluster Studies^a

group	ref	year	method	QM syst	opt	solvation	CP	ΔS	comments	receptor	no.	R^2
Pakkanen	187	1994	HF/6-31G*//AM1	L + 9 aa		SM2 (AM1)	yes		electrostatics with MM, $\epsilon = 4r$	L-arabinose-binding protein	3	0.37
Pakkanen	188	1995	HF/3-21G	L + 6 aa		SM2 (AM1)			electrostatics with MM, $\epsilon = 4r$	<i>p</i> -hydroxybenzoate hydroxylase	7	0.70
Sulimov	189	2004	PM3	L + 5 Å		some expl			only ΔH	six proteins	8	0.96
Villar	191	2005	AM1	L + 5 Å	L					five proteins	5	
Hannongbua	196	2005	MP2/6-31G*/B3LYP/6-31G**/PM3	L + 4 Å			yes			HIV reverse transcriptase	2	
Sulimov	190	2006	PM3	L + 5 Å		expl + COSMO				trypsin, thrombin, ribonuclease	12	
Houk	198	2007	MP2/6-31+G**//B3LYP/6-31+G**	L + 6 aa						avidin, streptavidin	2	
Gould	192	2008	B3LYP/6-31G**//HF/6-31G**	L + 1 lip			yes		eight conformations	lipids	12	0.55
Wang	193	2010	DFT/SZ(P)	L + 24 aa	L	PBSA (MM)				CDK2	5	0.87
Re	194	2010	B3LYP/LACV3P*/aug-cc-pVTZ(-f)//LACVP+/6-31+G*	L + 1 aa	all	PB		yes		cathepsin B	5	
Ryde	195	2011	TPSS/def2-SV(P)	L + 1 aa	all	COSMO		yes		cathepsin B	6	0.86
Hannongbua	197	2013	(SCS-)MP2/6-31G*//HF/3-21G	L + 19 aa	all					HIV reverse transcriptase	2	
Kongsted	199	2014	B3LYP or MP2/6-31G*	L + 2 M		C-PCM				HIV-1 RNase H	7	0.93
Svensson	201	2014	B3LYP/6-31+G**//6-31G**	L + 5 aa		PB				β -secretase	36	0.86

^aThe table lists the research group, the reference, the publication year, the QM method used (if two methods are given, the first is for energies and the second, after //, was used for geometries), the size of the QM system (L = ligand, aa = amino acids, lip = lipid, M = metal, and Å gives the maximum distance to the ligand), atoms that were optimized, the solvation method used (expl = explicit water molecules), whether CP corrections or an entropy term was included (if yes, the latter was obtained from the QM frequencies), possible comments, the receptor used, the number of systems studied, and the obtained correlation coefficient. A missing entry means this contribution was not included (or not specified in the original paper).

therefore, such an approach has probably been considered less realistic. A summary of QM-cluster calculations of binding affinities is given in Table 1.

In 1994, Peräkylä and Pakkanen used QM methods to study the binding of three monosaccharides to the L-arabinose-binding protein.¹⁸⁷ They calculated the QM interaction energy of the ligand with nine minimal models of protein side chains at the HF/6-31G* level of theory, including some CP corrections for the BSSE. To this was added a continuum desolvation energy of the ligand, calculated with AM1-SM2 and using structures optimized both in vacuum and in the solvent. Finally, the electrostatic interaction energy between the ligand and the protein was calculated at the MM level using a distance-dependent dielectric constant. Clearly, this was an impressive attempt to estimate ligand-binding affinities with QM methods, including the most important terms in a reasonable manner, considering the available computational resources. They obtained some correlation to the experimental data ($R^2 = 0.37$), but the estimated binding energies were almost 10 times larger than the measured binding affinities. The following year, they used a similar method to study the binding of seven ligands to *p*-hydroxybenzoate hydroxylase.¹⁸⁸ They included the ligand and six amino acid models in the QM calculations, which this time were performed at the HF/3-21G level, without any BSSE correction. Still, they obtained a better correlation to the measured affinities, $R^2 = 0.70$.

Ten years later, Sulimov and co-workers used PM3 to estimate ligand-binding affinities.¹⁸⁹ They included all protein residues with at least one atom within 5 Å of the ligand, giving a total of 293–455 atoms. The structures were optimized, keeping the

backbone atoms fixed. Only binding enthalpies were considered. Two approaches to treat water molecules were tested. In the first, only crystal water molecules were included, but this gave rather poor results, with an MAD of 24 kJ/mol and $R^2 = 0.3$ for eight protein–ligand complexes. However, when they added two water molecules to the free protein and ligand for each hydrogen bond present in the complex (i.e., giving some restricted explicit solvation), the results improved strongly to an MAD of 7 kJ/mol and an impressive $R^2 = 0.96$.

In a later study, they included a mixed explicit and implicit solvation model.¹⁹⁰ In the trimmed protein models, as well as in the free protein and ligand, water molecules were added to all potential hydrogen-bonding sites. The number of added water molecules was successively increased until the interaction energy converged to within ~4 kJ/mol, but the selection seems to have been guided also by the experimental data. All structures were optimized by PM3, keeping the heavy atoms of the backbone fixed. They studied 12 complexes with different ligands of trypsin, thrombin, and ribonuclease. The calculated and experimental binding enthalpies showed an excellent correlation with an RMSD of only 4 kJ/mol. PDDG/PM3 calculations gave similar results. For one complex, the dependence on the included residues was also studied. Models with only 1–3 residues gave totally unrealistic results, but with 7 residues, the difference was less than 8 kJ/mol. However, convergence to within 4 kJ/mol was not obtained until 19 residues were included.

Villar and co-workers used a similar approach.¹⁹¹ They first compared the performance of the AM1 and PM3 methods to that of MP2/6-31G* and B3LYP/6-311+G(2d,p) for the interaction energies of small models of typical protein–ligand interactions,

showing that AM1 gave much better results than PM3. Then, they calculated binding affinities for real ligands with all protein residues within 5 Å of the ligand with AM1. They started from crystal structures, optimizing the ligand in the rigid protein model. This gave reasonable structures, but no comparison with experimental energies was performed, and some binding energies were overwhelmingly negative (up to -1116 kJ/mol).

Several studies have instead used DFT methods. Gould et al. interpreted the nonspecific binding of ligands to lipid molecules.¹⁹² They employed a restricted conformational search, optimizing at least eight possible conformations of each complex at the HF/3-21G* level. The one with the strongest binding was reoptimized at the HF/6-31G** level, followed by CP-corrected B3LYP/6-31G** single-point energy calculations. A decent correlation to experimental nonspecific binding was observed, $R^2 = 0.55$.

Wang and co-workers also used DFT and a minimal SZ basis set for the protein and SZP for the ligand.¹⁹³ They included the ligand and the closest 24 amino acid residues (5.5 Å). Only the ligand and added H atoms were optimized in a fixed surrounding. To the QM energies were added PB + SASA continuum-solvation energies, calculated at the MM level with Mulliken charges for the ligand. They studied five inhibitors binding to CDK2 and obtained a good correlation to the experimental results with both the pure QM interaction energy and the full QM + PBSA energy ($R^2 = 0.90$ and 0.87). However, the variation in the calculated energies was almost 100 times larger than what was observed experimentally. They tested the convergence of the energies, by also including 50 amino acids. This changed the interaction energies by up to 25 kJ/mol, but the correlation was still 0.89.

Re and co-workers studied the binding of five metal complexes to cathepsin B.¹⁹⁴ They correlated the binding of the metal to a Cys model, using B3LYP calculations with a PB solvent and NMA entropy corrections. We also studied the six best Ru complexes with QM-cluster methods.¹⁹⁵ The ligands were optimized in vacuum, including a Cys model from the protein, and binding energies were calculated in a COSMO continuum solvent with a dielectric constant (ϵ) of 4 or 80, employing the TPSS/def2-SV(P) method. The vacuum energies gave the best correlation to the experimental affinities ($R^2 = 0.57$), but they were slightly deteriorated by including thermal and entropy corrections. On the other hand, the results were strongly improved if a conformational search of the flexible ligand was performed before the optimization. Then the best correlation was obtained with COSMO ($\epsilon = 4$), but the difference was not large ($R^2 = 0.81$ – 0.86). However, entropy corrections still deteriorated the results.

Four studies have instead used MP2 calculations. Hannongbua et al. used the two- and three-layered QM/QM ONIOM approach to study the binding of the 8-Cl TIBO ligand to the wild-type and a mutant HIV reverse transcriptase.¹⁹⁶ They included the ligand and 20 residues within 4 Å of the ligand at the PM3 level and various combinations of MP2/6-31G* and B3LYP or HF/6-31G** calculations for the ligand and two residues (sometimes only parts of them). All models correctly showed that the mutant reduced the binding energy, but the results at the various levels of theories differed by 16 kJ/mol in the estimated relative binding energy. In a later study of the same enzyme, they employed a divide-and-conquer MP2 and SCS-MP2 approach with the 6-31G* basis set to study the binding of a ligand to a 19 amino acid model of the enzyme.¹⁹⁷

DeChancie and Houk used QM cluster calculations to study the unusually strong interaction between biotin and avidin or streptavidin.¹⁹⁸ They employed MP2/6-31+G** calculations on B3LYP or MPWB1K/6-31+G** structures. They used biotin and six amino acid models (Figure 3a) to show that the five hydrogen bonds to the ligand in the active site are strongly cooperative.

Kongsted and co-workers studied the binding of seven ligands to HIV-1 RNase, including only the ligand and the two active-site Mg^{2+} ions in the QM calculations.¹⁹⁹ The QM system was solvated with a PCM solvent. Calculations with both the B3LYP and MP2/6-31G* methods gave a good correlation to experimental data ($R^2 = 0.93$ and 0.90 , respectively), much better than docking and scoring with the Glide²⁰⁰ software ($R^2 = 0.07$) and even FMO calculations ($R^2 = 0.86$). However, the range of the calculated affinities was 50 times larger than in the experiment. This simple approach was then employed as a final filter in a virtual-screening approach.

Recently, Svensson and co-workers published an interesting QM-cluster study of the relation between the measured and predicted affinities of 36 amidine and guanidine β -secretase inhibitors.²⁰¹ The calculations employed mainly the B3LYP method. Complexes were optimized with the 6-31G** basis set, and energies were evaluated with the 6-31+G** basis set in a PB or SM8 continuum solvent. A conformational search was first performed at the MM level. Two protein models were employed, one small one with only two acetate groups and the other with five amino acid side chain models and the backbone of three residues. The calculated affinities using the larger model and PB solvation correlated with experimental potencies with $R^2 = 0.73$ and 0.86 for bi- and monocyclic ligands, respectively, having correlation lines shifted by ~ 16 kJ/mol. For the SM8 solvation, both types of ligands gave a common correlation line with $R^2 = 0.65$. The maximum error in the predicted affinity was 6 kJ/mol. The correlation was appreciably better than what was obtained from docking or MM/GBSA calculations ($R^2 = 0.10$ – 0.17). Results with B3LYP-D3 or M06-2X were very similar. The smaller model gave somewhat worse results, but the calculations could be performed within 30 min on four CPUs. A slight problem of this study is that the calculations were not compared directly to experimental measurements, but to “core potencies” estimated via a structure–activity model obtained from measurements of a database of more complex molecules. The authors emphasize that such a study is possible only if the key interactions are well-defined, conserved, and dominated by electrostatics, and the binding pose is similar in all complexes.

In conclusion, QM-cluster calculations of binding affinities have been performed with methods ranging from SEQM, via HF and DFT, to MP2. However, with one exception, only small basis sets have been used (up to 6-31+G**), mostly without BSSE or dispersion corrections. The SEQM calculations typically included all residues within 4–5 Å of the ligand (a few hundred atoms), whereas the other studies mostly included only a few key residues. Most studies included a solvent correction, but only two have considered the entropy term. We doubt that QM-cluster approaches will give any predictive results, unless the binding free energy is dominated by a few well-defined, rigid, electrostatic interactions. So far, no really serious attempt has been made to combine an accurate QM method (large basis set with CP and dispersion corrections) with solvation and entropy estimates within a QM-cluster approach.

Table 2. Summary of Some QM Calculations on Host–Guest Systems^a

group	ref	year	method	opt	solvation	CP	ΔS	comments	host	no.	R^2
Houk	204	1999	HF/3-21G*	HF/3-21G*					[3] catenane	2	
Grimme	205	2005	BLYP-D2/TZVP	BLYP-D2/ TZVP				some SCS-MP2/aug-cc-pVTZ calculations	clip and tweezer	22	
Goddard	206	2008	DFT/6-311++G**	DFT/6-31G*	PB				[2] rotaxane	2	
Truhlar	207	2008	M06-2X/6-31+G**	M06-L/MIDI!		yes	M06-L/ MIDI! ^b		tweezers	2	
Jacquemin	99	2012	B97-D3/def2-QZVP	B97-D3/6-31G*	PCM	yes	B97/6-31G*	nonpolar PCM excluded	molecular tweezer	2	
Grimme	210	2012	PW6B95-D3abc/def2-QZVP'	TPSS-D3/ def2-TZVP	COSMO-RS		PM6-DH2 ^b	some conformational search	mixed	13	
Grimme	214	2014	PW6B95-D3abc/def2-QZVP'	TPSS-D3/ def2-TZVP	COSMO-RS		HF-3c ^b	some conformational search, special treatment of charges	cucurbit[7]uril octa-acid	14 9	0.90 0.42
Ryde	216	2014	TPSS-D3/def2-TZVP	TPSS-D3/ def2-SV(P)	COSMO-RS		MM	start from MD structures, fully charged	octa-acid	9	0.6–0.8
Grimme	217	2015	B3LYP, M06, PW6B95, B2PLYP, (SCS-)MP2/def2-QZVP, DLPNO-CCSD(T)/CBS	TPSS-D3/ def2-TZVP	COSMO-RS	yes	HF-3c ^b		frustrated Lewis-pair complexes	4	
Grimme	213	2015	many DFT/def2-QZVP' methods, HF-3c, several SEQM methods	TPSS-D3/ def2-TZVP	COSMO-RS		HF-3c ^b		mixed	30	0.80, 0.89

^aThe table lists the research group, the reference, the publication year, the QM method used for energies (abc represents three-body dispersion corrections) and for the geometry optimization, the solvation method used, whether CP corrections were included, the method used to obtain frequencies for the normal-mode analysis, possible comments, the host considered, the number of systems studied, and the obtained correlation coefficient. The QM calculations always involved the full host–guest system. ^bLow-lying vibrational modes were treated with a rigid-rotor harmonic-oscillator approximation.²¹⁰

3.2. Host–Guest Systems

Host–guest systems are macrocyclic organic molecules that can bind small (or medium-sized) molecules. Owing to their restricted size, 100–300 atoms, and typically a restricted flexibility, they are ideal model systems for computational studies, as the physical effects involved in the binding (e.g., hydrogen bonds, dispersion, hydrophobic effects, (de)solvation, and entropy) are expected to be the same as for biological macromolecules. Consequently, extensive MM and QM investigations have been performed on such systems.^{202,203} Although these are somewhat outside the scope of the present review, we will mention a few illustrative and important studies (summarized in Table 2), but refer to a recent review for a more complete account.²⁰²

Early studies employed methods that do not include explicit dispersion, using too small basis sets²⁰⁴ or excluded solvation or entropy effects.^{205–207} Therefore, they gave quite poor results or were not compared to experiments. However, in 2012, Jacquemin et al. studied two molecular tweezer complexes with the B97-D3 method.⁹⁹ Structures were optimized and frequencies were obtained with the 6-31G* basis set, whereas single-point energies were calculated with larger basis sets, up to def2-QZVP. The BSSE was corrected by the CP approach. PCM was used to estimate solvation effects, but only the electrostatic term was included, which according to the authors was to avoid double counting. However, DFT-D3 estimates the dispersion interactions between the atoms in the explicitly studied molecule, whereas the nonpolar PCM dispersion term calculates the dispersion between the explicit molecule and the continuum solvent. There is no overlap between these two effects, and both of them should be included to cover all energy terms and obtain valid solvation energies.^{208,209} They showed that the geometries are insensitive to the theoretical method and solvation effects. However, the energies were sensitive to the basis set, changing by ~35 kJ/mol between 6-31G* and def2-QZVP. For the small basis sets, the CP correction was very large, 53–72 kJ/mol, but it strongly overestimated the BSSE. With the def2-QZVP basis set, the CP correction was only 4 kJ/mol. Calculations with the largest CP-corrected basis set reproduce the experimental ΔG_{bind} within 4–14 kJ/mol.

The same year, Grimme suggested an approach to calculate binding free energies of supramolecular complexes.²¹⁰ The structures were optimized at the TPSS-D3/def2-TZVP level, using some restricted conformer scanning at the SEQM level. Energies were calculated with the TPSS and PW6B95 methods with the large def2-QZVP' basis set (omitting f- and g-type functions on H and non-H atoms, respectively), but without any correction for the BSSE. Dispersion corrections were estimated with the DFT-D3 method, including three-body terms. Solvation effects were estimated with the COSMO-RS method, based on BP86/TZVP calculations. Entropy and thermal corrections were obtained from frequencies calculated at the dispersion- and hydrogen-bond-corrected SEQM SCC-DFTB and PM6 levels, treating low-lying vibrational modes with a rigid-rotor harmonic-oscillator approximation (i.e., scaling down entropies from modes with frequencies below 100 cm⁻¹; a similar approach was also used by Truhlar et al.²⁰⁷). The method was applied to 13 complexes with 24–158 atoms, and experimental binding free energies were reproduced with an MAD of 9 kJ/mol and a maximum error of 20 kJ/mol. For the larger complexes, the three-body dispersion terms were significant, up to 19 kJ/mol. He estimated that the DFT-D3 energies, the solvation energies, and the vibrational entropies contribute roughly the same

uncertainty to the final results for the neutral systems, but the solvation term dominates the uncertainty for charged systems. The same host–guest systems were also later used to compare various methods to take into account the dispersion.⁸⁰ This study also showed an impressive performance of some SEQM methods, e.g., OM2-D3, with an MAD of 16 kJ/mol.

The same systems have recently also been studied with the other dispersion-corrected DFT methods,⁸² symmetry-adapted perturbation theory with DFT,²¹¹ random-phase approximation DFT, and quantum Monte Carlo calculations,²¹² but considering only the gas-phase energies. All these approaches gave results that agree within 4–13 kJ/mol on average, but identifying some systematic differences. The authors pointed out that the complexes are dominated by dispersive interactions, which are well described by dispersion-corrected pure functionals, whereas for complexes with hydrogen bonds and significant charge transfer, hybrid DFT methods are probably needed. The importance of many-body dispersion (beyond the three-body term) was also emphasized.

Recently, this set was extended to 30 host–guest systems with net charges from –1 to +4 and up to 200 atoms in a comparison of several QM methods.²¹³ The study indicated that PW6B95-D3/def2-QZVP' gave the most accurate results, in combination with HF-3c thermodynamic corrections and COSMO-RS solvation free energies (MAD = 10 kJ/mol). The results could be somewhat improved by using counterions for the charged complexes, and then the ω B97X-D3 method gave the best results (MAD = 9 kJ/mol). For 13 pairs of ligands binding to the same host, significant cancellation of systematic errors was obtained, and the difference in binding energy between the two ligands could be reproduced with an MAD of only 5 kJ/mol and a correct sign for all except two of the pairs ($\tau = 0.69$). PM6-D3H2 gave the best results among SEQM methods (MAD = 16 kJ/mol with counterions), but HF-3c gave structures that were most similar to those obtained at the TPSS/def2-TZVP level (RMSD = 0.17 Å) and also the best thermostatical correction. The authors showed that COSMO-RS gave better solvation free energies than SMD and that five parametrizations gave similar results. They suggested that the solvation contribution is the least accurate component of the calculated binding free energies. Grimme et al. have recently reviewed this approach for host–guest systems, claiming an average accuracy of 8 kJ/mol (after removal of two outliers).²⁰²

The same approach was applied also to two host–guest systems in the SAMPL4 blind-test competition.²¹⁴ The HF-3c approach was used both to calculate frequencies and to preoptimize the complexes and perform some manual conformational search. All complexes were first optimized without counterions, which were added afterward by hand and reoptimized in a COSMO continuum solvent. For the binding of 14 small amine ligands with a single or double positive charge to the neutral and rigid cucurbit[7]uril host, they obtained an MAD of 8 kJ/mol, $R^2 = 0.90$, and $\tau = 0.74$, which all were among the 3 best among the 21 submitted predictions in the competition (nearly all of the others were performed at the MM level), although the criteria used in the SAMPL4 overview paper²¹⁵ placed the method somewhat worse in the ranking. The second test case was the binding of nine carboxylate ligands to the octa-acid host. This was somewhat more demanding, owing to the –8 charge of the host and the fact that the host is quite flexible. Grimme and co-workers solved this problem by scanning 28 possible conformations of the ligand (at the HF-3c level) and starting the optimization of the free host from the geometry of

the complex. The host was fully protonated (neutralized) in most of the calculations, but this gave a systematic underbinding, making the calculated binding free energies among the 4 worst of the 13 submitted results. Compensating for the neutralization by extra calculations with 9 added counterions and 24 explicit water molecules improved the results strongly, giving an MAD of 10 kJ/mol and $R^2 = 0.4$. However, the results were still far worse than those obtained by the best MM methods in the competition (MAD = 4 kJ/mol and $R^2 = 0.84$ ²¹⁶), most likely because this test case was ideal for FES studies (small differences and a conserved charge among the guest molecules).

Interestingly, we also studied the octa-acid system with similar methods:²¹⁶ We optimized geometries with the TPSS-D3/def2-SV(P) method and obtained energies at the TPSS-D3/def2-TZVP level. Solvation energies were calculated with the COSMO-RS approach, and entropies were obtained from frequencies calculated at the MM level. In variance with Grimme et al., both the host and guest molecules were fully charged (-8 and -1 , respectively), and starting structures were taken from MD simulations at the MM level. To avoid the problem caused by the flexibility of the host molecule, we calculated rigid interaction energies (i.e., we used the geometry of the complex also for the monomer energies), but added a correction for the deformation of the ligand. Three different structures were tested, viz., optimized in vacuum, or in a COSMO continuum solvent without or with four explicit water molecules coordinating to the guest carboxylate group. There were systematic differences among the structures obtained with the three approaches, but all gave similar estimated binding affinities, with MAD = 5–9 kJ/mol (after removal of a systematic error of 3–14 kJ/mol) and $R^2 = 0.6$ – 0.8 , i.e., slightly better than the results obtained by Grimme et al.

Grimme and co-workers have also employed DLPNO-CCSD(T) calculations, extrapolated to a complete basis set to study the interaction between two borane–phosphine frustrated Lewis-pair complexes.²¹⁷ They used CP-corrected calculations with aug-cc-pVDZ and aug-cc-pVTZ basis sets to extrapolate to the CBS limit. They added solvation free-energy and entropy corrections calculated with COSMO-RS (BP86/TZVP) and HF-3c, respectively. Calculations were also performed with the dispersion-corrected (DFT-D3) B3LYP, M06, PW6B95, B2PLYP, and MP2 methods with the def2-QZVP basis set. All calculations gave results in reasonable accordance with the experimental measurement.

These studies of host–guest systems show how QM-minimization methods can be used to calculate ligand-binding affinities with an accuracy of ~ 8 kJ/mol in absolute binding free energies and ~ 5 kJ/mol for relative energies of different ligands binding to the same host, provided that accurate QM methods are used, typically DFT methods with very large basis sets and dispersion corrections including three-body terms with accurate estimates of both entropy and solvation (both polar and nonpolar terms). However, this good performance might be limited to complexes dominated by dispersion interactions and systems with a low flexibility. The next step would be to employ such methods also for biomacromolecules.

3.3. QM/MM Calculations

The second approach to study proteins is with QM/MM calculations. Such methods are available in several software products, and they have been much used to study ligand binding (especially the ONIOM approach), as can be seen in Table 3. However, most of the studies have employed only QM/MM

total energies and mainly discuss structural aspects and are therefore not explicitly reviewed. Already in 1997, Alex and Finn reported binding affinities calculated at the QM/MM level.²¹⁸ They studied 12 thermolysin inhibitors with an SEQM method. Very few details were given, but they presented a correlation line with two fitted parameters, giving $R^2 = 0.87$.

Gao and co-workers performed a detailed QM/MM study of electrostatic interactions between HIV-1 protease and three inhibitors, employing the AM1 method for the inhibitors.²¹⁹ They averaged the electrostatic interaction energies over snapshots from a 10 ps QM/MM MD simulation. The results showed that the polarization may contribute as much as one-third of the total electrostatic interaction energy. They also calculated contributions from the various residues in the protein, but did not compare them to experimental binding energies. Likewise, Yang et al. used AM1 calculations for 50 different peptides binding to HLA-A*0201, including interacting protein residues in the QM systems.²²⁰ With a parametrized SASA term for hydrophobic interactions, they obtained a decent correlation to measured pIC_{50} values ($R^2 = 0.56$).

However, most QM/MM studies have been performed with DFT calculations for the ligand and a few residues around it. For example, Hillier and co-workers included the inhibitor, two amino acid models, and one water molecule in the QM system.²²¹ The QM system was optimized by HF/3-21G calculations, but energies were calculated at the B3LYP/6-31G* level. They studied the binding of five inhibitors to adenosine deaminase and showed that the inhibitor reacts with a Zn-activated water molecule and that the QM/MM energies gave a much better correlation to experimental IC_{50} values than the vacuum QM energies or the binding energies of the inhibitors before the reaction, calculated at the MM level ($R^2 = 0.87$, 0.09 , and 0.00 , respectively). In a later investigation, they studied the binding of 10 fluorinated inhibitors of carbonic anhydrase II.²²² They used ME-QM/MM calculations with the ligand and five amino acid fragments treated by BLYP-D2/TZV(2d,2p). Interaction energies were also calculated for only the QM system with BH&HLYP/6-31+G* and CP-corrected MP2/aug-cc-pVDZ calculations. The obtained geometries were similar to crystallographic structures, but the interaction energies were not compared to experiments.

Likewise, we have applied QM/MM calculations to study the binding of six Ru complexes to cathepsin B.¹⁹⁵ The QM calculations involved the TPSS/def2-SV(P) method, and the QM system consisted of the Ru complex and the side chain of a Cys residue coordinating to the metal. EE-QM/MM optimizations were performed with either a fixed protein or by relaxing all atoms within 6 Å of the QM system. The latter approach gave the best geometries, whereas, with the fixed protein, typically some of the ligands dissociated from the metal. However, quite unexpectedly, the calculations with the fixed protein gave the best correlation to the experimental data, whereas those with an optimized protein gave no correlation ($R^2 = 0.58$ and 0.08 , respectively). In both cases, the correlation was improved by considering only the QM energy ($R^2 = 0.80$ and 0.19), showing that the problem comes from varying conformations of the surrounding protein.

Kovalenko and co-workers have studied the binding of biotin to streptavidin.²²³ They optimized geometries with HF/STO-3G for a 274-atom model involving the ligand and all residues within 3 Å. They calculated interaction energies with 16 different QM methods and 11 different basis sets, using the same QM system. Solvation effects were calculated for the isolated QM system with

Table 3. Summary of QM/MM Studies^a

group	ref	year	method	QM syst	E	opt	structure	solvation	CP	ΔS	comments	receptor	no.	R^2
Finn	218	1997	SEQM	L								thermolysin	12	0.87
Clark	230	2003	AM1	L	EE	yes	docked	$\epsilon = 4$				5 proteins	9	
Hillier	221	2003	B3LYP/6-31G**//HF/3-211W	L + 2 aa + 1W		yes						adenosine deaminase	5	0.87
Gao	219	2004	AM1	L			QM/MM MD					HIV-PT	3	
Hannongbua	228	2005	H: B3LYP/6-31G* M: PM6	L + 2 aa M: 5 Å								HIV-PT	2	
Hannongbua	229	2007	H: B3LYP/6-31G* M: PM6	L + 6 aa M: 5 Å			averaged MD					HIV-PT	3	
Wong	241	2007	DFT/SVP	L		L		PB (QM) + SASA				protein kinase	5	
Hillier	222	2008	MP2/aug-cc-pVDZ//BLYP-D2/TZV(2d2p)	L + 5 aa	ME	yes			yes			carbonic anhydrase	10	
Yang	224	2008	B3LYP/LANL2DZ	L + 1 aa + 1W	EE							CDK2	8	0.17
Yang	232	2008	B3LYP/6-31G*	L	ME	yes	docked	$\epsilon = 4r$				NSSB polymerase	20	
Yang	220	2009	AM1	L + n aa			built	parametrized SASA				HLA-A*0201	50	0.56
Shang	227	2009	mPWLYP/6-31G*	L + n aa		yes						3 proteins	3	0.90
Kovalenko	223	2009	B3LYP/6-31G**//HF/STO-3G	L + 3 Å		yes		PCM (QM)		NMA QM		streptavidin	1	
Gleeson	234	2009	B3LYP/6-31G**	L + 3 aa			docked					6 kinases	9	
Cho	236	2009	B3LYP/6-31G**	L + n aa		L	docked				max five steps of geo optimization	44 proteins	44	
Merz	245	2010	AM1	L + 5 Å		yes		PB + SASA		NMA QM		carbonic anhydrase	18	0.56
Ryde	195	2011	TPSS/def2-SVP(p)	L + 1 aa	EE	yes						carboxypeptidase	5	
Burger	233	2011	B3LYP/6-31G*	L	ME	yes	docked	L PCM		NMA QM		cathepsin B	6	0.58
Yang	237	2011	AM1	L + 6 aa	ME	MM	crystal	PB + SASA		rotatable bonds	max 20 iterations, electrostatics damped by $\epsilon = r$	cytochrome c peroxidase	60	0.50
Yang	238	2011	AM1	L + 4 aa	ME	yes	crystal	PB + SASA		rotamers		OppA	28	0.42
Liu	239	2012	AM1	L + 4 Å		yes		PB + SASA				PDZ3	30	0.30
Liu	240	2012	MP2/6-31G**	L + 4 Å		yes		PB + SASA			strain B3LYP/6-31G**/PCM	15 proteins	15	0.59
Chuman	226	2012	HF/6-31G*	L + 10 aa	EE	ME	MD	PB + SASA			two-param fit	8 proteins	20	0.68
Hobza	247	2013	TPSS-D3/TZVP//BLYP-D3/SVP	L + 4 aa	ME	L + 8 Å	average crystal or docked	GB, L SMD		rotatable bonds	L desolv and def	CDK2	31	0.64
Hobza	249	2013	PM6-D3H4X TPSS-D3/TZVP//BLYP-D3/SVP	+ 8 Å L + 4 Å		L + 8 Å	crystal	GB, L SMD			L desolv and def	aldolase reductase	7	0.59
Röhning	231	2014	PM6-D3H4X SCC-DFTB	+ 8 Å L + Zn + ligs		QM	docked	FACTS				Zn proteins	226	
Singh	225	2014	B3LYP/LACVP**	L + 6 aa								CDK2	29	0.78

Table 3. continued

group	ref	year	method	QM syst	E	opt	structure	solvation	CP	ΔS	comments	receptor	no.	R^2
Lu	242	2014	mPWLYP/6-31+G	L + 1 aa				PB + SASA				EGFR	426	0.48
Tan	243	2014	B3LYP/6-31G**	L + a few aa		AM1/ L + 4 Å		PB + SASA				thymidine kinase	18	0.44
Zhang	244	2014	PW91/DNP	L + 9 aa		yes	MD average	PB + SASA				MMP 9	5	0.96
Hobza	250	2015	TPSS-D3/TZVP//BLYP-D3/ SVP PM6-D3H4X	L + 4 Å + 8 Å		L + 8 Å	crystal	GB, L SMD			L desolv and def	aldolase reductase	3	0.87

^aThe table lists the research group, the reference, the publication year, the QM method used (if two methods are given, the first is for energies and the second, after //, was used for geometries), the size of the QM system (L = ligand, W = water, aa = amino acids, ligs = ligands, H = high-level system and M = medium-level system for three-level ONIOM calculations, and Å gives the maximum distance to the ligand), the QM/MM embedding scheme, if and how the system was optimized, structures used for the calculations, the solvation method used (expl = explicit water molecules), whether CP corrections were included, the method used to obtain entropy estimates, possible comments, the receptor used, the number of systems studied, and the obtained correlation coefficient.

PCM, and entropy and thermal effects were estimated from the harmonic frequencies at the HF/STO-3G level of theory. In most calculations, both the QM and MM systems were artificially neutralized. B3LYP/6-31G* was found to reproduce the experimental binding affinity best. Several other scientists have used similar methods to study ligand binding, e.g., to CDK2^{224,225} and MMP9,²²⁶ or to estimate the effect of fluorine substitution²²⁷ with varying success.

Hannongbua and co-workers used a more advanced approach in a study of the binding of saquinavir to the wild-type and a mutant HIV-1 protease.²²⁸ They used the three-layer ONIOM approach, using B3LYP/6-31G* for the ligand and the two active-site Asp groups, PM6 for 36 residues within 5 Å of the ligand, and the universal force field (UFF) for the remainder of the enzyme. They studied the protonation state of the two Asp residues, but failed to observe any significant difference in the ligand interaction energy between the wild-type and mutant enzymes. The studies were later extended to a double mutant and larger QM systems.²²⁹ Four extra residues were added to the DFT system in the three-layer ONIOM calculations, and all calculations were performed on averaged MD structures. The QM/MM calculations incorrectly indicated that the binding was stronger for the singly mutated enzyme. However, all calculations correctly indicated the double mutant has a much lower affinity, although the effect was grossly overestimated (e.g., 108 vs 15 kJ/mol).

An important use of QM/MM methods has been rescoring docked structures. Clark et al. described the first such approach in 2003.²³⁰ They performed QM/MM optimizations using AM1 only for the ligand. The QM–MM electrostatic interactions were scaled down by a dielectric constant of 4. The method worked well and allowed for some induced-fit effects in the otherwise rigid protein. They could also dock a ligand into two ligand-free crystal structures. However, no binding free energies were calculated.

Röhrig and co-workers also used a SEQM/MM approach for docking of Zn proteins.²³¹ They used SCC-DFTB for the ligand and the Zn ion and its first-sphere ligands. A total of 250 docking poses were optimized by 1000 iterations, keeping the MM system fixed. To the total QM/MM energy was added a polar solvation energy, based on the Mulliken charges of the QM system. The method was applied to 226 ligands bound directly to Zn in proteins, and it increased the successful docking from 62% to 77% (defined as an RMSD of less than 2 Å).

Other approaches have employed DFT methods. Yang et al. used B3LYP/6-31G* calculations for the ligand to rescore 20 docked poses of NSSB polymerase.²³² They used an ME-QM/MM scheme and scaled down the electrostatic interactions with a distance-dependent dielectric constant ($\epsilon = 4r$) to model solvation effects. They emphasized the importance of the internal energy of the ligand.

Burger et al. also used B3LYP/6-31G* only for the ligand.²³³ They first ran a short MD simulation on the five best docked poses, followed by a restricted QM/MM minimization (maximum of 20 iterations). Finally, the total QM/MM energy was supplemented by the desolvation energy of the ligand (calculated with B3LYP/6-31G* PCM). They damped the electrostatic interactions by a distance-dependent dielectric constant ($\epsilon = r$); i.e., the QM energy was calculated for a polarized wave function, but the electrostatic interactions were calculated by MM, using an ESP-charge model of the QM system (i.e., charges fitted to the QM electrostatic potential). The method was developed on a trypsin inhibitor and then applied for

17 decoys and 43 binders to cytochrome *c* peroxidase. It was shown that the approach performed significantly better than standard docking, giving an $R^2 = 0.50$ to the experimental data for the binding ligands.

Still other studies used DFT for the ligand and a few nearby residues: Gleeson and Gleeson used the B3LYP/6-31G** method for the ligand and the backbone of three amino acid residues when they rescored nine cross-docked protein–ligand complexes.²³⁴ They showed that they could identify the correct pose from a set of plausible decoys 77% of the time, which was appreciably better than for standard docking with the GOLD²³⁵ software (44%). HF/3-21G* and PM3 calculations gave somewhat worse results. Likewise, Cho and co-workers used B3LYP/6-31G** for the ligand and possibly a few protein residues.²³⁶ The 10 top-scoring docked poses were evaluated by QM/MM, and only the ligand was optimized by at most five steps. The pose with the lowest QM/MM energy was selected. The method performed better than standard docking for 44 tested systems, especially for those involving hydrophobic interactions. However, no attempt was made to compare the results with measured binding affinities.

Several groups have added PB + SASA continuum-solvation energy terms to the QM/MM energy, similarly to the MM/PBSA approach, but without the use of MD snapshots. Yang and co-workers studied the binding of 28 tripeptides to the OppA protein.²³⁷ They used ME-ONIOM with AM1 for the peptide and six selected protein residues interacting with the tripeptide. Single-point QM/MM energy calculations were performed on MM-minimized crystal structures. To the QM/MM interaction energy, they added a PB + SASA solvation energy. They obtained some correlation to the experimental data, $R^2 = 0.42$. In a subsequent study, they added an entropy term, estimated from the rotamers of the peptide side chains, compared to a library for the free peptides.²³⁸ They studied 30 penta- to heptapeptides binding to the PDZ3 domain. The peptides and four selected protein residues were treated by AM1. They obtained a weak correlation to the experimental binding affinities ($R^2 = 0.30$), which could be improved to 0.43 when a multiple linear fit to the QM/MM, PBSA, and entropy terms was performed.

Liu and co-workers have applied a similar approach to study the binding of 10 substrates to enzymes.²³⁹ They used AM1 for the substrate and all residues with a heavy atom within 4 Å, using the ONIOM QM/MM approach. To the total QM/MM interaction energy, they added a PB + SASA solvation energy. Only single QM/MM-optimized structures were employed. Still, they obtained a decent correlation to experimental binding free energies, $R^2 = 0.59$, but the RMS error was large, 19 kJ/mol. They emphasized the role of the strain energy in both the protein and the ligand. The latter was calculated at the B3LYP/6-31G**/PCM level of theory, after a conformational search. They also used a similar approach to study the binding of 20 drugs to a varied set of proteins.²⁴⁰ They compared the results of using four different QM methods, AM1, PM3, B3LYP/6-31G**, and MP2/6-31G**, as well as two different MM force fields, Amber or UFF. All methods gave some correlation to experimental data, $R^2 = 0.43$ – 0.68 (MP2 was best), but the RMS error was high, 24–41 kJ/mol (B3LYP was best). However, the error was quite systematic, so in the end they recommended the simpler and cheaper AM1/UFF approach.

However, most studies have been performed with DFT for the ligand and a few surrounding residues: Wang and Wong studied the binding of balanol and four derivatives to protein kinase A.²⁴¹ The PB solvation energy was solved self-consistently using the

QM density and the MM charges, rather than using the normal point-charge model of the QM system. They employed a single structure, in which only the ligand was optimized. The results were quite poor, and the best and worst binding ligands could be distinguished only if the protein dielectric constant was set to 1.5.

Lu et al. have employed a QM/MM method to study the binding of 6 EGFR inhibitors to 71 mutant enzymes.²⁴² They used the ONIOM approach on MM-minimized structures in a GB solvent, employing the mPWLYP/6-31+G* method for the ligand and the mutated residue. To this was added a PB + SASA solvation energy, obtained with restrained ESP (RESP) charges for the QM system. The QM and solvation methods were selected after a comparison with AM1, HF, and B3LYP calculations with the same basis set on a set of 20 known interaction energies. The selected method gave a correlation of $R^2 = 0.48$.

Tan et al. studied the binding of nine inhibitors to two virus thymidine kinases.²⁴³ They employed structures minimized by QM/MM with AM1 used for the ligand and all residues within 4 Å. Binding energies were calculated with B3LYP/6-31G** calculations for the ligand and a few key residues. To this were added PB and SASA energies, but no entropy term. This gave an appreciably better correlation to the experimental data than the pure QM/MM energies or MM/PBSA calculations ($R^2 = 0.44$, compared to 0.09 and 0.03). Zhang and co-workers used similar methods in a study of MMP-9.²⁴⁴ They performed docking, QM/MM minimization, MD simulations, MM/PBSA, and QM/MM-PBSA on the average structure from the MD simulations. They obtained a nearly perfect correlation to experimental EC₅₀ data, $R^2 = 0.96$, but much overestimated differences between the various ligands.

In 2010, Merz and co-workers suggested a QM/MM variant²⁴⁵ of their linear-scaling SEQM approach (QMScore).²⁴⁶ They studied 23 Zn proteins and included the ligand and all residues within 5 Å of the Zn ion in the QM system (150–311 atoms). The complexes were fully minimized in vacuum before the energy calculation. The SEQM calculations were performed at the AM1 level, and the solvation free energy was calculated in the SEQM/MM calculations with the PB method, also including an SASA term. The entropy was calculated by NMA of the QM system. They obtained an R^2 of 0.56 and a root mean square error of 9 kJ/mol. This could be slightly improved by using only the QM energy and not the full QM/MM energy ($R^2 = 0.64$). Omitting the minimization and calculating entropies instead from the number of fixed rotatable bonds (as in QMScore) gave results of a similar quality if only the QM energy was used, but much worse if the full QM/MM energy was used. In fact, this alternative entropy estimate also improved the correlation with minimization. Calculating the vibrational entropy only for the ligand gave the same results as if it was calculated for the whole QM system. The best result was only slightly worse than that obtained with SEQM calculations of the full protein ($R^2 = 0.69$) for the same systems.²⁴⁶

In 2013, Hobza and co-workers suggested another approach to calculate binding affinities,²⁴⁷ again as an extension of their approach involving all-protein linear-scaling SEQM methods.²⁴⁸ They used a three-layer ME-QM/SEQM/MM approach. For the residues within 4 Å of the ligand (~400 atoms), they employed a DFT-D3 method, BLYP-D3 for geometries and TPSS-D3/TZVP for energies. For residues within 8 Å of the ligand (~1000 atoms), they used the PM6-D3H4X method. For the remainder of the protein, MM was used together with a GB continuum solvent. Structures were optimized by QM/SEQM/MM

Table 4. Summary of Fragmentation Studies^a

group	ref	year	variant	QM method	frgm size	incl	opt	solvation	ΔS	comments	receptor	no.	R^2
Maseras	251	2001	PA	B3LYP/6-31+G	1 aa	8 aa					acetylcholine receptor	3	
Zhang	259	2003	MFCC	HF/3-21G	1 aa		MM				streptavidin	1	
Zhang	260	2004	MFCC	HF/3-21G	1 aa		partly rigid				trypsin	1	
Zhang	261	2004	MFCC	HF/3-21G	1 aa						adipocyte lipid binding protein, streptavidin	2	
Zhang	262	2005	MFCC	HF/3-21G	1 aa						HIV-pT	6	
Zhang	263	2005	MFCC	HF/3-21G, B3LYP/6-31G*, MP2/6-31G*	1 aa		rigid HF/3-21G				HIV-RT	4	
Kitaura	275	2005	FMO	HF/STO-3G	1 aa						estrogen receptor	11	0.70
Kitaura	277	2006	FMO	HF or MP2/6-31G*	1 aa						estrogen receptor	1	
Tanaka	281	2006	FMO	MP2/6-31G	1 aa						cAMP receptor protein	1	
Chuman	276	2006	FMO	HF/STO-3G	1 aa					visualize and cluster	estrogen receptor	31	
Hannongbua	229	2007	PA	B3LYP/6-31(+)/G**	1 aa	8 aa					HIV-1 protease	3	
Bettens	264	2007	SMF	MP2/6-311+G(2d,p)	1 aa		L B3LYP/6-31(+)/G**				neuraminidase	1	
Tanaka	280	2007	FMO	MP2/6-31G	1 aa						retinoid X receptor	1	
Kiso	284	2007	FMO	HF/STO-3G	1 aa						hemagglutinin	4	
Kitaura	285	2007	FMO	MP2/6-31G*	1 or 2 aa		L HF/3-21G	PB (MM) + SASA			FK506 binding protein	4	-0.33
Zhang	265	2008	MFCC	MP2/cc-pVTZ	1 aa		MD snapshots				p53-MDM2	3	
Ryde	112	2009	PMISP	HF and MP2/6-31G*	1 aa	4 Å					avidin	7	
Ryde	273	2009	PMISP	MP2/aug-cc-pVTZ	1 aa	all					avidin	2	
Cafilisch	255	2010	PA	PM6	1 aa	5 aa, 6 aa MM	some aa			dock + MM	tyrosine kinase	2.7M	
Yamada	278	2010	FMO	MP2/6-31G*	1 aa						vitamin D receptor	1	
Yamada	279	2010	FMO	MP2/6-31G*	1 aa						PPAR γ	2	
Kitaura	286	2010	FMO	MP2/6-31G*	2 aa		MM		MM NMA		hemagglutinin	4	
Vivas-Reyes	252	2011	PA	M06-2X/6-311G**	1 aa	24 aa		PCM			butyrylcholine esterase	14	
Nowosielski	254	2011	PA	CP-MP2/6-31G*	1 aa	5 Å		SASA		dock + MD + av	squalene epoxidase	1	
Merz	258	2011	PA	HF and M06-L/6-31G*, PM6-DH2	1 aa	18 aa					HIV-II protease	1	
Takano	282	2011	FMO	HF, MP2, MP3/6-31G	1 aa						hemagglutinin-antibody	1	
Mazanetz	287	2011	FMO	MP2/6-31G*	1 aa			PB + SASA (MM)	L rotatable bonds	fitted model	CDK2	26	0.94
Kurita	289	2011	FMO	MP2 and HF/6-31G	1 aa		MM	explicit	MM NMA		thermolysin	4	0.94
Kurita	292	2011	FMO	MP2/6-31G	1 aa		MM	explicit 5 Å			plasminogen activator receptor	2	
Caetano	266	2012	MFCC	LDA/DNP	1 aa	12 Å					HMGR	6	
Grimme	272	2012	MFCC	B97-D3/def2-TZVPP	1-17 aa		B97-D3/def2-TZVPP	COSMO			three proteins	3	
Kurita	290	2012	FMO	MP2 and HF/6-31G	1 aa		MM	S Å explicit			thermolysin	6	0.72
Kitaura	294	2012	FMO	B3LYP-D or MP2/6-31G*	10 aa		FMO (HF/6-31G*)	EFP			griffithsin	1	

Table 4. continued

group	ref	year	variant	QM method	frgm size	incl	opt	solvation	ΔS	comments	receptor	no.	R^2
Merz	296	2012	ONIOM/ FMO	MP2/CBS//FMO (MP2/6-31G)	1 aa						insulin	1	
Nowosielski	253	2013	PA	M06-2X/6-31G*	1 aa	5.5 Å				dock + MD + MM	pantothenate synthetase	3	0.91
Xu	256	2013	XO	ω B97X-D/6-311+G**/ PM6		300–400/ ~1100 atoms	ω B97X-D/6- 31G*/PM6	SMD (B3LYP/6- 31G*)	50% L NMA ω B97X-D/6- 31G*		CDK2PAK1	8020	0.86, 0.76
Caetano	267	2013	MFCC	PBE-TS/DNP	1 aa	10 Å					Glu receptor	4	
Caetano	268	2013	MFCC	PBE-D2/DNP	1 aa	8 Å		one explicit shell			tropocollagen	1	
Takano	283	2013	FMO	MP2/6-31G*	1 aa						antibody 2G12	1	
Kurita	295	2013	FMO	MP2/6-31G	1 aa		MD cluster	723 explicit water molecules			amyloid- β peptides	109	
Caetano	269	2014	MFCC	PWC/DNP	1 aa	8.5 Å		some explicit water molecules			inhA reductase	1	
Caetano	270	2014	MFCC	GGA-TS/DNP	1 aa	10 Å	QM/MM				dopamine D3R receptor	1	
Ryde	274	2014	PMISP	LCCSD(T)/CBS		whole host	TPSS/def2- SV(P)	COSMO-RS (MP2/cc- pVTZ)	MM NMA		octa-acid host	9	0.20
Takano	293	2014	FMO	MP2/6-31G*	1 aa			PCM or explicit	MM NMA		antibody 2G12	2	
Kurita	291	2014	FMO	MP2/6-31G	1 aa		MM	5 Å explicit			buthylcholinesterase	4	0.54
Kongsted	199	2014	FMO	MP2/6-31G*	1 aa		QM/MM	PCM		docked	HIV-1 RNase H	7	0.86
Caetano	271	2015	MFCC	PBE-D2/DNP	1 aa	12 Å		COSMO, $\epsilon = 40$			albumin	1	
Kosenkov	288	2015	FMO	MP2/6-31G**	1 aa			PCM	L QM NMA		G-quadruplex DNA	4	0.94

^aThe table lists the research group, the reference, the publication year, the fragmentation approach, the QM method used, the number of amino acids (aa) in each fragment, the part of the receptor included (Å gives the maximum distance to the ligand), the method used to optimize the geometry, the solvation method used, the method used to obtain the entropy, possible comments, the receptor used, the number of systems studied (M = million), and the obtained correlation coefficient (a negative sign denotes anti-correlation.)

calculations with the MM system fixed. To the QM/MM interaction energy and MM GB solvation energy was added a more accurate ligand solvation energy (calculated with SMD at the HF/6-31G* level), as well as deformation energies of the protein and the ligand (calculated at the QM/QM/MM and HF/6-31G* levels, respectively) and an entropy estimate from the number of rotatable bonds in the ligand that are restricted in the protein. With this approach they studied 31 inhibitors of CDK2. If the calculations were performed on a manually modified crystal structure (of one of the inhibitors), a good correlation with experimental results was obtained ($R^2 = 0.64$). However, if docked structures were used instead, the results were poor. This was attributed to a high sensitivity of the SEQM and DFT-D calculations to the structural details. A similar approach was also used to study the importance of a halogen bond for the binding of eight inhibitors of aldose reductase.^{249,250}

In conclusion, a great variety of QM/MM methods have been used to study ligand binding. In general, quite small QM systems have been used, and most have been studied by SEQM or DFT methods. The basis sets have in general been small, and only a few studies have employed CP corrections or entropies. The recent approaches by Merz²⁴⁵ and Hobza²⁴⁷ stand out as the most serious attempt to obtain accurate energies, involving all important components, but no method has found any general use. The prime use of QM/MM calculations has instead been to describe the binding of the ligands and to pinpoint important interactions with the receptor.

3.4. Fragmentation Calculations

Many groups have employed different QM fragmentation approaches to estimate binding affinities and to point out important interactions in the binding. The studies are summarized in Table 4, and a schematic view of various fragmentation approaches is shown in Figure 2. In the simplest variant, pairwise interactions between the ligand and various groups of the receptor are calculated without any strict aim of getting correct total binding energies or avoiding double counting, and they will be called pairwise-additive (PA) approaches. More common is the use of the strict MFCC and FMO approaches, which try to approximate total binding energies and total energies, respectively.

3.4.1. PA and Similar Approaches. In 2001, Maseras and co-workers used a simple fragmentation approach to study the binding of three molecules to the acetylcholine receptor.²⁵¹ After some testing on a small model system, they selected B3LYP/6-31+G as their theoretical method. Each ligand was divided into two fragments, and their pairwise interaction energies with 5 + 3 minimal amino acid models were calculated. Structures were taken from the end of MD simulations at the MM level. The total interaction energies (sum of all pairwise terms) gave a correct ordering of the three ligands, but they were much too large, owing to the missing solvation energy and entropy. For one of the ligands, a full geometry optimization of each pair was also tested, but the residue models then ended up in overlapping positions.

Hannongbua and co-workers also used B3LYP/6-31(+)G** with up to eight residues in the QM system when they compared the binding of saquinavir to the wild-type and two mutant HIV-1 proteases.²²⁹ The various QM models gave varying (by 28 kJ/mol) and inconclusive results for the single mutant. However, all calculations correctly indicated that the double mutant had the lowest affinity. Likewise, Vivas-Reyes et al. studied the binding of 14 ligands to BACE using fragmentation methods.²⁵² They

included 24 residues within 5 Å of the center of the ligand at the PM6 level to study the protonation state of the active site. Then binding energies were calculated by PA fragment calculations at the M06-2X/6-311G** level of theory. No comparison with experimental data was attempted.

Nowosielski and co-workers have developed an automatic tool to study protein–ligand complexes.²⁵³ It involves docking, MD simulations (at the MM level), averaging and minimization of the MD snapshots, and PA QM calculations for all ligand–amino acid pairs within a specified distance (possibly mediated by water molecules). As an application, they studied the binding of three sulfonamide ligands to pantothenate synthetase. Using M06-2X/6-31G* calculations for all residues within 5.5 Å of the ligand, they obtained a good correlation with experimental data ($R^2 = 0.91$). However, the interaction energies were 10 times larger than the experimental binding free energies. In another study of the binding of terbinafine to squalene epoxidase, they instead used MP2/6-31G* calculations with CP correction for all residues within 5 Å of the ligand.²⁵⁴

Cafilisch and Zhou suggested an interesting QM approach to high-throughput virtual screening.²⁵⁵ They described the binding site by a few probes, represented by very small molecular fragments (2–10 atoms): They represented the polar group in the protein by minimal models of amino acid side chains, but water and HF were used for the amide CO and NH groups, respectively. The ligands were first docked into the protein and then minimized by MM. Finally, interaction energies with each of the QM probes were calculated, first without minimization and then by optimizing a few atoms in some of the functional groups. They used the PM6 method and added the MM van der Waals interaction energy between the molecule and six residues in the binding site. They screened 2.7 million ligands for the binding to a tyrosine kinase, employing 50 docked poses per ligand on average, and using five probes, representing one side chain and four backbone groups. Moreover, a shape Tanimoto score was calculated after minimization of the free ligand with RM1. Twenty-three ligands were selected from the screening, and three of them were found to bind with an IC_{50} of 5–18 μ M.

Xu and co-workers have developed a QM scoring function based on QM fragmentation calculations.²⁵⁶ The protein was neutralized and divided into high- and low-level regions with 300–380 and 1000–1100 atoms, on the basis of the distance to the ligand. The high-level region was optimized by the extended ONIOM QM/QM fragmentation approach,²⁵⁷ using ω B97X-D/6-31G* and PM6 calculations for the two regions. Single-point energies were then calculated after water molecules were stripped off with ω B97X-D or XYG3 using the 6-311+G** basis set. To these interaction energies were added solvation energies calculated with SMD at the B3LYP/6-31G* level, as well as an entropic penalty consisting of 50% of the entropy of the free ligand, calculated from ω B97X-D/6-31G* frequencies. The method was tested on the binding of 80 inhibitors of CDK2 and 20 organometallic PAK1 inhibitors. For both systems, they obtained good correlation to experimental data, $R^2 = 0.76$ –0.88.

Merz and co-workers have examined the accuracy and convergence of a PA fragmentation approach for the calculation of the interaction energy between indinavir and HIV protease.²⁵⁸ With a ~300-atom model of the binding site, they compared full and fragmentation energies obtained with the ligand and 18 fragments (minimal models of amino acid side chains or backbones, in a few cases joined to avoid overlapping atoms). The fragmentation calculations were performed with dimers, trimers, tetramers, and pentamers and at three levels of theory,

HF/6-31G*, M06-L/6-31G*, and PM6-DH2. Unfortunately, the results depended strongly on the level of theory. With dimers, the error was 1–14 kJ/mol. The three-body terms were 8–19 kJ/mol, and for HF and PM6, the error was decreased to 3–4 kJ/mol. However, for M06-L, the error instead increased to 18 kJ/mol. Four- and five-body terms were calculated only with PM6-DH2 (for which the three-body term was smallest) and amounted to 3.2 and 0.3 kJ/mol.

3.4.2. MFCC and Similar Approaches. The MFCC method was developed in 2003 by Zhang and co-workers with the aim of calculating ligand-binding affinities.^{109,111} In variance with the calculations in the previous section, it includes the whole protein in the calculations, systematically dividing it into overlapping fragments and correcting for double counting by subtracting the energy of the joined capping fragments (Figure 1). In the first application, they studied the binding of biotin to streptavidin.²⁵⁹ They employed the HF/3-21G method and included one capped amino acid in each fragment. They studied the crystal structure and an MM-optimized structure. The MFCC energies were found to be ~125 kJ/mol larger than the MM binding energies, probably an effect of the small basis set, partly counteracted by the missing dispersion interactions. Similar results were obtained for the binding of benzamidine to trypsin, but in that study, they also showed that the total binding energy can be decomposed into residue contributions.²⁶⁰ In the next application, they performed a rigid geometry optimization of the protein–ligand complex for two proteins, still at the HF/3-21G level of theory.²⁶¹ In a later study of HIV-1 protease at the same level of theory, the ligand was also divided into five fragments, providing an even more detailed partitioning of the binding energy.²⁶² For the interaction of efavirenz with HIV-1 reverse transcriptase, they first calculated all residue interaction energies with HF/3-21G and then recalculated the larger terms with B3LYP/6-31G* and MP2/6-31G*.²⁶³ Similar methods were used to study several other systems,¹¹¹ but no attempt was made to quantitatively compare the results to experimental binding affinities (and such a comparison would give quite poor results owing to the small basis sets used, as well as the missing dispersion, solvation, and entropy effects).

Bettens and Lee used a similar approach to calculate the interaction energy for the binding of an inhibitor to neuraminidase.²⁶⁴ The calculations were performed at the MP2/6-311+G(2d,p) level of theory, thereby representing the first attempt to calculate binding energies at a level of theory for which there starts to be a hope to cover all important interactions in a nearly converged manner (the previous studies are substantially affected by BSSE and missing dispersion interaction). They showed that the vast majority of the QM pair calculations could be avoided by a prescreening of the electrostatic, induction, and dispersion interactions at the MM level. The year after, Zhang and co-workers employed MP2/cc-pVDZ calculations with middle-bond functions (and also some MP2/cc-pVTZ calculations) to study the interaction between p53 and the oncoprotein MDM2.²⁶⁵ They employed three snapshots from MD simulations (those with the strongest interaction energy). On the basis of MM interaction energies, they selected only the strongest interactions, which were recalculated by MFCC.

In a series of papers, Caetano and co-workers used the MFCC approach to calculate binding affinities and residue contributions for a number of different systems.^{266–271} They used crystal structures and standard MFCC calculations with one amino acid per fragment, although they sometimes tried two-residue

fragments. They employed a variety of DFT methods, often with dispersion corrections, and a numerical DNP basis set. In variance with other MFCC calculations, they only included parts of the protein in the calculations, determined by the distance from the ligand, 8–12 Å depending on the protein. The first studies were performed in vacuum, whereas later studies included some explicit water molecules and the latest a COSMO continuum solvent with a dielectric constant of 40. The latter strongly stabilized the convergence of the energies with respect to the cutoff radius. For example, the change between 11 and 12 Å was 8 kJ/mol in the COSMO solvent, but ~160 kJ/mol in vacuum.²⁷¹ They mainly discussed which amino acids interact strongly with the ligand, but they did not compare estimated absolute binding affinities to experimental data, which would be hard because entropy estimates are missing.

In 2012, Antony and Grimme used MFCC to estimate the binding affinity for three protein–ligand complexes with 1060–3680 atoms.²⁷² They used the B97-D3/def2-TZVPP method. The calculations were performed on crystal structures with added hydrogen atoms optimized by SEQM. They did not include any explicit water molecules. Two sets of calculations were performed, one with all amino acids neutralized and one with the standard protonation state of amino acids. They studied how the energies varied with the size of the fragments, including 1–17 residues in each. With neutralized side chains, the net MFCC binding energy varied by 10–13 kJ/mol depending on the number of residues in each fragment. A total of 3–11 residues per fragment gave the fastest calculations, depending on the protein, and they recommended 5 or 6 in routine applications. The three-body term, which normally is not estimated by MFCC, amounted to 21–23 kJ/mol. Calculations on different subunits of one of the proteins gave energies that differed by 70–77 kJ/mol, illustrating the large problem of single-structure approaches. The CP correction amounted to 23 kJ/mol, and increasing the basis set to def2-QZVP changed the interaction energy by 17 kJ/mol.

With charged residues, the MFCC results depended much more on the number of residues per fragment, viz., by 73–127 kJ/mol. Moreover, severe convergence problems in the QM energy calculations are observed. Fortunately, these problems could be reduced by running the calculations in a COSMO continuum solvent with a dielectric constant of 4, giving a variation of only 8–14 kJ/mol and no convergence problems.

For the smallest protein with neutral residues, they estimated the accuracy of the MFCC calculation by comparing B97-D3/def2-SVP interaction energies obtained with and without MFCC fragmentation. The error of the MFCC calculations decreased from 22 kJ/mol with 1-residue fragments to less than 1 kJ/mol for fragments with 29 residues (i.e., only two fragments). However, it was still 14 kJ/mol with 15-residue fragments. The three-body MFCC energies converged faster, with errors of 14, 4, and 0 kJ/mol for fragments of 2, 8, and 15 residues, respectively. This investigation nicely sets the frame of future DFT-D calculations of binding affinities, showing the severe challenges posed by the use of single structures, fragmentation approaches, and the BSSE.

We have developed the PMISP approach to calculate accurate binding affinities at a high level of QM theory.¹¹² It involved MFCC calculations for the ligand and all chemical groups within 4 Å. In addition, many-body effects were estimated by MM calculations with an unusually detailed force field, including anisotropic polarizabilities and multipoles up to quadrupoles for all atoms and bond centers. These polarizabilities and multipoles

were obtained from QM calculations of capped amino acids in an MFCC manner. Thus, the approach can also be considered as a very accurate MM force field, in which the closest interactions between the ligand and the protein are treated by QM fragment calculations (to accurately model exchange repulsion, charge transfer, charge penetration, and other short-range effects).

The approach was first calibrated on a 247-atom model of the avidin binding site with seven different biotin analogues, for which the full HF and MP2/6-31G* energies can be calculated. The model consisted of 14 protein fragments, 1 of which contained the backbone of six residues. Test calculations showed that dividing the latter fragment into five changed the energy by less than 1 kJ/mol, illustrating the accuracy of the MFCC approach. Likewise, the total PMISP energy reproduced the true QM energy within 2 kJ/mol for neutral ligands at the HF level. However, for ligands with a net negative charge, the error was larger, 10 ± 3 kJ/mol (using different geometries). The results were similar at the MP2 level, 5 and 9 ± 3 kJ/mol, respectively. This means that if you can afford to calculate the full HF energy, the PMISP MP2 energy could be corrected for the error at the HF level, giving accuracies of 4 and 1 ± 1 kJ/mol. Another way to reduce the error (to 6 and 2 ± 3 kJ/mol) was to embed all QM calculations in the surrounding polarized multipoles. Comparison with other fragmentation methods showed that PMISP performed better than the PA, EE-PA, and even FMO2 approaches, even if the latter is theoretically more stringent. The error comes almost entirely from three-body terms; both FMO3 and PMISP3 gave errors of less than 1 kJ/mol. It comes from the coupling of polarization and exchange repulsion, and it shows that any polarizable MM methods can be expected to give errors of ~ 10 kJ/mol owing to the omission of three-body effects.

In a subsequent paper, the PMISP model of the binding site was supplemented by the same polarizable multipole model for the whole protein, as well as a standard MM Lennard-Jones model, in a QM/MM manner.²⁷³ It was shown that octupoles had a small effect on the binding energies, whereas quadrupoles and polarizabilities were important. On the other hand, the multipoles and polarizabilities could be calculated with DFT, rather than MP2, calculations, without any loss in accuracy. The distance dependence of the various terms was also estimated. PMISP models of different sizes (up to 7 Å from the ligand) were tested, and it was shown that the binding energy changed by only 0.1 kJ/mol between 6 and 7 Å for neutral ligands, but by 2 kJ/mol for the charged ligand. At the end, interaction energies for biotin and one analogue were calculated at the MP2/aug-cc-pVTZ level of theory.

We have also used the PMISP approach to study the binding of nine carboxylate ligands to the octa-acid host at the LCCSD(T0) level (198–207 atoms).^{216,274} The complicated macrocyclic host molecule was divided into 24 fragments, but test calculations showed that we still could keep the error from the fragmentation below 10 kJ/mol, after an improvement in the treatment of intramolecular polarization. The LCCSD(T0) calculations were performed with the cc-pVTZ basis set, and the energies were extrapolated to a complete basis set employing canonical MP2 calculations with the aug-cc-pVTZ and aug-cc-pVQZ basis sets. These energies were supplemented by COSMO-RS solvation energies (LMP2/cc-pVDZ), the zero-point energy, and entropic and thermal corrections from MM calculations. Unfortunately, the final binding free energies reproduced the experimental data quite poorly, with $R^2 = 0.2$ and an MAD of 12 kJ/mol, even after the removal of the systematic overbinding by 31 kJ/mol. This problem was assigned to the use of single optimized structures.

3.4.3. FMO. Numerous applications of the FMO fragmentation approach to study the binding of small ligands to biomacromolecules have been published.^{103,104} However, most of them are based on similar methods and discuss mainly the geometry of RL complex and specific interactions between the ligand and the receptor. Therefore, we restrict the discussion to some typical cases. In the first FMO study of binding affinities, Kitaura and co-workers considered the binding of 11 steroid ligands to the estrogen receptor.²⁷⁵ They used the HF/STO-3G approach on a 50-residue model of the binding site. For four ligands, the whole ligand-binding domain (241 residues) was also tested, giving no significant difference in the binding affinities. In spite of the low level of theory and the missing dispersion, solvation, and entropy effects, good correlation with experimental data was obtained, $R^2 = 0.70$. They observed significant charge transfer between the protein and the ligand. Chuman et al. used the same method, but also developed a method to visualize ligand–residue interactions for different ligands and cluster the results.²⁷⁶

However, the great majority of the FMO studies have been performed with MP2 and the 6-31G basis set with or without polarization functions, e.g., for the estrogen receptor,²⁷⁷ vitamin D receptor,²⁷⁸ PPAGγ,²⁷⁹ retinoid X receptor,²⁸⁰ and even a DNA fragment binding to the cAMP receptor protein.²⁸¹ In the latter, the interactions differed significantly between FMO and MM, owing to charge transfer from the DNA to the receptor and polarization effects, modifying the relative strengths of the base pairing and stacking within the DNA before and after the binding. In a later study, Tanaka and co-workers employed even MP3/6-31G to study the binding of hemagglutinin to an antibody.²⁸² In another investigation, they studied the variation of the energies over 10 snapshots from a 10 ns MD simulation, showing fluctuations of over 200 kJ/mol in the total energy.²⁸³ Another study showed 220 kJ/mol differences between calculations involving only the binding domain of hemagglutinin and the entire protein.²⁸⁴

In a study of the binding of four ligands to the FK506 binding protein, Kitaura et al. used appreciably improved methods.²⁸⁵ The geometry of the ligand was optimized by HF/3-21G for a model involving protein residues within 5.5 Å. Then the energy was calculated at the MP2/6-31G* level of theory, including two residues in each fragment. Moreover, solvent effects were calculated by the PB method at the MM level, and an SASA term was also included. However, a negative correlation with experimental values was found. Quite large differences were found between calculations involving one- or two-residue fragments, up to 20 kJ/mol in the total interaction energies. They also showed that the correlation energy dominated the binding energy. In a subsequent study, they used instead a PCM model for the implicit solvation (including both polar and nonpolar terms) and an entropy term, calculated at the MM level.²⁸⁶ With this approach, they could rationalize the binding of human and avian influenza A virus hemagglutinin to α -sialosides. Likewise, Kongsted and co-workers obtained a good correlation with experiment ($R^2 = 0.86$) for seven ligands binding to HIV-1 RNase using a C-PCM solvent model and QM/MM structures.¹⁹⁹ However, the differences in binding energies were grossly overestimated (39–53 times larger than the experimental range).

Mazanetz et al. studied the binding of 28 inhibitors to CDK2 and showed that the pure FMO energy gave mediocre correlation to the experimental data ($R^2 = 0.68$).²⁸⁷ However, when enhanced with PB + SASA solvation (calculated at the MM

Table 5. Summary of Linear-Scaling Studies^a

group	ref	year	method	opt	solvation	disp	ΔS	comments	receptor	no.	R^2
Bliznyuk	297	2004	AM1	120–180 atm	COSMO				33-residue RNA aptamer trypsin	66	0.38
Pichierri	298	2004	AM1, PM3, PM5		COSMO				Lck kinase		
Merz	246	2004	AM1		PB + SASA	LJ	rotatable bonds		carbonic anhydrase	185	0.69
Merz	308	2005	AM1, PM3	no or MM	PB + SASA	LJ	rotatable bonds		carboxypeptidase	165	0.48
Sakurai	299	2005	AM1		COSMO + SASA		MM NMA		antibody	2	
Cadisch	302	2008	RM1 + MM-disp	all	PB (MM)				West Nile virusHIV-1 proteaseCDK2	442473	
Anikin	303	2008	AM1, PM3	L					FKB	1783	
Monard	305	2009	PM3	docking					urate oxidase	2	
Reynolds	300	2009	PM5		COSMO + SASA				stromelysin	6	0.93
Hobza	248	2010	PM6-DH2	all	COSMO, SMD(L)	DH2	MM NMA	R and L def energy	HIV-PT	22	0.62
Hobza	311	2011	PM6-DH2	all	COSMO, SMD(L)	DH2	MM NMA	L def energy	CDK2	15	0.52
Hobza	312	2011	PM6-DH2X//PM6-DH2	all	COSMO, C-PCM(L)	DH2	MM NMA	L def energy	casein kinase 2	25	0.24
Kolinsky	301	2012	PM6-DH2	all	COSMO	DH2	MM NMA	P and L def energy	VDR receptor	4	
Merz	310	2012	PM6-DH2		COSMO or PBSA		MM NMA		trypsin	40	0.06
Hobza	313	2013	TPSS-D3/TZVPP//BLYP-D2/SVP (L+3aa)/PM6-D3H4X	L+8 Å	COSMO, SMD(L)	D3H4X	rotatable bonds	L def energy	cathepsin B1	20	0.47
Miyazaki	318	2013	PBE/DZP	MM					FK506 binding protein	3	0.99

^aThe table lists the research group, the reference, the publication year, the QM method used (if two methods are given, the first is for energies and the second was used for geometries), atoms that were optimized (atm = atoms, L = ligand, Å gives the maximum distance to the ligand), the solvation method used, the method used to treat dispersion effects, the method used to obtain the entropy, possible comments, the receptor used, the number of systems studied, and the obtained correlation coefficient. The calculations always involved the full receptor–ligand complex.

level) and an entropy term from the number of rotatable bonds in the ligand, the fitted scoring function gave a much better correlation ($R^2 = 0.94$). Likewise, Kosenkov and co-workers obtained an excellent correlation with experiment ($R^2 = 0.94$) when employing a PCM solvation model and ligand entropies from M06-2X/6-31G* frequency calculations.²⁸⁸

Several other FMO studies have instead considered explicit water. For example, Kurita and co-workers have studied the binding of four inhibitory dipeptides to thermolysin.²⁸⁹ They used the MP2/6-31G method for the ligand, the catalytic Zn ion, and all protein residues and water molecules within 5 Å, whereas the remainder of the enzyme, as well as a 2 Å solvation shell, was treated at the HF/6-31G level of theory. Calculations were performed on structures from an MD simulation after clustering, minimization, and selection of the lowest energy structure. Thus, the complex was explicitly solvated, but not the free ligand. They added an entropy estimate, obtained from MM frequencies. They obtained a good correlation to the experimental data ($R^2 = 0.94$), but the absolute affinities were ~20 times larger than the experimental ones. In a later study of six inhibitors binding to the same enzyme, they obtained a somewhat poorer correlation ($R^2 = 0.72$, without entropy correction),²⁹⁰ and the correlation was even worse for the binding of four ligands to butylcholinesterase (still without any entropy correction), $R^2 = 0.54$.²⁹¹ Explicit water molecules have also been included in studies of the plasminogen activator²⁹² and the 2G12 antibody.²⁹³ They often gave unrealistically large absolute binding energies, because fixed water molecules underestimate the electrostatic screening.

Another way to include solvation is to use the EFP force field (which is polarizable and contains many nonstandard terms).²⁹⁴ This was tested for the binding of a carbohydrate to griffithsin, analyzing contributions to the interaction energy from individual fragments and their corresponding solvation effects. Unfortunately, the errors in the total energy (compared to full FMO calculations) were quite extensive, from 16 kJ/mol for MP2/6-31G* to 72 kJ/mol for B3LYP-D/6-31G*.

Total FMO energies have been used to decide the best structure of ligands bound to amyloid- β peptides, obtained from a cluster analysis of MD snapshots, i.e., as a simple docking approach.²⁹⁵ The calculations employed the MP2/6-31G method with explicit water molecules. The energies showed very large variations (by up to 3000 kJ/mol), indicating that they will depend more on the inconsistency between the MM and QM potential surface than on the actual interactions between the receptor and the ligand.

Merz and co-workers have developed the overlapping-multicenter ONIOM/FMO method to calculate accurate interaction energies.²⁹⁶ The high-level layer consisted of several overlapping QM calculations at the CCSD(T) or MP2 level, extrapolated to a complete basis set, whereas FMO calculations were employed for the low-level layer to estimate many-body effects. The approach was used to calculate the vacuum interaction energy of the insulin dimer with 4'-hydroxyacetanilide at the MP2/CBS level.

In conclusion, fragmentation methods have been much used to rationalize observed binding affinities. By their construction, they directly give contributions from each amino acid residue to the binding energy. Interestingly, FMO calculations have mainly employed the MP2 method, in variance to the great majority of the other approaches reviewed in this article, which have used SEQM, HF, or DFT. On the other hand, all FMO calculations and most MFCC calculations use much too small basis sets to give any reliable absolute affinities. It is a serious drawback of

FMO that it cannot use large and diffuse basis sets. Therefore, methods based on MFCC, but designed to include many-body effects, such as PMISP, seem to be more promising approaches for ligand binding, especially when combined with proper solvation, entropy estimates, and possibly sampling (see below). On the other hand, it is not certain whether fragmentation approaches really are needed except perhaps for CCSD(T) calculations, considering that DFT-D approaches give accurate results and can be employed for quite large systems.

3.5. Linear-Scaling Calculations

At the next level of theory, the whole receptor–ligand complex is included in the calculation, using various linear-scaling approaches. As can be seen in Table 5, all such calculations have been performed at the SEQM level with one single exception. In 2004, Vasilyev and Bliznyuk published an SEQM study of six ligands binding to a 33-residue RNA aptamer and six ligands binding to trypsin, involving QM systems of 1118 and 3720 atoms.²⁹⁷ They employed the AM1 method with the linear-scaling MOZYME approach. The structures were partly optimized (120–180 atoms) in the gas phase, before binding energies were calculated with a COSMO continuum-solvation model. For the aptamer, with neutral ligands, the COSMO calculations gave poor results, whereas the gas-phase calculations gave a reasonable correlation ($R^2 = 0.56$). However, for trypsin (with ligands of varying charges), only COSMO gave any correlation ($R^2 = 0.38$). For all complexes, the COSMO binding energies were positive. No attempt was made to predict the entropies, but the results were compared to binding free energies.

Similar studies with MOZYME and COSMO solvation have been performed by several other groups at the AM1, PM3, PM5, and PM6 levels of theory.^{298–301} Two of them added a nonpolar SASA term,^{299,300} two an entropy correction obtained at the MM level,^{299,301} and the latest study also a DH2 dispersion correction.³⁰¹ They typically gave too strong interactions and overestimated the difference between different ligands.

In 2008, Caflisch and co-workers developed a LIE-like approach.³⁰² It was based on their continuum-solvation LIE approach with minimized structures (i.e., without sampling).¹⁶⁵ The approach was tested for three proteins, 44, 24, and 73 inhibitors of West Nile virus BS3 protease, HIV-1 protease, and CDK2, respectively. The structures were first minimized with MM in vacuum. Then single-point SEQM energies with the RM1 method were calculated for the entire protein–ligand complex. To this energy were added an MM van der Waals interaction energy and a continuum-electrostatic PB solvation energy, both calculated at the MM level. For all proteins, the QM term gave similar or slightly improved results compared to an MM electrostatic term, e.g., decreasing the RMSD from 4 to 3 kJ/mol for the BS3 protease. However, different terms were fitted for each of the three proteins, and the fitted parameters were not transferable between the various proteins.

Anikin et al. have suggested a method to rescore many docked structures, speeding up the calculations by taking advantage of the fact that many ligands are docked to the same rigid part of the protein.³⁰³ They employed the AM1 and PM3 methods and showed that the method works well, but did not compare the results to experimental data. With this approach the binding energy of each protein–ligand complex could be obtained in 5 min. Further developments of the approach reduced the time to 15 s per ligand for a rigid docking and 153 s for flexible docking.³⁰⁴

Likewise, Thiriot and Monard have developed a combination of a genetic algorithm and linear-scaling SEQM calculations to perform a full SEQM docking procedure.³⁰⁵ The method was tested for the docking of two molecules into a 700-atom model of urate oxidase, closely reproducing the corresponding crystal structures using the PM3 method. This approach was later improved and integrated with MOPAC.³⁰⁶

However, the most serious approaches to calculated binding affinities with linear-scaling SEQM methods have been developed by the Merz and Hobza groups. Already in 2004, Raha and Merz developed a linear-scaling all-protein SEQM method to score inhibitors binding to a protein.²⁴⁶ They studied 18 + 5 inhibitors binding to the zinc ion in carbonic anhydrase or carboxypeptidase. The calculations were based on crystal structures, which were minimized by MM. The binding affinity was estimated by the AM1 method for the entire protein–ligand complex in a PB continuum solvent. Dispersive interactions were taken from the attractive Lennard-Jones part of the Amber FF96 calculation, and the entropy was estimated from the buried surface area and the number of degrees of freedom lost from the ligand and the protein side chains upon ligand binding. They obtained a correlation of $R^2 = 0.69$ compared to the experimental data. They also showed that the SEQM energy could be decomposed, allowing for a discussion of the importance of specific protein residues or parts of the ligand for the observed affinity.³⁰⁷

This approach was later applied in a large-scale test of scoring functions.³⁰⁸ Both the AM1 and PM3 methods were employed, and the method was tested on 165 complexes, giving an R^2 of 0.48. It could be increased to 0.55 by fitting a coefficient before each term in the binding energy (SEQM, solvation, dispersion, SASA, entropy), giving the QMScore. The results were not significantly improved if the complexes were fully optimized with MM before the calculations. The method has also been used for a set of protein kinase inhibitors, identifying the most important residues for binding by a pairwise decomposition scheme.³⁰⁹

This approach was used to estimate the binding free energy of 34 fragment-like ligands of trypsin (17 binders and 17 nonbinders) in the SAMPL3 blind-test competition.³¹⁰ Energies were calculated with the PM6-DH2 method on docked structures, but were corrected for systematic errors from error distributions obtained from calibration calculations, divided into polar and van der Waals interactions.^{148,149} The entropy was obtained from a normal-mode analysis at the MM level. Unfortunately, the calculations gave a poor correlation to experiments, $R^2 = 0.06$, and rather large MADs, 8 kJ/mol, even after the energy terms were scaled using a training set of similar ligands. The effect of the systematic-error corrections was small.

In 2010, Hobza and co-workers suggested a method to rescore docked ligand poses.²⁴⁸ They employed the PM6-DH2 method with dispersion and hydrogen-bond corrections and started from the two best docked structures, which were fully optimized in a COSMO continuum solvent (without nonpolar terms). For the ligand, more accurate desolvation energies were calculated with the SMD model, based on IEFPCM calculations at the HF/6-31G* level, using structures either from the optimized complex or from a short MD simulation, followed by a minimization, both at the PM6-DH2/COSMO level. This also gave a ligand deformation energy, which was calculated at the PM6-DH2 level. The deformation energy of the protein was calculated at the PM6-DH2 level from optimized structures. Normal-mode entropies were estimated from MM frequencies after reoptimization in a GB solvent, and a zero-point vibrational energy term was

also included. The method was tested on 22 diverse ligands of HIV-1 protease, 11 known binders and 11 false binders. They could discriminate binders from nonbinders (which also was possible with docking and MM methods) and obtained a good correlation to the experimental data for the binders ($R^2 = 0.62$, appreciably better than that of the DOCK or MM results, $R^2 = 0.10$ – 0.15). However, even better results were obtained if the deformation energy of the protein was ignored ($R^2 = 0.71$). Unfortunately, most binding affinities were strongly positive, and the range of the calculated binding affinities was almost 10 times larger than the experimental range. The calculations took 3–4 days on a single processor, dominated by the geometry optimization.

The method was also applied on 15 diverse ligands binding to CDK2.³¹¹ The calculations differed in some aspects from the previous ones: They were started from crystal structures, the protein deformation energy was omitted, and the free ligand was only minimized (i.e., no MD was performed). The full method gave a decent correlation of $R^2 = 0.52$, but the PM6-DH2 interaction term alone gave an appreciably better correlation, $R^2 = 0.87$. The other terms deteriorated the results, especially the entropy term. The results were much better than what was obtained with the Amber 99 or 03 force fields ($R^2 = 0.06$ and 0.00).

A similar approach was also applied to the binding of two sets of halogenated inhibitors of casein kinase 2.³¹² As the complexes involve halogen bonds, the authors employed the PM6-DH2X method, involving halogen-bond corrections. The structures were optimized with the PM6-D2X/COSMO approach (i.e., without hydrogen-bond corrections), followed by single-point PM6-DH2X/COSMO energy calculations. Otherwise, the calculations were similar to those in the CDK2, except that the ligand desolvation energy was calculated with C-PCM using the B3LYP/6-31G* method. The full scoring function gave a poor correlation to experimental data, $R^2 = 0.24$ and 0.19 for the two sets of ligands. Again, the entropy term was problematic; without it, the correlation was much better, $R^2 = 0.81$ and 0.71 . A standard MM calculation failed to reproduce the halogen bonds and gave poor correlations ($R^2 = 0.04$ and 0.08). This may explain why the entropy term was so poor for this system (it was calculated at the MM level).

The same group has also suggested a variant of the method for covalently bound inhibitors.³¹³ BLYP-D2/SVP was used for optimization and TPSS-D3/TZVPP for single-point energy calculations of the ligand and three protein residues, whereas PM6-D3H4X was used for the rest of the protein (truncated after 10 Å and fixed outside 8 Å in the geometry optimizations). The approach was employed for 20 inhibitors of cathepsin B1. With the standard score, they obtained a modest correlation of $R^2 = 0.47$, but taking only the covalent energy term, a much better correlation was obtained, $R^2 = 0.81$. However, in both cases, a few complexes were excluded as outliers.

Hobza and co-workers have also examined how the result depends on the structure used for the ligand.¹⁷⁸ They considered the same nine inhibitors of HIV-1 protease as in their first study.²⁴⁸ They compared the energy of the ligand optimized from the structure in the protein and the probability density obtained from an MD simulation at the MM level with 10 different sets of RESP charges. All MD structures were optimized with PM6-DH2 in a COSMO solvent. Finally, vacuum energies were calculated with PM6-DH2 and SMD solvation energies at the HF/6-31G* level of theory. A total of 50 snapshots from a 50 ps PM6-DH2/COSMO MD simulation were also included. The

results show a variation of ~ 80 kJ/mol in energies obtained from the various snapshots (although all were optimized with the same method). The single optimized structure differed from the MD average by an MAD of 13 kJ/mol for the nine ligands with no systematic bias. However, the averages obtained from the MD simulations with MM and SEQM showed a systematic bias of 25 kJ/mol and an MADtr of 9 kJ/mol. These results clearly illustrate the risks of using a single structure for binding-affinity estimates as well as of using a method for sampling different from that used for the energy calculations. Moreover, these errors apply for the isolated ligand; even larger problems can be expected from the protein–ligand complex.

An important component in ligand binding is the strain energy, i.e., the difference in the internal energy of the ligand in the binding site and in solution.³¹⁴ One common way to estimate it is by comparison of the energy of the ligand at a certain level of theory calculated in a crystal structure and in continuum solvation after some conformational search.^{315,316} However, this will include possible errors in the crystal structure, as well as the disagreement between the energy method used to measure the strain and that used to obtain the crystal structure. A more satisfying approach is to re-refine the crystal structure with a QM/MM approach¹⁸⁶ and use the same method also in solvent. Merz and co-workers have shown that such an approach decreases the estimated strain energy by 80% for a charged ligand.³¹⁷

In 2013, the first study of ligand binding, using linear-scaling DFT calculations, was published.³¹⁸ Miyazaki and co-workers used PBE/DZP calculations to calculate the binding energy of three ligands to the FK506 binding protein. Although they did not include any solvation, dispersion, or entropy effects, they obtained a perfect correlation to experiments, $R^2 = 0.99$. They also obtained an only slightly overestimated range for the binding affinities of the three ligands, 20 compared to 14 kJ/mol.

In conclusion, a number of groups have used linear-scaling SEQM methods to calculate binding affinities. Most of them have used the freely available MOZYME approach in the Mopac package, and they then also include the COSMO continuum-solvation model. However, it is only the Merz and Hobza groups that have systematically included SASA, dispersion, and entropy corrections, and these are also the only groups that have employed the approach in several studies. Hobza also included a more accurate ligand-solvation energy and a deformation energy of the ligand. In one study, Hobza has supplemented the approach with DFT-D calculations for the most important residues around the ligand. Recently, the first study entirely at the DFT level was presented, but it did not consider any solvation, dispersion, or entropy contributions. Still, such approaches may be promising in the future.

4. END-POINT APPROACHES

In the end-point approaches, a conformational sampling is performed, but only of the actual states in eq 1, i.e., of the receptor–ligand complex, and possibly also of the free receptor and the free ligand. This is expected to improve the ΔG_{bind} estimates, but it still does not provide true free energies. These calculations often follow the MM/PBSA or LIE approaches, replacing the MM energies by QM, and they will be discussed in separate subsections.

4.1. MM/PBSA Approaches

Several approaches have been presented to introduce QM calculations in MM/PB(GB)SA (i.e., MM/PBSA or MM/

GBSA) calculations. The studies are summarized in Table 6. In most studies, QM/MM methods have been used, giving QM/MM-PBSA approaches: In 2005, Fischer and co-workers suggested the first such approach.³¹⁹ They used AM1 for the ligand and the CHARMM force field for the protein. Starting structures were obtained by a conformational search (giving up to seven conformations per ligand). All structures were optimized by QM/MM and then clustered, but only a single structure was used for the free ligands and proteins. During the geometry optimization, the point charges were scaled down to reproduce electrostatic interactions observed in a PB calculation at the MM level. The solvation energy was calculated by PB with an ionic strength of 0.1 M. A dielectric constant of 4 was used for the electrostatic interactions and the solvation energy. The nonpolar solvation energy was taken to be proportional to the SASA. An NMA entropy correction was calculated at the MM level. As the structures were not taken from MD simulations, the various structures were instead Boltzmann weighted according to their estimated free energy. For 47 benzamidine derivatives bound to trypsin, the calculated and experimental affinities agreed well with an RMSD of 5 kJ/mol (after a scaling constant for the protein–ligand van der Waals interactions was fitted) without any bias and with a similar range. However, the correlation was poor, $R^2 = 0.04$, owing to the relatively small range of the experimental affinities, 15 kJ/mol. Similar results were also obtained for three small ligands of the FK506 binding protein, refitting the parameter, with RMSDs of 3 and 6 kJ/mol for a flexible and rigid protein, respectively.

Jamet and co-workers also treated the ligand by AM1, but employed a more typical QM/MM-PBSA approach, in which they replaced the first three terms in eq 8 by the QM energy.³²⁰ A total of 51 snapshots were obtained from a 1 + 0.5 ns QM/MM MD simulation. The entropy term was omitted, and PB was used for the polar solvation energy. The binding free energy was decomposed by calculating the QM/MM energies with point charges from only a single residue. They studied the binding of five bromobenzimidazole inhibitors to the kinase CK2. The raw QM/MM energies gave a poor correlation with experimental affinities, $R^2 = 0.14$, but this was improved to 0.69 for the full QM/MM-PBSA energy, owing to the compensation of the electrostatic QM/MM interactions with the PB solvation energy.

Ibrahim also used a similar approach (but with GB solvation) to study eight halogen-containing inhibitors of CDK2.³²¹ He obtained poor results, with a negative correlation, owing to missing halogen-bond corrections. Ojha and co-workers used SEQM for the ligand only, but tested five different methods, PM3, MNDO, PDDG–PM3, PDDG–MNDO, and SCC-DFTB (also for MD).³²² They claimed that the best results were obtained with SCC-DFTB, but this is questionable considering that all methods gave identical results within the large reported standard error (14–36 kJ/mol).

On the other hand, Wang and Chen also included eight active-site residues in the QM system (treated by SCC-DFTB).³²³ They studied the binding of four inhibitors of neuraminidase and obtained a good correlation of $R^2 = 0.78$ to the experimental binding affinities. Barbault and Maurel used AM1 for the ligand and all residues within 6 Å.³²⁴ They studied five inhibitors of the urokinase plasminogen activator. With a single structure (the one closest to the MD average), they obtained a poor correlation to experimental data ($R^2 = 0.16$). This could be improved by using 18 snapshots from the MD simulation (at the MM level), $R^2 = 0.68$, especially after removal of 1–3 outliers. Even better results were obtained after SEQM minimization of the structures ($R^2 =$

Table 6. Summary of MM/PBSA-like Approaches^a

group	ref	year	variant	method	QM syst	opt	structure	solvation	ΔS	comments	receptor	no.	R^2
Merz	341	2005	LS-SEQM	AM1 and PM3	all	L + 6 aa + 1 W	MD	COSMO + SASA	MM	MM dispersion	TEM-1 R-lactamase	2	
Fischer	319	2005	QM/MM (EE)	AM1	L	yes	docking + Boltzmann weighting	PB + SASA	MM	electrostatics scaled down by $\epsilon = 4$	trypsinFKS06	473	0.04
Ryde	328	2008	QM/MM (ME)	TPSS/def2-SV (P)	L + 1 aa		MD or min	PB + SASA	NMA		cathepsin B	6	0.91
Jamet	320	2009	QM/MM	AM1	L		MD	PB + SASA			CK2	5	0.69
Zhan	330	2010	QM/MM	B3LYP/6-31G*	L + 6 aa + 3 W	yes	min	PB + SASA	rotatable bonds		phosphodiesterase 10	2	
Wang	193	2010	QM	DFT/SZ(P)	L + 24 aa		QM	PBSA			CDK2	5	0.87
Ryde	336	2010	PMISP	MP2/cc-pVTZ	L + 4 A		MD	PCM (QM)	MM		avidin	7	
Zhan	331	2011	QM/MM	B3LYP/6-31+G*	L + 6 aa + 3 W	yes	min	PB + SASA	rotatable bonds		phosphodiesterase 4	1	
Ibrahim	321	2011	QM/MM	AM1	L		MD	GB + SASA			CDK2	8	0.00
Ojha	322	2011	QM/MM	5 SEQM	L		MD	PB + SASA	MM	one fitted param	c-Abl tyrosine kinase	1	
Cavasotto	342	2011	LS-SEQM	PM3	all	100 steps	MD	COSMO + SASA	MM		Lck SH2	5	0.68
Cavasotto	343	2011	LS-SEQM	PM3	all	100 steps	MD	COSMO + SASA	MM		BRCA1	5	0.47
Ryde	344	2012	LS-SEQM	AM1, RM1, PM6	all		MD	GB + SASA	MM	dispersion needed, H-bond not essential	avidin	7	0.86
											factor Xa	9	0.12
											ferritin	9	0.92
											urokinase plasminogen activator	5	0.96
Maurel	324	2012	QM/MM	AM1, PM3	L + 6 A	yes	MD	PB + SASA	MM		glycogen phosphorylase	2	
Leonidas	333	2012	QM/MM	B3LYP/6-31+G*	L		docked	PB (QM) + SASA	MM		glycogen phosphorylase	4	
Leonidas	334	2012	QM/MM	B3LYP/6-31+G*	L		docked	PB (QM) + SASA	MM		glycogen phosphorylase	4	
Gilson	156	2012	MM2	PM6-DH+	all		MM2	COSMO			cucurbit[7]uril	29	0.91
Leonidas	335	2013	QM/MM	M06-2X/6-31+G*	L + 2 aa	yes	docked	PB (QM) + SASA	MM		glycogen phosphorylase	3	
Kuwata	339	2013	FMO	MP2/cc-pVTZ	1 aa		MD	explicit 8 Å			lysozyme	2	
Shigemitsu	340	2013	FMO	HF or MP2/6-31G*	1 aa		MD	PB + SASA (MM)	MM		DJ-1	3	
Sippl	327	2014	QM/MM	RM1	L + 5 A	yes	MD	GB + SASA	rotatable bonds		Myt1 kinase	23	0.12
Zhan	332	2014	QM/MM	B3LYP/6-31+G*	L + ~10 aa	yes	MD	PB + SASA	rotatable bonds		cytochrome P450 2A6	4	0.87
Wang	323	2014	QM/MM	SCC-DFTB	L + 8 aa		MD	GB + SASA	MM		neuraminidase	4	0.78
Skylaris	345	2014	LS-QM	PBE + D	all		MD	PB + SASA	MM	polar solvation energy scaled	RAD51	2	
Skylaris	347	2014	LS-QM	PBE + D	all		MD	PCM (QM) + SASA	MM	corrections for nonpolar solvation	T4 lysozyme mutant	8	0.00
Gilson	361	2014	M2	PM6-DH+	all		M2	COSMO	MM		cucurbit[7]uril	14	0.24

Table 6. continued

group	ref	year	variant	method	QM syst	opt	structure	solvation	ΔS	comments	receptor	no.	R^2
Merz	157	2014	LS-SEQM	PM6-DH2	all		systematic search L	COSMO SMD			T4 lysozyme mutant	8	0.68 0.56

^aThe table lists the research group, the reference, the publication year, the type of QM calculations, the QM method used, the size of the QM system (L = ligand, aa = amino acids, W = water, and Å gives the maximum distance to the ligand), atoms that were optimized, structures used for the calculations, the solvation method used, the method used to obtain entropies, possible comments, the receptor used, the number of systems studied, and the obtained correlation coefficient.

0.96). Similar results were obtained with the PM3 method ($R^2 = 0.91$). Unfortunately, uncertainties of the estimated affinities were not reported, so it is not possible to judge the statistical significance of the reported results, because MM/PBSA typically gives a poor precision when based on averages over only 18 snapshots.^{29,167}

The MMPBSA.py script in the AMBER software allows running QM/MM-PB(GB)SA with SEQM methods in an automatic manner, in the same way as standard MM-PB(GB)SA postprocessing of MD snapshots.³²⁵ This means that the three first terms in eq 8 are replaced by the QM/MM energy in AMBER,³²⁶ whereas the three last terms are kept. Sippl et al. applied this implementation for the rescoring of potential inhibitors of Myt1 kinase.³²⁷ The QM system included the ligand and residues within 5 Å, and it was treated by the AM1 and RM1 methods. The entropy was estimated from the number of rotatable bonds in each ligand. They showed that QM/MM-GBSA successfully could discriminate 5 active inhibitors from 11 nonbinders, in contrast to docking with the GOLD software²³⁵ and MM/PB(GB)SA calculations. RM1 gave the best results, whereas AM1 gave one incorrect prediction. Calculations based on minimized structures or MD snapshots gave similar results. Then they used QM/MM-GBSA with RM1 to predict the binding of 23 known kinase inhibitors. Five of these were predicted to bind, and they were subsequently tested for binding, showing three of them actually inhibited the enzyme. However, the correlation between the predicted and measured binding strengths was poor ($R^2 = 0.12$).

Many studies have instead used DFT calculations for the ligand and a few nearby groups. We developed the first such approach by replacing the first three terms in eq 8 with a QM/MM energy.³²⁸ The method was primarily directed toward metalloproteins, for which it is hard to obtain accurate MM force fields. Therefore, the entropy was calculated only for the QM system, whereas the entropy of the MM system was omitted (as is often done also in standard MM/PBSA¹⁶⁷). The solvation energy was calculated with either the PB or GB method, and both EE and ME approaches were used for the QM/MM calculations. Moreover, we tested basing the calculations on QM/MM-minimized structures or ensembles from MD simulations, in which the QM system was kept fixed. Finally, we tested whether crystal water molecules should be treated as a part of the protein or as a part of the solvent. All these approaches gave comparable results and reproduced strict QM/MM-FES results for reaction energies in two enzymes appreciably better than standard QM/MM energies (MADs of 4–22 kJ/mol, compared to 29–32 kJ/mol). The only exception was when separate MD simulations of the reactant and product states were used, which gave a useless precision.

This method was then used to study the binding of six Ru-containing ligands to cathepsin B.¹⁹⁵ The TPSS/def2-SV(P) method was used for the ligand and the side chain of the Cys residue that coordinated to the Ru ion. Only the ME-QM/MM variant and PB solvation were used, but we tested to calculate the point charges of the QM system either from a vacuum wave function or from a wave function polarized by point charges of the MM surroundings. The QM/MM-PBSA energies gave a decent correlation to the experimental affinities if the protein was kept fixed in the optimizations ($R^2 = 0.59$), whereas no correlation was found if the protein was relaxed, owing to the local-minimum problem.³²⁹ The results with the fixed protein were strongly improved by performing QM/MM-PBSA on snapshots from MD simulations with a fixed QM system ($R^2 =$

0.91). In this case, the full energy function also gave a better correlation than the QM energy alone ($R^2 = 0.76$). However, the estimated free energies showed a much larger range than the experimental ones (176 kJ/mol, compared to 12 kJ/mol), indicating that the energies are overestimated and that the good correlation comes mainly from the correct identification of the best and worst binders.

Zhan and co-workers have used a similar approach for metalloenzymes.^{330–332} They combined pseudobond QM/MM energies with PBSA solvation, using RESP charges from the QM/MM calculation, and an entropy term from a simple count of the number of rotatable bonds lost during the binding and the number of water molecules displaced by the ligand. They used the B3LYP density functional with either the 6-31G* or 6-31+G* basis set for the ligand and the metal ion(s), together with their first-sphere ligands, as well as a few nearby residues. In the first studies, a single QM/MM-optimized structure was used, but in the later study, 10 structures were optimized, starting from snapshots from an MD simulation. The method was employed for two phosphodiesterases and cytochrome P450 2A6 with good results after the fitting of one parameter (the entropy of each rotatable bond), e.g., $R^2 = 0.87$ for the binding of four inhibitors to CYP 2A6 (but the standard errors in the calculated estimates are not reported).

Leonidas and co-workers have also used a similar approach in a series of studies of phosphorylase b.^{333–335} They employed a single docked structure (sometimes relaxed by a QM/MM optimization) and used DFT (B3LYP or M06-2X) with the 6-31+G* basis set for the ligand only or for the ligand and two nearby residues. The PB solvation energy was calculated from the QM charge density. They used a standard MM NMA entropy. In several cases, they showed that QM/MM-PBSA, but not the docking score, could explain experimental ranking of small sets of ligands, owing to important desolvation, π -stacking, and σ -hole binding.

In one case, instead a QM-cluster approach has been used: Wang and co-workers used a DFT method with a SZP basis set for the ligand but a minimal SZ basis for the closest 24 amino acid residues (5.5 Å) in a study of five inhibitors binding to CDK2.¹⁹³ They performed a 1 ps QM MD simulation of the complex. For 800 snapshots, they added PBSA continuum-solvation energies, calculated at the MM level with Mulliken charges for the ligand. Unfortunately, this is shorter than the typical correlation time of binding interaction energies,¹⁷⁷ so in practice this means that they have sampled the same energy 800 times. Still, they obtained good correlation to experimental data, $R^2 = 0.87$.

The PMISP method has been used in an MM/PBSA-like approach to compute binding free energies for seven ligands to avidin at the MP2/cc-pVTZ level.³³⁶ The calculations were performed on 10 snapshots per ligand from an MD simulation at the MM level. Entropies were taken directly from the corresponding MM/PBSA calculation. Solvation energies were calculated for the full protein with the polarizable multipole model (obtained at the B3LYP/6-31G* level). However, if both the polar and nonpolar PCM terms were included, poor results were obtained (positive binding affinities and $R^2 = 0.27$). Appreciably better results were obtained if instead the standard SASA nonpolar solvation energy was employed ($R^2 = 0.52$ and MADtr = 19 kJ/mol). However, the results were still worse than the MM/PBSA results ($R^2 = 0.96$ and MADtr = 14 kJ/mol). Later, we showed that the problem of the nonpolar energy was caused by the fact that continuum-solvation models fill the

binding cavity with solvent.^{337,338} If this was avoided, PCM gave the more accurate results.

A few FMO calculations have also been performed on MD snapshots. Kuwata et al. have studied a trisaccharide binding in two modes to lysozyme at the MP2/cc-pVDZ level.³³⁹ The calculations were based on 40 snapshots from a 50 ps MD simulation, and the calculations explicitly included all water molecules within 8 Å from the ligand. No additional implicit solvation or entropy effects were considered. Unfortunately, the uncertainty in such explicitly solvated calculations was very large (in that case 13 kJ/mol for the difference of the two binding modes). They observed transfer of ~ 3 electrons from the solvent to the protein.

On the other hand, Shigemitsu developed a true FMO/PBSA approach.³⁴⁰ He studied the binding of three ligands to the DJ-1 protein. For four snapshots from an MD simulation, he calculated the FMO energy at the HF and MP2/6-31G* levels (the former both with and without an empirical dispersion correction). These energies replaced the $E_{\text{int}} + E_{\text{el}} + E_{\text{vdW}}$ energies of standard MM/PBSA and MM/GBSA calculations (with 100 snapshots). Unfortunately, both the MM/PB(GB)SA and FMO/PB(GB)SA methods gave strongly positive binding energies (but a correct ranking of the two ligands with experimental affinities). Docking calculations gave reasonable absolute affinities but an incorrect ranking. Moreover, the MM/PB(GB)SA had an uncertainty of ~ 10 kJ/mol, indicating that the FMO results (based on only four snapshots) would have a 5-fold larger standard error (not reported).

Several studies have instead used linear-scaling SEQM methods: Already in 2005, Merz and co-workers developed an all-protein linear-scaling SEQM variant of MM/PBSA, QM-PBSA.³⁴¹ They used the same approach as for their single-point calculations on crystal structures.^{246,308} SEQM energies were calculated for the whole protein–ligand complex, including a PB continuum-solvation model. To this was added an MM dispersion term, together with an SASA term for the nonpolar solvation free energy. However, the conformational entropy was calculated by an MM NMA, as in standard MM/PBSA. The calculations were performed on 50 snapshots from an MD simulation at the MM level, but each snapshot was minimized by QM/MM using AM1 or PM3 for the ligand, six protein side chains, and a water molecule. The method was employed to calculate the affinity of benzylpenicillin and cephalosporin to the TEM-1 β -lactamase, showing that the former binds strongest, although the difference was not statistically significant, owing to the poor precision of the method (standard errors of 20–36 kJ/mol). The results of the AM1 and PM3 methods agreed mutually within 4 kJ/mol.

In 2011, Anisimov and Cavasotto suggested the MM/QM-COSMO method.³⁴² In this method, the energy of the full protein was calculated with the PM3 method, including COSMO continuum solvation and an SASA term. The SEQM calculations were performed on 1000 snapshots from an MD simulation of the complex at the MM level, followed by 100 steps of energy minimization at the PM3 level. To this was added an MM NMA entropy correction, but also terms for the change in the translational and rotational energies obtained from configurational integrals based on the movement of the ligand in the MD simulations. After optimization of the COSMO atomic radii for PM3, they obtained a good agreement between experimental and MM/QM-COSMO binding energies with an MAD of 3 kJ/mol and $R^2 = 0.68$ for the binding of five tetrapeptides to the Lck SH2 domain. This was much better than standard MM/PB(GB)SA

Table 7. Summary of LIE-Type Approaches^a

group	ref	year	variant	method	QM	MD	structure	solvation	fit	comments	receptor	no.	R ²
Balaz	349	2005	QM/MM (EE)	B3LYP/LAV3P**	L + 5 aa	MM	average MD	SASA	3		MMP-9	28	0.90
Balaz	350	2007	QM/MM (EE)	B3LYP/LAV3P**	L + 5 aa	MM	MD	polar and nonpolar SASA	4		MMP-9	28	0.90
Balaz	351	2007	QM/MM (EE)	B3LYP/LAV3P**	L + 5 aa	MM	average MD	SASA	3		MMP-3	28	0.90
Tuñón	353	2007	QM/MM	AM1	L	QM/MM	MD		2		HIV-1 integrase	11	0.82
Tuñón	354	2007	QM/MM (ME)	BLYP/6-31G*	L + Mg	QM/MM (AM1,L)	single from MD		2		HIV-1 integrase	3	
Tuñón	356	2007	QM/MM	AM1	L	QM/MM	MD		3		CDK2	5	0.95
Tuñón	355	2008	QM/MM (ME)	BLYP/6-31G*	L + Mg	QM/MM (AM1,L)	single from MD		2		HIV-1 integrase	2	
Chuman	358	2008	FMO	HF/6-31G	1 aa	MM	MD	SASA	3		HIV-1 PT	12	0.81
Chuman	359	2010	FMO	HF/6-31G	1 aa	EE-QM/MM (HF/6-31G*)	MD clustered	GB + SASA (MM)	2	deprotonation energy	carbonic anhydrase	16	0.91
Chuman	360	2011	FMO	MP2/6-31G	1 aa	MM	minimized	PB	2		neuraminidase	6	0.96
Balaz	352	2012	QM/MM (EE)	B3LYP/6-31G**	L + 5 aa	MM	MD for solv	GB + SASA	3	multiple protonation and tautomeric states	protein kinase	66	0.88
Xiang	357	2012	QM/MM	AM1	L	QM/MM	MD	SASA	3		$\alpha\beta_3$ integrin	8	0.88

^aThe table lists the research group, the reference, the publication year, the type of QM calculation, the QM method used, the size of the QM system (L = ligand, and aa = amino acids), the method used for the MD simulations, structures used for the energy calculations, the solvation method used, the number of fitted terms, possible comments, the receptor used, the number of systems studied, and the obtained correlation coefficient.

calculations which gave large absolute errors (>40 kJ/mol) and $R^2 = 0.01$ – 0.14 . The same method was also used for the binding of five tetrapeptides to BRCA1. This gave $R^2 = 0.47$, slightly better than for the MM/PBSA method ($R^2 = 0.37$).³⁴³

We have used a similar approach to calculate binding free energies.³⁴⁴ We replaced the first four terms in eq 8 with an SEQM energy, calculated in COSMO solvent for the whole protein–ligand complex, but used the standard MM/PBSA terms for the entropy and the nonpolar solvation energy. Structures were obtained from MD simulations at the MM level (40 snapshots), without any optimization. We compared the performance of three SEQM methods, AM1, RM1, and PM6, and tested the inclusion of two types of dispersion corrections and one type of hydrogen-bond correction. The method was tested for the binding of seven biotin analogues to avidin, nine inhibitors to blood-clotting factor Xa, and nine phenol derivatives to ferritin. As often observed with end-point methods,¹⁶⁷ the results varied and were nonconclusive, except that a dispersion correction was mandatory. On average, AM1 with the DH2 correction gave the best results, but the results were not significantly better than those of the standard MM/GBSA approach. The time consumption was only ~ 1.5 times larger than for MM/GBSA, because it was dominated by the time for the MD simulations and the entropy calculation.

Finally, Skylaris and co-workers have suggested a QM-PBSA method in which the entire protein was treated by a linear-scaling DFT method (PBE with pseudopotentials).³⁴⁵ The DFT energy was complemented with a dispersion correction. The polar solvation energy was obtained with PB at the MM level, but it was scaled by the quotient between the DFT energy and the electrostatic MM energy raised to the power of 0.91 (obtained from a fit). To this was added an unscaled SASA energy, whereas the entropy term was obtained from an NMA at the MM level. They studied the binding of two 15-peptide moieties to 163 residues of RAD51 (2800 atoms) and employed averages over 40 snapshots. Unfortunately, no comparison with experimental data was done, only to standard MM/GBSA calculations. The approach was then used for the tennis-ball host–guest system, using a slightly different scaling of the solvation energies.³⁴⁶ The QM-PBSA ΔH_{bind} values agreed with experimental data much better than MM/PBSA. However, QM-PBSA overestimated the binding by 23–35 kJ/mol, although the correlation for the three ligands was reasonable, $R^2 = 0.66$.

In 2014, they applied the QM-PBSA method to the binding of eight ligands to a T4 lysozyme mutant (2602 atoms).³⁴⁷ This time they had implemented a continuum-solvation model in the DFT calculations, thereby avoiding the doubtful scaling of the MM solvation energy. A total of 50 snapshots were employed for the energies, giving a statistical precision of 2–3 kJ/mol. Special corrections were added for the nonpolar solvation term for the buried binding site. Two of the studied ligands were nonbinders according to experiments, but QM-PBSA could identify only one of them (none with MM/PBSA). Excluding these ligands, QM-PBSA gave a decent MAD of 7 kJ/mol compared to the experimental results, appreciably better than that of MM/PBSA (23 kJ/mol). On the other hand, it gave a correlation line with an incorrect slope, whereas MM/PBSA gave a correct correlation with $R^2 = 0.51$. However, the range of the experimental estimates was only 6 kJ/mol, which would be very hard to reproduce (the ranges of the QM-PBSA and MM/PBSA methods were 18 and 23 kJ/mol, respectively).

In conclusion, a variety of QM(/MM)-PBSA approaches have been suggested. These have employed many different QM

approaches, using QM only for the ligand, also for the nearest amino acids, or for the full protein. Docked, minimized structures or MD snapshots have been used. When employed for several systems, no uniformly improved performance has been observed. This has also been observed at the MM level;¹⁶⁷ the MM/PB(GB)SA approach seems to give an uneven performance for different systems, and it is very sensitive to the continuum-solvation model used, giving binding affinities that can vary by 210 and 85 kJ/mol in absolute and relative terms.³⁴⁸ Therefore, we doubt that MM/PB(GB)SA is accurate enough to allow for a consistent improvement by the use of QM calculations. On the other hand, it is quite clear that the continuum-solvation energy provides a consistent improvement over plain QM/MM energies³²⁸ and that the QM(/MM)-PBSA approach provides an interesting paradigm to include most effects being important for ligand binding.

4.2. LIE-Type Approaches

Fewer groups have used LIE-type approaches to include QM effects into binding-affinity estimates, as can be seen in Table 7. In 2005, Balaz et al. developed a QM/MM-LIE approach.³⁴⁹ They studied 28 hydroxamate inhibitors of matrix metalloproteinase 9. Structures were first docked by FlexX. The best structure with the ligand binding to Zn was then optimized by EE-QM/MM. The QM system involved the ligand, the Zn ion, side chains of the three His Zn-coordinating residues, one Glu side chain (accepting a hydrogen bond from the ligand), and the backbone between two of the residues. Only protein atoms within 5 Å of the ligand were optimized. The B3LYP method was used for the QM system and the OPLS-AA force field for the MM system. Next, MD simulations at the MM level were performed with Zn–ligand distances restrained to those found in the QM/MM structures and Mulliken charges for the QM system. Only residues within 5 Å of the ligand were allowed to move. The simulation was run for 200 ps, and 2000 structures were collected, averaged, and minimized. Therefore, only a single structure was studied in the final step, in which a single-point QM/MM energy was calculated, together with an SASA term. Three terms were fitted to the experimental data, viz., the QM/MM and SASA energies, as well as a constant term. The docking score gave no correlation with the experimental data ($R^2 = 0.04$), but the QM/MM energies gave a much improved correlation ($R^2 = 0.50$), although they were completely dominated by the SASA term, giving the same correlation alone. Even better correlation was obtained from the MD-averaged structures ($R^2 = 0.76$), again dominated by the SASA term. However, the best correlation was obtained from the QM/MM + SASA calculations ($R^2 = 0.90$), although it should be remembered that this involved the fitting of three parameters.

Two years later, they studied the same system, but extended the number of parameters by considering both polar and nonpolar SASA. They also treated averages over each 25 ps simulation as a separate binding mode.³⁵⁰ The results were somewhat improved for the pure MM approach ($R^2 = 0.84$, most likely owing to the increased number of fitting parameters), but not for the QM/MM-LIE approach ($R^2 = 0.90$). They also used the original approach to study the binding of the same ligands to a related protein, MMP3.³⁵¹ The results were similar: The correlation increased steadily from the docking ($R^2 = 0.06$), the QM/MM minimization ($R^2 = 0.46$), MM-LIE ($R^2 = 0.81$), and QM/MM-LIE ($R^2 = 0.90$). If the three adjustable parameters were fitted for both MM3 and MMP9 simultaneously, the fit was

Table 8. Summary of Strict FES Binding Studies^a

group	ref	year	FES	QM method	QM syst	comments	receptor	no.	R ²
Reddy	363	2007	EA	AM1	L		fructose-1,6-bisphosphatase	5	0.98
Essex	376	2011	elstat-ssEA	B3LYP/6-31G**	L	3000 QM evaluations	COX2	2	
Reddy	364	2012	EA	AM1	L		fructose-1,6-bisphosphatase	14	0.99
Moliner	365	2012	EA, US	AM1	L		HIV-1 RT	5	
Ryde	216	2014	ssEA, NBB	TPSS-D3/def2-QZVP'	L + H + 6 Å W		octa-acid host	8	0.6–0.7
Mulholland	377	2015	MH-MC	BLYP/aug-cc-pVDZ	L	180000 QM evaluations	neuraminidase	8	
Ryde	378	2015	ssEA, NBB	BLYP-D3/def2-TZVP	L + 4.5 Å	polarized multipole MM	galectin 3	2	
Ryde	379	2016	ssEA NBB	PM6-DH2X	L + 4.5 Å	60000 QM evaluations	octa-acid host	8	0.32 0.15

^aThe table lists the research group, the reference, the publication year, the FES method used (US = umbrella sampling, MH-MC = Metropolis-Hastings Monte Carlo, ssEA = single-step exponential averaging, NBB = non-Boltzmann BAR), the QM method used, the size of the QM system (L = ligand, H = host, W = water, and Å gives the maximum distance to the ligand), possible comments, the receptor used, the number of systems studied, and the obtained correlation coefficient. All calculations employed QM/MM methods.

deteriorated to $R^2 = 0.77$, and nearly identical results were obtained without the QM/MM term ($R^2 = 0.76$).

In 2012, the method was extended to also consider multiple protonation and tautomeric states.³⁵² They studied the binding of 66 inhibitors of a protein kinase with up to five different ionization states and seven tautomers. The QM system involved the ligand, two full residues, and the backbone of three other residues, and it was treated at the B3LYP/6-31G** level. Only a single SASA term was included. Again, the results were strongly improved when going from docking, via QM/MM minimization and MM-LIE, to QM/MM-LIE ($R^2 = 0.00, 0.20, 0.35$, and 0.91). Without the multistate treatment of the tautomers and ionization states, the correlation was appreciably worse, $R^2 = 0.66$.

Tuñón and co-workers have developed another QM/MM-LIE approach in which they evaluated the average QM/MM interaction energy between a QM ligand and an MM protein from 1 ns QM/MM-MD simulations of 11 inhibitors of HIV-1 integrase.³⁵³ They employed the AM1 method and obtained a quite good correlation with experimental affinities, $R^2 = 0.82$. However, the calculated differences between the various inhibitors were more than 10 times larger than the experimental ones. In a related study of the same enzyme with three inhibitors, they calculated interaction energies at the ME-QM/MM level with BLYP/6-31G* calculations for the ligand and a single Mg ion in the QM system, using a single structure optimized from the last MD snapshot.³⁵⁴ In the QM/MM MD simulation, the ligand was treated by AM1, whereas the rest of the protein was described by MM. In another investigation, they studied a mutant of the enzyme, reproducing the experimentally observed decreased affinity of the ligand.³⁵⁵

They also used the original method to study the binding of five inhibitors to CDK2.³⁵⁶ The QM/MM-MD simulation was 350 ps. They obtained a good correlation between experimental IC₅₀ values and QM/MM interaction energies ($R^2 = 0.85$), although the calculated energies were very large (up to -520 kJ/mol) as were the reported uncertainties ($12-34$ kJ/mol). They also attempted an LIE-like fit to the electrostatic and van der Waals QM/MM components, which increased the correlation to $R^2 = 0.95$.

Xiang et al. used a similar approach to study the binding of eight cyclic peptides to $\alpha_v\beta_3$ integrin.³⁵⁷ They performed short (150 ps) QM/MM MD simulations on docked structures, employing AM1 for the peptide inhibitors only. They showed

that a linear fit of the average QM/MM interaction energy correlated with the binding affinity ($R^2 = 0.80$). Even better correlation was obtained by fitting separately the electrostatic and van der Waals components of the QM/MM energy ($R^2 = 0.88$).

Finally, FMO interaction energies have been used as a descriptor in LIE (or almost QSAR-like) approaches: Chuman and co-workers studied the binding of 12 inhibitors to HIV-1 protease.³⁵⁸ They employed the HF/6-31G method on 10 MM-minimized snapshots from an MD simulation without any solvation. The fit was based on the binding or interaction energies, supplemented with SASA and constant terms. They obtained a good correlation to experimental affinities ($R^2 = 0.81$). In a later study, they used a similar approach to study the binding of 16 sulfonamide ligands to carbonic anhydrase.³⁵⁹ However, they used only five structures obtained from a cluster analysis of the MD snapshots and then optimized by EE-QM/MM using HF/6-31G* for the ligand and the catalytic Zn ion and its three His ligands. In a later study, they used single structures for the FMO calculations, but averages over 50 MD structures for the solvation energies.³⁶⁰ They obtained a good correlation to experimental data for both PB and GB solvation (calculated at the MM level), after fitting two parameters, $R^2 = 0.96$ and 0.88 , respectively, for the binding of six ligands to neuraminidase.

Thus, only four groups have employed QM-LIE approaches, all based on QM/MM or FMO calculations, but three groups have used this approach systematically for several different systems. Only a single study used a QM method which includes dispersion effects, and all studies have been performed with too small basis sets to give any reliable results. Still, quite good results have been obtained, but it is not clear whether this is mainly an effect of the fitting of some parameters or is really caused by the QM calculations.

4.3. Other Approaches

Muddana and Gilson have rescored 29 small ligands docked to the cucurbit[7]uril host systems with the mining minima (M2) approach, using the PM6-DH method coupled with the COSMO implicit solvation model.¹⁵⁶ After removal of a systematic error, they obtained an MAD of 7 kJ/mol and $R^2 = 0.91$ to experimental affinities. The SEQM results were better than those obtained by MM. However, two years later, they used the same approach to calculate binding free energies for 14 small ligands binding to the cucurbit[7]uril host in the SAMPL4 blind challenge.³⁶¹ In this

case, they obtained a much better correlation with MM + PBSA than with SEQM ($R^2 = 0.74$ and 0.24 , respectively).

Merz and co-workers have suggested another method to estimate free energies.¹⁵⁷ They studied the L99A T4 lysozyme mutant with eight different ligands. Protein residues within 5 Å from the ligand were minimized with MM without the ligand and solvent. The ligands were then put into the rigid binding site and were systematically translated and rotated, and all rotatable bonds were systematically sampled. All poses that did not overlap with protein atoms were added to an ensemble of reasonable structures. The free ligand was treated in a similar way (no translation or rotation needed). Free energies were directly estimated from conformational integrals. The best results were obtained with the PM6-DH2 method combined with the COSMO model ($R^2 = 0.68$), whereas the SMD model and MM calculations gave slightly worse results ($R^2 = 0.56$ and ~ 0.5). However, the calculated energies were much too negative (e.g., by ~ 40 kJ/mol for PM6-DH2/COSMO), the slopes were far from unity, and the maximum relative error was ~ 20 kJ/mol. They suggested that this is probably an effect of the rigid protein and the implicit solvent. They also tried to improve the results by adding corrections for systematic errors from reference calculations,^{148,149} which changed the absolute and relative affinities by ~ 4 and ~ 2 kJ/mol, respectively.

5. FREE-ENERGY SIMULATIONS

The statistically mechanically strict way to obtain binding free energies is to perform free-energy simulations (FESs). However, these require extensive sampling of the receptor–ligand complex and various intermediate states, making them computationally very demanding. Therefore, full FES simulations for ligand binding have been performed only at the SEQM/MM level and in only a few cases. It has been more common to perform the sampling at the MM level and then try to extrapolate these results to the QM level. The studies are summarized in Table 8 and are described in two separate subsections.

5.1. FES Simulations

Reddy and Erion have used QM/MM-FES to calculate the binding free energies of five inhibitors of fructose-1,6-bisphosphatase.³⁶² They used AM1 for the ligand and MM for the protein and solvent. With standard EA, they obtained results with a suspiciously high accuracy: Five relative binding affinities were reproduced with an error of less than 1.4 kJ/mol, although the reported statistical uncertainties of the calculated affinities were 1.9–2.5 kJ/mol. The results obtained at the MM level were almost equally good, with a maximum error of 2.1 kJ/mol. The SEQM calculations increased the computational time by a factor of 5. The same approach was later used to study the binding of some other inhibitors to the same enzyme.³⁶³ Again, excellent results were obtained for 22 relative binding affinities, with maximum errors of 1.7 and 3.3 kJ/mol for SEQM and pure MM, respectively, although the reported uncertainty in the relative energies is 3.8 kJ/mol.

Likewise, Moliner et al. have used QM/MM MD simulations to perform two types of free-energy calculations, alchemical FES calculations and umbrella sampling potential-of-mean-force calculations, for five ligands binding to HIV-1 reverse transcriptase.³⁶⁴ Only the ligand was in the QM system, and the AM1 method was employed. They used 100 MD simulations of 100 ps each to turn off first the charges and then the van der Waals interactions, thereby giving absolute binding affinities. The study analyzed the sampling requirements, but unfortunately, the

demanding energy function prohibited a proper convergence of any of the methods.

5.2. Reference-Potential Methods

A slightly more common approach has been to perform the sampling at the MM level and then evaluate QM/MM energies only for a restricted number of snapshots. The problem with such an approach is that the energy functions used for the simulations and the perturbations are not the same, so that eq 7 (or similar formulas) cannot directly be applied to the QM/MM energies. Instead, valid QM/MM free energies should be obtained either by an MM \rightarrow QM/MM FES calculation, employing the thermodynamic cycle in Figure 7a,^{129,365,366} or by reweighting

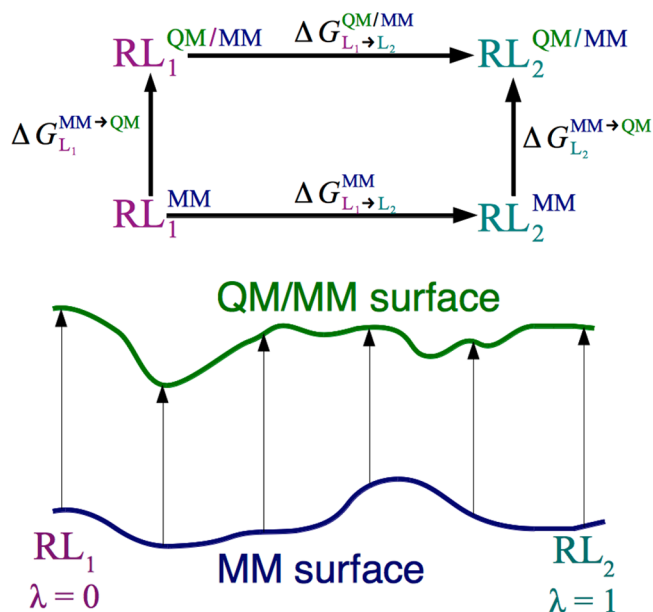


Figure 7. (a, top) Thermodynamic cycle to obtain relative QM/MM binding free energies. We can obtain the desired binding energy by $\Delta G_{L_1 \rightarrow L_2}^{QM/MM} = \Delta G_{L_1 \rightarrow L_2}^{MM} - \Delta G_{L_1}^{MM \rightarrow QM/MM} + \Delta G_{L_2}^{MM \rightarrow QM/MM}$ (and similar for the free ligands in water solution). If the QM/MM and MM potentials are similar enough, it may be enough to use sampling at the MM level. (b, bottom) Method of reweighting MM simulations to conform to the QM potential surface. In many applications, only the first and last points are reweighted to the QM/MM surface, whereas the remainder of the binding is studied only on the MM surface.

the MM snapshots with the QM/MM energy function (Figure 7b), e.g., by the non-Boltzmann BAR approach (NBB).³⁶⁷ Such approaches have been used quite extensively for enzyme reactions,^{44,129,365,366,368,369} for solvation free energies,^{370–375} and in a few cases also for ligand binding.^{216,376–379} The challenge with these approaches is to obtain converged results for the MM \rightarrow QM/MM perturbation, which must be performed in a single step to avoid the need of QM/MM sampling, i.e., to ensure that the overlap of the distributions generated by the MM and QM/MM potentials is large enough. For enzyme reactions, proper convergence has been obtained by keeping the QM system fixed,^{129,365,366} but for binding affinities, such an approximation seems inappropriate, because the entropy and reorganization of the ligand is crucial for the binding.

In 2011, Essex and co-workers suggested a method to include QM calculations in binding free-energy calculations.³⁷⁶ They first performed a standard FES calculation at the MM level. For a number of snapshots of the end states, they then performed QM/

MM single-point energy calculations to estimate the free energy of going from MM to QM/MM using a single-step EA (ssEA) calculation (Figure 7a). However, to avoid convergence problems, they considered only the electrostatic interaction energy between the ligand and the surroundings, calculated either with QM/MM or with MM (i.e., two QM calculations were performed for each snapshot and state, one with a point-charge model of the surroundings and one in vacuum). After testing and evaluating the method on the difference in hydration energy of CH₄ and H₂O, they applied it to study the difference in binding affinity of two inhibitors of COX-2, differing in one single group (–OH or –CH₃). They used the B3LYP/6-31G** method for the ligand only and performed the calculations on 3000 snapshots for each state, both inside the protein and in water solution. They obtained a result that was appreciably closer to experiments than that obtained at the MM level (deviations of 1 and 7 kJ/mol, respectively, for the difference in affinity of 19 kJ/mol). The uncertainty was only 2 kJ/mol (but this was still 5–10 times larger than at the MM level, owing to the lower number of snapshots employed for the averages).

Mulholland and co-workers have used a different approach to calculate the absolute binding affinity of water molecules in two conserved binding sites of neuraminidase.³⁷⁷ The water molecules were rigid and were treated at the BLYP/aug-cc-pVDZ level of theory, whereas the surroundings were treated by MM. They employed eight λ values, i.e., performing sampling with QM/MM, using Monte Carlo methods. However, they used the Metropolis–Hastings MC (MH-MC) approach³⁷⁰ to reduce the number of QM calculations by a factor of 500. Still, 160 000 QM energy evaluations were used for each state. They found that the TIP4P \rightarrow QM correction was significant for all eight studied water molecules, amounting to 2–12 kJ/mol, more for the polar site than for the hydrophobic site. The statistical uncertainty was up to 4 kJ/mol. Unfortunately, there were no experimental affinities for comparison.

Both these studies included only the ligand in the QM system. However, to fully exploit the advantage of the QM methods, it is necessary to also include the nearest surroundings of the ligand. We have done this in three studies: In the SAMPL4 blind-test competition, we tried to improve MM FES results by DFT-D3 calculations for the octa-acid host–guest system.²¹⁶ For 100 snapshots from the end states and from the intermediate $\lambda = 0.5$ state, we performed QM/MM calculations at the TPSS-D3 level of theory (including three-body dispersion corrections), using the def2-QZVP' basis set for the ligands and the def2-TZVP basis set for the host and water molecules within 6 Å of the ligand (287–312 atoms in total). To make the energies more stable, only the difference in interaction energies between QM/MM and MM was considered (i.e., $E(\text{RL}) - E(\text{R}) - E(\text{L})$) using the same geometry for all three calculations; this has been shown to be a valid approximation in another study involving full QM/MM FES³⁸⁰). If the MM \rightarrow QM/MM correction was used as an extrapolation, a reasonable standard error could be obtained (2–3 kJ/mol). However, if the strict ssEA approach was used (Figure 7a), the standard errors were much larger, 3–23 kJ/mol. Reweighting with the NBB approach (Figure 7b) gave a slightly lower uncertainty, 5–13 kJ/mol. All three approaches reproduced experimental affinities worse than FES at the MM level, with $R^2 = 0.6$ –0.7 and MAD = 13–23 kJ/mol (0.84 and 4 kJ/mol at the MM level), probably owing to the large uncertainties.

We have also used a similar approach for a protein system, viz., the relative binding affinity of two substituted disaccharides to the carbohydrate-recognition domain of galectin 3.³⁷⁸ For 100

snapshots of the end states and the $\lambda = 0.3$ state, we calculated BLYP-D3/def2-SV(P) interaction energies. The QM system included the full ligand, as well as all protein groups and water molecules within 6 Å, in total 744–748 atoms. For 20 snapshots, CP corrections were calculated, and for 10 snapshots, more accurate BLYP-D3/def2-TZVP energies were calculated. The effect of the basis set was significant, 6–7 kJ/mol, and the CP correction for the def2-TZVP basis set was still 2–4 kJ/mol. The surroundings were modeled by the same polarizable multipole (up to quadrupoles) description as in the PMISP approach, also obtained at the MFCC/BLYP/def2-SV(P) level of theory. As for the octa-acid system, we had major problems converging the MM \rightarrow QM/MM perturbations: ssEA and NBB calculations gave standard errors of 14 and 23 kJ/mol, respectively. Therefore, we had to employ BAR calculations directly on the QM/MM energies, although this ignores the differences in the structures sampled by MM and QM/MM potentials. Still, this gave a difference in the binding affinity of the two ligands of 3 ± 3 kJ/mol, which was essentially identical to that obtained at the MM level, 3.6 ± 0.5 kJ/mol, and quite far from the experimental estimate of 10 kJ/mol.

Very recently, we have studied how many QM calculations are needed to obtain converged MM \rightarrow QM/MM perturbations for the octa-acid system.³⁷⁹ We sped up the calculations by using a neutralized host molecule, slightly smaller QM systems (waters within 4.5 Å of the ligand, 158–224 atoms), and the much cheaper PM6-DH2X method. Then we could obtain converged QM/MM binding energies (a standard error of 1 kJ/mol for all eight perturbations) with 60 000 snapshots for each of the end states, employing ssEA with a cumulant expansion.^{381,382} On the other hand, the NBB result still showed an uncertainty of 2–7 kJ/mol, and it required twice as many QM evaluations. All except one (small) MM \rightarrow QM/MM correction was in the correct direction (i.e., toward experimental data), but they were mostly too large so that no net improvement of the binding affinities was observed ($R^2 = 0.0$ was much worse and MAD = 5 kJ/mol was slightly worse than for MM). However, this was not the aim of the study, and it was perhaps not expected for such a simple SEQM method.

In conclusion, QM methods have also started to be used for FES calculations. Undoubtedly, this is the ultimate goal of the QM methods, because the FES approaches are limited only by the sampling and the energy function. Therefore, it is only for such methods that a consistent gain of improving the energies can be expected. However, we have seen that such calculations are extremely demanding and that there are great problems to obtain converged results. Clearly, a large number of QM evaluations are needed for accurate results, but it is so far not certain whether these are most efficiently used for single-point energy evaluations on MM snapshots or directly in QM/MM MD simulations.

6. CONCLUDING REMARKS

This review has illustrated the great interest of using QM calculations to improve estimates of binding affinities. This is quite natural, considering the increasing awareness of the shortcomings of standard MM force fields. In particular, QM calculations automatically include effects of polarization, charge transfer, charge penetration, and the coupling of the various terms. Moreover, QM avoids the need of parametrization of force fields for the ligands, which is a tedious and time-consuming procedure, if you aim at accurate results. QM can also

consistently treat the formation of covalent or metal-coordination bonds.

Many different QM methods have been employed, ranging from cheap SEQM approaches, via DFT, to strict MP2 and CCSD(T) calculations. In the latest decade, numerous calibration studies of various QM methods have been presented and dispersion corrections to DFT have been developed, giving strongly improved results for nonpolar interactions and large systems. Thereby, DFT methods have become a competitive alternative to the more expensive MP2 calculations. Likewise, the SEQM methods have been extended with dispersion and hydrogen- and halogen-bond corrections, bringing them appreciably closer to CCSD(T) reference values.

The calibrations have also emphasized the importance of large basis sets for DFT and, in particular, correlated QM methods. SVP calculations give poor results and enormous BSSEs, which seem to be overestimated by CP corrections. Not even TZVP calculations are converged (within the desired accuracy of ~ 6 kJ/mol), so basis sets of QZVP quality seem to be required (at the DFT level) to obtain reliable results. For correlated methods, basis-set extrapolations or explicitly correlated calculations should be used. The need for large basis sets is very problematic for FMO, which breaks down for large basis sets. A problem for DFT calculations with large (and diffuse) basis sets is that the energy calculations sometimes can converge to multiple states or saddle points.^{125,383} Finally, it should be noted that the self-interaction error in DFT methods often leads to a partial transfer of charge between zwitterionic systems, which can give rise to wrong electronic states when applied to significant parts of a receptor or a charged ligand.³⁸⁴ Large portions of HF exchange or range-separated functionals seem to be needed to avoid that problem.

Still, the calibration studies show that there is a significant improvement in the results going from SEQM, via DFT-D, to CCSD(T). On the other hand, the time consumption also increases strongly along this series, e.g., by a factor of ~ 1000 between SEQM and DFT-D. This determines the size of the systems that can be studied by the various methods. With SEQM, a full protein can be studied, with DFT-D up to ~ 2000 atoms, and with local CCSD(T) methods ~ 200 atoms. Fragmentation approaches can increase this limit, but they may introduce approximations (e.g., exclusion of many-body effects) that easily may limit the accuracy. On the other hand, there are many studies that indicate that it may be enough to include groups within 4.5–6 Å of the ligand (with a proper embedding),^{121,130,273} but it is unlikely that calculations involving only the ligand in the QM system will provide all improvements expected from QM methods.

Finally, the amount of sampling is crucial for the results. The statistical mechanically proper way to obtain binding free energies is the use of free-energy simulations. So far, this has only been performed with SEQM and only the ligand in the QM system. Valid free energies can also be obtained by reference-potential simulations (i.e., sampling at the MM level) followed by reweighting or MM \rightarrow QM perturbations (Figure 7). Unfortunately, the large difference between MM and QM makes the convergence of the MM \rightarrow QM poor, requiring a large number of QM evaluations (~ 60000).

Consequently, the bulk of the studies have used more approximate approaches involving restricted or no sampling, primarily MM/PBSA-like approaches (based on a number of MD snapshots of the receptor–ligand complex) or minimization approaches (based on a single structure, possibly preceded by a

docking or some sort of conformational search). We have emphasized in this review the importance of including all important terms for ligand binding, i.e., large basis sets, dispersion corrections, polar and nonpolar solvation, and entropy. Otherwise, it is unlikely that the method will give reliable and transferable results (but proper trends can be obtained for certain systems dominated by one type of interaction, and for most systems good geometries are obtained by QM/MM minimization). In this respect, the approaches by the Merz, Hobza, and Grimme groups show the largest promise, but also the QM(/MM)-PBSA approaches include the important terms. However, there is always the risk that the missing sampling may make these approaches too approximate, hiding the gain of the use of QM. In fact, this was our conclusion after trying to improve the MM/GBSA approach with QM methods in a series of ~ 10 studies.¹⁶⁷

From reading this paper, you can easily get the impression that inclusion of QM methods nearly always improves calculated binding affinities. This is not an accurate picture; in our hands, QM methods mostly have given comparable or even worse results than MM methods.^{216,344,336} The apparent success is probably an effect of the fact that it is easier to publish success stories.^{385,386} Moreover, the performance of a method depends on the quality measures used: Methods not based on FES or fitting tend to overestimate energies and energy differences, and QM methods often increase this overestimation. However, this typically improves the correlation between experimental and calculated affinities. Therefore, a correlation coefficient should always be supplemented by a measure of the agreement in terms of the free energy (MAD or RMSD), but such results are much more seldom reported. We have tried to emphasize this problem frequently in this review.

Therefore, the best estimates of the true accuracy of QM-affinity methods come from blind-test competitions, in which the results are not biased by experimental data. For the octa-acid host–guest system in the SAMPL4 competition, the best results were obtained by FES calculations at the MM level (MAD = 4 kJ/mol; this system was ideal for an FES study of relative energies).^{215,216} A similar accuracy (4–6 kJ/mol) was obtained in three recent large-scale tests of MM FES of relative affinities in a range of proteins.^{387–389} Attempts to extrapolate the octa-acid results to the DFT-D level completely failed. On the other hand, both we and the Grimme group obtained reasonable results (MADs of 8–10 kJ/mol) with a DFT-D minimization approach, although this was worse than for most MM methods.^{90,216} Similar results (MAD = 8 kJ/mol) were obtained also for the binding to the cucurbit[7]uril host, which was more similar to the results for MM methods (because this test case was less appropriate for FES calculations for relative affinities). On the other hand, Gilson and co-workers obtained better results with MM than with QM for the same system ($R^2 = 0.74$ and 0.24 , respectively).³⁶¹ Thus, we tend to conclude that QM methods do not currently automatically provide a clear improvement in computational estimates of binding affinities. This is probably caused by a combination of several effects: insufficient sampling and treatment of entropy effects, the use of rather crude continuum-solvation methods, and the fact that a QM treatment of most interactions (e.g., electrostatics, polarization, and repulsion) gives rise to larger energy components (of opposite signs) that require a higher precision to give accurate final results (MM methods gain much from error cancellation). However, this may change as it becomes possible to perform valid FES simulations at the QM(/MM) level.

AUTHOR INFORMATION

Corresponding Author

*E-mail: Ulf.Ryde@teokem.lu.se. Phone: +46-46 2224502. Fax: +46-46 2228648.

Notes

The authors declare no competing financial interest.

Biographies

Ulf Ryde received his Ph.D. in biochemistry from Lund University, Sweden, under the supervision of Prof. G. Pettersson in 1991. He then moved into the field of theoretical chemistry at the same university as a postdoctoral fellow of Prof. Björn Roos. He became a docent in 1996 and a full professor in 2004. From 2001 to 2007 he had a senior research position at the Swedish Research Council. He has published over 200 papers. He studies the structure and function of proteins, in particular metalloproteins, such as blue copper proteins, heme enzymes, vitamin B₁₂ enzymes, hydrogenases, and multicopper oxidases. He has developed QM/MM methods for an accurate treatment of environmental effects, e.g., using accurate MM force fields with multipole expansions and anisotropic polarization, and combinations of QM/MM with free-energy methods or experimental approaches, such as X-ray crystallography, NMR, and extended X-ray absorption fine structure (EXAFS) spectroscopy. He also studies and develops methods to calculate ligand-binding affinities, in particular MM/PBSA (MM combined with Poisson–Boltzmann and solvent-accessible surface area continuum solvation) and free-energy simulations, as well as various combinations of MM and QM methods.

Pär Söderhjelm received his M.Sc. degree in chemistry from Lund University, Sweden. He obtained his Ph.D. from the same university under the supervision of Prof. Ulf Ryde. His main topics were the development of polarizable force fields, QM fragmentation methods, and QM/MM methods for ligand binding. After receiving his Ph.D. in 2009, he spent two years with Prof. Michele Parrinello at Eidgenössische Technische Hochschule/Università della Svizzera Italiana (ETH/USI) in Lugano, Switzerland, applying and developing enhanced-sampling methods for biological systems. Currently, he is employed as an associate lecturer at the Division of Biophysical Chemistry at Lund University, mainly applying enhanced-sampling methods to systems in which protein dynamics play a significant role. He is also active in organizing school contests in informatics.

ACKNOWLEDGMENTS

This investigation has been supported by grants from the Swedish Research Council (Project 2014-5540) and from the Knut and Alice Wallenberg Foundation (KAW 2013.0022). The computations were performed on computer resources provided by the Swedish National Infrastructure for Computing (SNIC) at Lunarc at Lund University and HPC2N at Umeå University.

ABBREVIATIONS

6-31+G*	split-valence basis set with diffuse functions
6-31G*	split-valence basis set
6-311G(2df,sp)	triple- ζ basis set
AM1	Austin model 1 (semiempirical method)
aug-cc-pVTZ	triple- ζ basis set with diffuse functions
B3LYP	hybrid Becke and Lee–Yang–Parr density-functional method
BAR	Bennett acceptance ratio FES method
BH&HLYP	Becke half-and-half density-functional method

BP86	Becke–Perdew 1986 density-functional method
BSSE	basis-set superposition error
CBS	complete basis set
cc-pVDZ	split-valence basis set
cc-pVTZ	triple- ζ basis set
cc-pVQZ	quadruple- ζ basis set
CCSD(T)	coupled-cluster calculations with single, double, and perturbatively treated triple excitations
COSMO	conductor-like solvent model
COSMO-RS	COSMO for real solvent full solvation method
CP	counterpoise correction for the basis-set superposition error
def2-SV(P)	split-valence basis set
def2-TZVP	triple- ζ basis set
def2-TZVPD	triple- ζ basis set with diffuse functions
def2-QVP	quadruple- ζ basis set
DFT	density-functional theory
DFT-D3	Grimme's dispersion correction
D3H4	dispersion and hydrogen-bond corrections to semiempirical methods
D2H	dispersion and hydrogen-bond corrections to semiempirical methods
DH	dispersion and hydrogen-bond corrections to semiempirical methods
DH2X	dispersion, hydrogen-bond, and halogen-bond corrections to semiempirical methods
DLPNO-CCSD(T)	domain-based local-pair natural-orbital coupled-cluster method
EA	exponential averaging
EE	electrostatic embedding
EE-PA	electrostatically embedded pairwise additive fragmentation method
EE-GMFCC	electrostatically embedded generalized MFCC approach
EFMO	combination of FMO and EFP
EFP	effective fragment potential force field
FES	free-energy simulation
FMO	fragment molecular orbital
GB	generalized Born solvation
ΔG_{bind}	binding free energy
HF	Hartree–Fock method
L	ligand
LCCSD(T0)	local coupled-cluster method
LIE	linear interaction energy method
M06-L	Minnesota 2006 pure density-functional method
M06-2X	Minnesota 2006 hybrid density-functional method with double exact exchange
MAD	mean absolute deviation
MADtr	mean absolute deviation after removal of the systematic error (MSD)
MBAR	multistate Bennett acceptance ratio FES method
MC	Monte Carlo
MD	molecular dynamics
ME	mechanical embedding (for QM/MM)
MFCC	molecular fractionation with conjugate caps
MH-MC	Metropolis–Hastings Monte Carlo

MM	molecular mechanics
	molecular mechanics with generalized Born and solvent-accessible surface-area solvation
MM/GBSA	
MM/PBSA	molecular mechanics with Poisson–Boltzmann and solvent-accessible surface-area solvation
MP2	Møller–Plesset many-body perturbation theory to the second order
MP3	Møller–Plesset many-body perturbation theory to the third order
MP4	Møller–Plesset many-body perturbation theory to the fourth order
MSD	mean signed error
NBB	non-Boltzmann BAR
NEMO	polarizable force field
NMA	normal-mode analysis
OM2	semiempirical method
ONIOM	our own <i>N</i> -layered integrated MO and MM, a QM/QM or QM/MM approach
mPWLYP	modified Perdew–Wang Lee–Yang–Parr density-functional method
PA	pairwise-additive fragmentation method
PB	Poisson–Boltzmann solvation
PBE	Perdew–Burke–Ernzerhof density-functional method
PCM	polarized continuum model solvation method
PDDG/PM3	pairwise distance-directed Gaussian PM3 method (semiempirical method)
PE	polarized embedding for QM/MM
PI	predictive index
PM3	parametrized model 3 (semiempirical method)
PM6	parametrized model 6 (semiempirical method)
PMISP	polarizable multipole interaction with supermolecular pair fragmentation method
PW6B95	Truhlar hybrid functional for kinetics
QM	quantum mechanics
QM/MM	combined QM and MM calculations
QM/QM	combination of several QM methods
QSAR	quantitative structure–activity relationship
QZP	quadruple- ζ basis set
R	receptor
R^2	correlation coefficient
RL	receptor–ligand complex
RM1	reparametrized model 1 (semiempirical method)
RMSD	root-mean-squared deviation
SASA	solvent-accessible surface-area solvation
SCC-DFTB	self-consistent charge density-functional-based tight binding semiempirical method
SEQM	semiempirical quantum-mechanical methods
SIBFA	sum of interactions between fragments ab initio computed polarizable force field
SMD	solvation model based on density
ssEA	single-step exponential averaging
SVP	split-valence basis set
SZ	minimal basis set
SZP	minimal basis set with polarizing functions

TPSS	Tao–Perdew–Staroverov–Scuseria density-functional method
TZP	triple- ζ basis set
τ	Kendall's rank correlation coefficient
τ_{90}	Kendall's rank correlation coefficient, based on only statistically significant pairs

REFERENCES

- (1) Gohlke, H.; Klebe, G. Approaches to the Description and Prediction of the Binding Affinity of Small-molecule Ligands to Macromolecular Receptors. *Angew. Chem., Int. Ed.* **2002**, *41*, 2644–2676.
- (2) Warren, G. L.; Andrews, C. W.; Capelli, A.-M.; Clarke, B.; LaLonde, J.; Lambert, M. H.; Lindvall, M.; Nevins, N.; Semus, S. F.; Senger, S.; et al. A Critical Assessment of Docking Programs and Scoring Functions. *J. Med. Chem.* **2006**, *49*, 5912–5931.
- (3) Cross, J. B.; Thompson, D. C.; Rai, B. K.; Baber, J. C.; Fan, K. Y.; Hu, Y.; Humblet, C. Comparison of Several Molecular Docking Programs: Pose Prediction and Virtual Screening Accuracy. *J. Chem. Inf. Model.* **2009**, *49*, 1455–1474.
- (4) Brandsdal, B. O.; Österberg, F.; Almlöf, M.; Feierberg, I.; Luzhkov, V. B.; Åqvist, J. Free Energy Calculations and Ligand Binding. *Adv. Protein Chem.* **2003**, *66*, 123–158.
- (5) Kollman, P. A.; Massova, I.; Reyes, C.; Kuhn, B.; Huo, S.; Chong, L.; Lee, M.; Lee, T.; Duan, Y.; Wang, W.; et al. Calculating Structures and Free Energies of Complex Molecules: Combining Molecular Mechanics and Continuum Models. *Acc. Chem. Res.* **2000**, *33*, 889–897.
- (6) Hansen, N.; van Gunsteren, W. F. Practical Aspects of Free-Energy Calculations: A Review. *J. Chem. Theory Comput.* **2014**, *10*, 2632–2647.
- (7) Mobley, D. L.; Klimovich, P. V. Perspective: Alchemical Free Energy Calculations for Drug Discovery. *J. Chem. Phys.* **2012**, *137*, 230901.
- (8) Peters, M. B.; Raha, K.; Merz, K. M. Quantum Mechanics in Structure-Based Drug Design. *Curr. Opin. Drug Discovery Dev.* **2006**, *9*, 370–379.
- (9) Cavalli, A.; Carloni, P.; Recanatini, M. Target-Related Applications of First Principles Quantum Chemical Methods in Drug Design. *Chem. Rev.* **2006**, *106*, 3497–3519.
- (10) Raha, K.; Peters, M. B.; Wang, B.; Yu, N.; Wollacott, A. M.; Westerhoff, L. M.; Merz, K. M. The Role of Quantum Mechanics in Structure-Based Drug Design. *Drug Discovery Today* **2007**, *12*, 725–731.
- (11) Gleeson, M. P.; Gleeson, D. QM/MM Calculations in Drug Discovery: A Useful Method for Studying Binding Phenomena? *J. Chem. Inf. Model.* **2009**, *49*, 670–677.
- (12) Zhou, T.; Huang, D.; Cafilisch, A. Quantum Mechanical Methods for Drug Design. *Curr. Top. Med. Chem.* **2010**, *10*, 33–45.
- (13) Menikarachchi, L. C.; Gascón, J. A. QM/MM Approaches in Medicinal Chemistry Research. *Curr. Top. Med. Chem.* **2010**, *10*, 46–54.
- (14) Söderhjelm, P.; Kongsted, J.; Genheden, S.; Ryde, U. Estimates of Ligand-Binding Affinities Supported by Quantum Mechanical Methods. *Interdiscip. Sci.: Comput. Life Sci.* **2010**, *2*, 21–37.
- (15) Jing, Y.-Q.; Han, K.-L. Quantum Mechanical Effect in Protein–Ligand Interaction. *Expert Opin. Drug Discovery* **2010**, *5*, 33–49.
- (16) De Vivo, M. Bridging Quantum Mechanics and Structure-Based Drug Design. *Front. Biosci., Landmark Ed.* **2011**, *16*, 1619–1626.
- (17) Söderhjelm, P.; Genheden, S.; Ryde, U. Quantum Mechanics in Structure-Based Ligand Design. In *Protein–Ligand Interactions*; Gohlke, H., Ed.; Methods and Principles in Medicinal Chemistry, Vol. 53; Wiley-VCH Verlag: Weinheim, Germany, 2012; pp 121–143.
- (18) Lodola, A.; De Vivo, M. The Increasing Role of QM/MM in Drug Discovery. *Adv. Protein Chem. Struct. Biol.* **2012**, *87*, 337–362.
- (19) Lepšák, M.; Rezác, J.; Kolár, M.; Pecina, A.; Hobza, P.; Fanfrlík, J. The Semiempirical Quantum Mechanical Scoring Function for in Silico Drug Design. *ChemPlusChem* **2013**, *78*, 921–931.
- (20) Mucs, D.; Bryce, R. A. The Application of Quantum Mechanics in Structure-Based Drug Design. *Expert Opin. Drug Discovery* **2013**, *8*, 263–276.

- (21) Wong, C. F.; Bairy, S. Drug Design for Protein Kinases and Phosphatases: Flexible-Receptor Docking, Binding Affinity and Specificity, and Drug-Binding Kinetics. *Curr. Pharm. Des.* **2013**, *19*, 4739–4754.
- (22) Ilatovskiy, A. V.; Abagyan, R.; Kufareva, I. Quantum Mechanics Approaches to Drug Research in the Era of Structural Chemogenomics. *Int. J. Quantum Chem.* **2013**, *113*, 1669–1675.
- (23) Bryce, R. A. Physics-Based Scoring of Protein–Ligand Interactions: Explicit Polarizability, Quantum Mechanics and Free Energies. *Future Med. Chem.* **2011**, *3*, 683–698.
- (24) Bryce, R. A.; Hillier, I. H. Quantum Chemical Approaches: Semiempirical Molecular Orbital and Hybrid Quantum Mechanical/Molecular Mechanical Techniques. *Curr. Pharm. Des.* **2014**, *20*, 3293–3302.
- (25) Reddy, M. R.; Reddy, C. R.; Rathore, R. S.; Erion, M. D.; Aparoy, P.; Reddy, R. N.; Reddanna, P. Free Energy Calculations to Estimate Ligand-Binding Affinities in Structure-Based Drug Design. *Curr. Pharm. Des.* **2014**, *20*, 3323–3341.
- (26) Jensen, J. H. Predicting Accurate Absolute Binding Energies in Aqueous Solution: Thermodynamic Considerations for Electronic Structure Methods. *Phys. Chem. Chem. Phys.* **2015**, *17*, 12441–12451.
- (27) Li, X.; He, X.; Wang, B.; Merz, K. Conformational Variability of Benzamidinium-Based Inhibitors. *J. Am. Chem. Soc.* **2009**, *131*, 7742–7754.
- (28) Cho, A. E.; Guallar, V.; Berne, B. J.; Friesner, R. Importance of Accurate Charges in Molecular Docking: Quantum Mechanical/Molecular Mechanical (QM/MM) Approach. *J. Comput. Chem.* **2005**, *26*, 915–931.
- (29) Weis, A.; Katebzadeh, K.; Söderhjelm, P.; Nilsson, I.; Ryde, U. Ligand Affinities Predicted with the MM/PBSA Method: Dependence on the Simulation Method and the Force Field. *J. Med. Chem.* **2006**, *49*, 6596–6606.
- (30) Söderhjelm, P.; Ryde, U. Conformational Dependence of Charges in Protein Simulations. *J. Comput. Chem.* **2009**, *30*, 750–760.
- (31) Genheden, S.; Söderhjelm, P.; Ryde, U. Transferability of Conformational Dependent Charges From Protein Simulations. *Int. J. Quantum Chem.* **2012**, *112*, 1768–1785.
- (32) Fischer, B.; Fukuzawa, K.; Wenzel, W. Receptor-Specific Scoring Functions Derived From Quantum Chemical Models Improve Affinity Estimates for in-Silico Drug Discovery. *Proteins: Struct., Funct., Genet.* **2008**, *70*, 1264–1273.
- (33) Liu, J.; He, X.; Zhang, J. Z. H. Improving the Scoring of Protein–Ligand Binding Affinity by Including the Effects of Structural Water and Electronic Polarization. *J. Chem. Inf. Model.* **2013**, *53*, 1306–1314.
- (34) Wang, J.; Shao, Q.; Cossins, B. P.; Shi, J.; Chen, K.; Zhu, W. Thermodynamics Calculation of Protein-Ligand Interactions by QM/MM Polarizable Charge Parameters. *J. Biomol. Struct. Dyn.* **2016**, *34*, 163–176.
- (35) Tripathi, S. K.; Soundarya, R. N.; Singh, P.; Singh, S. K. Comparative Analysis of Various Electrostatic Potentials on Docking Precision Against Cyclin-Dependent Kinase 2 Protein: A Multiple Docking Approach. *Chem. Biol. Drug Des.* **2015**, *85*, 107–118.
- (36) Karelson, M.; Lobanov, V. S.; Katritzky, A. R. Quantum-Chemical Descriptors in QSAR/QSPR Studies. *Chem. Rev.* **1996**, *96*, 1027–1044.
- (37) Helguera, A. M.; Combes, R. D.; Gonzalez, M. P.; Cordeiro, M. N. D. S. Applications of 2D Descriptors in Drug Design: A Dragon Tale. *Curr. Top. Med. Chem.* **2008**, *8*, 1628–1655.
- (38) De Benedetti, P. G.; Fanelli, F. Multiscale Quantum Chemical Approaches to QSAR Modeling and Drug Design. *Drug Discovery Today* **2014**, *19*, 1921–1927.
- (39) Alzate-Morales, J.; Caballero, J. Computational Study of the Interactions between Guanine Derivatives and Cyclin-Dependent Kinase 2 (CDK2) by CoMFA and QM/MM. *J. Chem. Inf. Model.* **2010**, *50*, 110–122.
- (40) El Kerdawy, A.; Güssregen, S.; Matter, H.; Hennemann, M.; Clark, T. Quantum Mechanics-Based Properties for 3D-QSAR. *J. Chem. Inf. Model.* **2013**, *53*, 1486–1502.
- (41) Braga, R. C.; Andrade, C. H. *Mini-Rev. Med. Chem.* **2012**, *12*, 573–582.
- (42) Blomberg, M. R. A.; Borowski, T.; Himo, F.; Liao, R.-Z.; Siegbahn, P. E. M. Quantum Chemical Studies of Mechanisms for Metalloenzymes. *Chem. Rev.* **2014**, *114*, 3601–3658.
- (43) Siegbahn, P. E. M.; Himo, F. Recent Developments of the Quantum Chemical Cluster Approach for Modeling Enzyme Reactions. *J. Biol. Inorg. Chem.* **2009**, *14*, 643–651.
- (44) Senn, H. M.; Thiel, W. QM/MM Methods for Biomolecular Systems. *Angew. Chem., Int. Ed.* **2009**, *48*, 1198–1229.
- (45) Lin, H.; Truhlar, D. G. QM/MM: What Have We Learned, Where Are We, and Where Do We Go From Here? *Theor. Chem. Acc.* **2007**, *117*, 185–199.
- (46) Jensen, F. *Introduction to Computational Chemistry*; John Wiley & Sons: Chichester, U.K., 2007.
- (47) Cramer, C. J. *Essentials of Computational Chemistry: Theories and Models*; John Wiley & Sons: Chichester, U.K., 2006.
- (48) Hartree, D. R. The Wave Mechanics of an Atom with a Non-Coulomb Central Field. Part I. Theory and Methods. *Math. Proc. Cambridge Philos. Soc.* **1928**, *24*, 89–132.
- (49) Fock, V. Selfconsistent Field mit Austausch für Natrium. *Eur. Phys. J. A* **1930**, *62*, 795–805.
- (50) Møller, C.; Plesset, M. S. Note on an Approximation Treatment for Many-Electron Systems. *Phys. Rev.* **1934**, *46*, 618–622.
- (51) Raghavachari, K.; Trucks, G. W.; Pople, J. A.; Head-Gordon, M. A Fifth-Order Perturbation Comparison of Electron Correlation Theories. *Chem. Phys. Lett.* **1989**, *157*, 479–483.
- (52) Thiel, W. Semiempirical Quantum–Chemical Methods. *WIREs Comput. Mol. Sci.* **2014**, *4*, 145–157.
- (53) Dewar, M. J. S.; Zoebisch, E. G.; Healy, E. F.; Stewart, J. J. P. AM1: A New General Purpose Quantum Mechanical Molecular Model. *J. Am. Chem. Soc.* **1985**, *107*, 3902–3909.
- (54) Rocha, G. B.; Freire, R. O.; Simas, A. M.; Stewart, J. J. P. *J. Comput. Chem.* **2006**, *27*, 1101.
- (55) Stewart, J. J. P. Optimization of Parameters for Semiempirical Methods I. Method. *J. Comput. Chem.* **1989**, *10*, 209–220.
- (56) Repasky, M. P.; Chandrasekhar, J.; Jorgensen, W. L. PDDG/PM3 and PDDG/MNDO: Improved Semiempirical Methods. *J. Comput. Chem.* **2002**, *23*, 1601–1622.
- (57) Stewart, J. J. P. Optimization of Parameters for Semiempirical Methods V: Modification of NDDO Approximations and Application to 70 Elements. *J. Mol. Model.* **2007**, *13*, 1173–1213.
- (58) Weber, W.; Thiel, W. Orthogonalization Corrections for Semiempirical Methods. *Theor. Chem. Acc.* **2000**, *103*, 495–506.
- (59) Rezáč, J.; Fanfrlík, J.; Salahub, D.; Hobza, P. Semiempirical Quantum Chemical PM6Method Augmented by Dispersion and H-Bonding Correction Terms Reliably Describes Various Types of Noncovalent Complexes. *J. Chem. Theory Comput.* **2009**, *5*, 1749–1760.
- (60) Korth, M.; Pitonák, M.; Rezáč, J.; Hobza, P. A Transferable H-Bond Correction for Semiempirical Quantum-Chemical Methods. *J. Chem. Theory Comput.* **2010**, *6*, 344–352.
- (61) Rezáč, J.; Hobza, P. A Halogen-Bonding Correction for the Semiempirical PM6Method. *Chem. Phys. Lett.* **2011**, *506*, 286–289.
- (62) Rezáč, J.; Hobza, P. Advanced Corrections of Hydrogen Bonding and Dispersion for Semiempirical Quantum Mechanical Methods. *J. Chem. Theory Comput.* **2012**, *8*, 141–151.
- (63) Hohenberg, P.; Kohn, W. Inhomogeneous Electron Gas. *Phys. Rev.* **1964**, *136*, B864–B871.
- (64) Kohn, W.; Sham, L. J. Self-Consistent Equations Including Exchange and Correlation Effects. *Phys. Rev.* **1965**, *140*, A1133–A1138.
- (65) Becke, A. D. Density-functional Exchange-Energy Approximation with Correct Asymptotic Behavior. *Phys. Rev. A: At., Mol., Opt. Phys.* **1988**, *38*, 3098–3100.
- (66) Perdew, J. P. Density-functional Approximation for the Correlation Energy of the Inhomogeneous Electron Gas. *Phys. Rev. B: Condens. Matter Mater. Phys.* **1986**, *33*, 8822–8824.
- (67) Perdew, J. P.; Burke, K.; Ernzerhof, M. Generalized Gradient Approximation Made Simple. *Phys. Rev. Lett.* **1996**, *77*, 3865–3868.
- (68) Tao, J.; Perdew, J. P.; Staroverov, V. N.; Scuseria, G. E. Climbing the Density Functional Ladder: Nonempirical Meta-Generalized

Gradient Approximation Designed for Molecules and Solids. *Phys. Rev. Lett.* **2003**, *91*, 146401.

(69) Zhao, Y.; Truhlar, D. G. The M06 Suite of Density Functionals for Main Group Thermochemistry, Thermochemical Kinetics, Non-covalent Interactions, Excited States, and Transition Elements: Two New Functionals and Systematic Testing of Four M06-Class Functionals and 12 Other Functionals. *Theor. Chem. Acc.* **2008**, *120*, 215–241.

(70) Adamo, C.; Barone, V. Exchange Functionals with Improved Longrange Behavior and Adiabatic Connection Methods without Adjustable Parameters: The Mpw and Mpw1pw Models. *J. Chem. Phys.* **1998**, *108*, 664–675.

(71) Lee, C. T.; Yang, W. T.; Parr, R. G. Development of the Colle-Salvetti Correlation-Energy Formula into a Functional of the Electron Density. *Phys. Rev. B: Condens. Matter Mater. Phys.* **1988**, *37*, 785–789.

(72) Becke, A. D. Density-functional Thermochemistry. III. The Role of Exact Exchange. *J. Chem. Phys.* **1993**, *98*, 5648–5652.

(73) Becke, A. D. A New Mixing of Hartree-Fock and Local Density-Functional Theories. *J. Chem. Phys.* **1993**, *98*, 1372–1377.

(74) Zhao, Y.; Truhlar, D. G. Design of Density Functionals That Are Broadly Accurate for Thermochemistry, Thermochemical Kinetics, and Nonbonded Interactions. *J. Phys. Chem. A* **2005**, *109*, 5656–5667.

(75) Grimme, S.; Antony, J.; Schwabe, T.; Mück-Lichtenfeld, C. Density Functional Theory with Dispersion Corrections for Supramolecular Structures, Aggregates, and Complexes of (Bio)Organic Molecules. *Org. Biomol. Chem.* **2007**, *5*, 741–758.

(76) Grimme, S. Density Functional Theory with London Dispersion Corrections. *WIREs Comput. Mol. Sci.* **2011**, *1*, 211–228.

(77) Grimme, S. Semiempirical GGA-type Density-Functional Constructed with A Long-Range Dispersion Correction. *J. Comput. Chem.* **2006**, *27*, 1787–1799.

(78) Grimme, S.; Antony, J.; Ehrlich, S.; Krieg, H. A Consistent and Accurate Ab Initio Parametrization of Density Functional Dispersion Correction (DFT-D) for the 94 Elements H–Pu. *J. Chem. Phys.* **2010**, *132*, 154104.

(79) Grimme, S.; Ehrlich, S.; Goerigk, L. Effect of the Damping Function in Dispersion Corrected Density Functional Theory. *J. Comput. Chem.* **2011**, *32*, 1456–1465.

(80) Risthaus, T.; Grimme, S. Benchmarking of London Dispersion-Accounting Density Functional Theory Methods on Very Large Molecular Complexes. *J. Chem. Theory Comput.* **2013**, *9*, 1580–1591.

(81) Burns, L. A.; Vázquez-Mayagoitia, A.; Sumpter, B. G.; Sherrill, C. D. Density-functional Approaches to Noncovalent Interactions: A Comparison of Dispersion Corrections (DFT-D), Exchange-Hole Dipole Moment (XDM) Theory, and Specialized Functionals. *J. Chem. Phys.* **2011**, *134*, 084107.

(82) Otero-de-la-Roza, A.; Johnson, E. R. Predicting Energetics of Supramolecular Systems Using the XDM Dispersion Model. *J. Chem. Theory Comput.* **2015**, *11*, 4033–4040.

(83) Porezag, D.; Frauenheim, T.; Köhler, T.; Seifert, G.; Kaschner, R. Construction of Tight-Binding-Like Potentials on the Basis of Density-Functional Theory: Application to Carbon. *Phys. Rev. B: Condens. Matter Mater. Phys.* **1995**, *51*, 12947–12957.

(84) Elstner, M.; Porezag, D.; Jungnickel, G.; Elsner, J.; Haugk, M.; Frauenheim, T.; Suhai, S.; Seifert, G. Self-Consistent-Charge Density-Functional Tight-Binding Method for Simulations of Complex Materials Properties. *Phys. Rev. B: Condens. Matter Mater. Phys.* **1998**, *58*, 7260–7268.

(85) Gaus, M.; Cui, Q.; Elstner, M. DFTB3: Extension of the Self-Consistent-Charge Density-Functional Tight-Binding Method (SCC-DFTB). *J. Chem. Theory Comput.* **2011**, *7*, 931–948.

(86) Elstner, M.; Hobza, P.; Frauenheim, T.; Suhai, S.; Kaxiras, E. Hydrogen Bonding and Stacking Interactions of Nucleic Acid Base Pairs: A Density-Functional-Theory Based Treatment. *J. Chem. Phys.* **2001**, *114*, 5149.

(87) Brandenburg, J. G.; Hochheim, M.; Bredow, T.; Grimme, S. Low-Cost Quantum Chemical Methods for Noncovalent Interactions. *J. Phys. Chem. Lett.* **2014**, *5*, 4275–4284.

(88) Hehre, W. J.; Ditchfield, R.; Pople, J. A. Self-Consistent Molecular Orbital Methods. 12. Further Extensions of Gaussian-type Basis Sets for use in Molecular-orbital Studies of Organic-molecules. *J. Chem. Phys.* **1972**, *56*, 2257.

(89) Weigend, F.; Ahlrichs, R. Balanced Basis Sets of Split Valence, Triple Zeta Valence and Quadruple Zeta Valence Quality for H to Rn: Design and Assessment of Accuracy. *Phys. Chem. Chem. Phys.* **2005**, *7*, 3297–3305.

(90) Kendall, R. A.; Dunning, T. H.; Harrison, R. J. Electron Affinities of the First-Row Atoms Revisited. Systematic Basis Sets and Wave Functions. *J. Chem. Phys.* **1992**, *96*, 6796–6806.

(91) Krishnan, R.; Binkley, J. S.; Seeger, R.; Pople, J. A. Self-Consistent Molecular Orbital Methods. 20. A Basis Set for Correlated Wave Functions. *J. Chem. Phys.* **1980**, *72*, 650–654.

(92) Rappoport, D.; Furche, F. Property-Optimized Gaussian Basis Sets for Molecular Response Calculations. *J. Chem. Phys.* **2010**, *133*, 134105.

(93) Boys, S. F.; Bernardi, F. The Calculation of Small Molecular Interactions by the Differences of Separate Total Energies. Some Procedures with Reduced Errors. *Mol. Phys.* **1970**, *19*, 553–566.

(94) Halkier, A.; Klopper, W.; Helgaker, T.; Jørgensen, P.; Taylor, P. R. Basis Set Convergence of the Interaction Energy of Hydrogen-Bonded Complexes. *J. Chem. Phys.* **1999**, *111*, 9157–9167.

(95) Tarakeswar, P.; Choi, H. S.; Lee, S. J.; Lee, J. Y.; Kim, K. S.; Ha, T.-K.; Jang, J. H.; Lee, J. G.; Lee, H. A Theoretical Investigation of the Nature of the π -H interaction in ethene-H₂O, benzene-H₂O, and benzene-(H₂O)(2). *J. Chem. Phys.* **1999**, *111*, 5838–5850.

(96) Kim, K. S.; Tarakeswar, P.; Lee, J. Y. Molecular Clusters of π -Systems: Theoretical Studies of Structures, Spectra, and Origin of Interaction Energies. *Chem. Rev.* **2000**, *100*, 4145–4186.

(97) Valdés, H.; Sordo, J. A. Ab Initio Study on the (OCS)₂-CO₂ van der Waals Trimers. *J. Phys. Chem. A* **2002**, *106*, 3690–3701.

(98) Antony, J.; Grimme, S.; Liakos, D. G.; Neese, F. Protein-Ligand Interaction Energies with Dispersion Corrected Density Functional Theory and High-Level Wave Function Based Methods. *J. Phys. Chem. A* **2011**, *115*, 11210–11220.

(99) Graton, J.; Le Questel, J.-Y.; Legouin, B.; Uriac, P.; Van de Weghe, P.; Jacquemin, D. A DFT-D Evaluation of the Complexation of a Molecular Tweezer with Small Aromatic Molecules. *Chem. Phys. Lett.* **2012**, *522*, 11–16.

(100) Hampel, C.; Werner, H.-J. Local Treatment of Electron Correlation in Coupled Cluster Theory. *J. Chem. Phys.* **1996**, *104*, 6286–6295.

(101) Werner, H.-J.; Schütz, M. An Efficient Local Coupled Cluster Method for Accurate Thermochemistry of Large Systems. *J. Chem. Phys.* **2011**, *135*, 144116.

(102) Riplinger, C.; Sandhoefer, B.; Hansen, A.; Neese, F. Natural Triple Excitations in Local Coupled Cluster Calculations with Pair Natural Orbitals. *J. Chem. Phys.* **2013**, *139*, 134101.

(103) Fedorov, D. G.; Kitaura, K. Extending the Power of Quantum Chemistry to Large Systems with the Fragment Molecular Orbital Method. *J. Phys. Chem. A* **2007**, *111*, 6904–6914.

(104) Fedorov, D. G.; Nagata, T.; Kitaura, K. Exploring Chemistry with the Fragment Molecular Orbital Method. *Phys. Chem. Chem. Phys.* **2012**, *14*, 7562–7577.

(105) Fedorov, D. G.; Kitaura, K.; Li, H.; Jensen, J. H.; Gordon, M. S. The Polarizable Continuum Model (PCM) Interfaced with the Fragment Molecular Orbital Method (FMO). *J. Comput. Chem.* **2006**, *27*, 976–985.

(106) Watanabe, H.; Okiyama, Y.; Nakano, T.; Tanaka, S. Incorporation of Solvation Effects Into the Fragment Molecular Orbital Calculations with the Poisson-Boltzmann Equation. *Chem. Phys. Lett.* **2010**, *500*, 116–119.

(107) Nagata, T.; Fedorov, D. G.; Kitaura, K.; Gordon, M. S. A Combined Effective Fragment Potential-fragment Molecular Orbital Method. I. The Energy Expression and Initial Applications. *J. Chem. Phys.* **2009**, *131*, 024101.

- (108) Söderhjelm, P.; Öhrn, A.; Ryde, U.; Karlström, G. Accuracy of Typical Approximations in Classical Models of Intermolecular Polarization. *J. Chem. Phys.* **2008**, *128*, 014102.
- (109) Zhang, D. W.; Zhang, J. Z. H. Molecular Fractionation with Conjugate Caps for Full Quantum Mechanical Calculation of Protein–Molecule Interaction Energy. *J. Chem. Phys.* **2003**, *119*, 3599–3605.
- (110) Dahlke, E. E.; Truhlar, D. G. Electrostatically Embedded Many-Body Expansion for Large Systems, with Applications to Water Clusters. *J. Chem. Theory Comput.* **2007**, *3*, 46–53.
- (111) He, X.; Zhu, T.; Wang, X.; Liu, J.; Zhang, J. Z. H. Fragment Quantum Mechanical Calculation of Proteins and Its Applications. *Acc. Chem. Res.* **2014**, *47*, 2748–2757.
- (112) Söderhjelm, P.; Ryde, U. How Accurate Can A Force Field Become? - A Polarizable Multipole Model Combined with Fragment-Wise Quantum-Mechanical Calculations. *J. Phys. Chem. A* **2009**, *113*, 617–627.
- (113) Steinmann, C.; Fedorov, D. G.; Jensen, J. H. Effective Fragment Molecular Orbital Method: A Merger of the Effective Fragment Potential and Fragment Molecular Orbital Methods. *J. Phys. Chem. A* **2010**, *114*, 8705–8712.
- (114) Ochsenfeld, C.; Kussmann, J.; Lambrecht, D. S. Linear-Scaling Methods in Quantum Chemistry. In *Reviews in Computational Chemistry*; Lipkowitz, K. B., Cundari, T. L., Eds.; VCH Publishers: New York, 2007; Vol. 23, pp 1–82.
- (115) Yang, W. Direct Calculation of Electron Density in Density-Functional Theory. *Phys. Rev. Lett.* **1991**, *66*, 1438–1441.
- (116) Lopes, P. E. M.; Roux, B.; MacKerell, A. D. Molecular Modeling and Dynamics Studies with Explicit Inclusion of Electronic Polarizability: Theory and Applications. *Theor. Chem. Acc.* **2009**, *124*, 11–28.
- (117) Gresh, N.; Cisneros, G. A.; Darden, T. A.; Piquemal, J.-P. Anisotropic, Polarizable Molecular Mechanics Studies of Inter- and Intramolecular Interactions and Ligand-Macromolecule Complexes. A Bottom-Up Strategy. *J. Chem. Theory Comput.* **2007**, *3*, 1960–1986.
- (118) Gordon, M. S.; Slipchenko, L. V.; Li, H.; Jensen, J. H. The Effective Fragment Potential: A General Method for Predicting Intermolecular Interactions. *Annu. Rep. Comput. Chem.* **2007**, *3*, 177–193.
- (119) Engkvist, O.; Åstrand, P.-O.; Karlström, G. Accurate Intermolecular Potentials Obtained from Molecular Wave Functions: Bridging the Gap between Quantum Chemistry and Molecular Simulations. *Chem. Rev.* **2000**, *100*, 4087–4108.
- (120) Sumowski, Ochsenfeld. A Convergence Study of QM/MM Isomerization Energies with the Selected Size of the {Qm} Region for Peptidic Systems. *J. Phys. Chem. A* **2009**, *113*, 11734–11741.
- (121) Hu, L.; Eliasson, J.; Heimdal, J.; Ryde, U. Do Quantum Mechanical Energies Calculated for Small Models of Protein Active Sites Converge? *J. Phys. Chem. A* **2009**, *113*, 11793–11800.
- (122) Sumner, S.; Söderhjelm, P.; Ryde, U. Effect of Geometry Optimisations on QM-Cluster and QM/MM Studies of Reaction Energies in Proteins. *J. Chem. Theory Comput.* **2013**, *9*, 4205–4214.
- (123) Liao, R.-Z.; Thiel, W. On the Effect of Varying Constraints in the Quantum Mechanics Only Modeling of Enzymatic Reactions: The Case of Acetylene Hydratase. *J. Phys. Chem. B* **2013**, *117*, 3954–3961.
- (124) Svensson, M.; Humbel, S.; Froese, R. D. J.; Matsubara, T.; Sieber, S.; Morokuma, K. NIOM: A Multilayered Integrated MO + MM Method for Geometry Optimizations and Single Point Energy Predictions. A Test for Diels-Alder Reactions and Pt(P(t-Bu)₃)₂ + H₂ Oxidative Addition. *J. Phys. Chem.* **1996**, *100*, 19357–19363.
- (125) Hu, L.; Söderhjelm, P.; Ryde, U. On the convergence of QM/MM energies. *J. Chem. Theory Comput.* **2011**, *7*, 761–777.
- (126) Poulsen, T. D.; Kongsted, J.; Osted, A.; Ogilby, P. R.; Mikkelsen, K. V. The Combined Multiconfigurational Self-Consistent-Field Molecular Mechanics Wave Function Approach. *J. Chem. Phys.* **2001**, *115*, 2393–2400.
- (127) Söderhjelm, P.; Husberg, C.; Strambi, A.; Olivucci, M.; Ryde, U. Protein Influence on Electronic Spectra Modelled by Multipoles and Polarizabilities. *J. Chem. Theory Comput.* **2009**, *5*, 649–658.
- (128) Hu, H.; Yang, W. Development and Application of Ab Initio QM/MM Methods for Mechanistic Simulation of Reactions in Solution and in Enzymes. *J. Mol. Struct.: THEOCHEM* **2009**, *898*, 17–30.
- (129) Rod, T. H.; Ryde, U. Quantum Mechanical Free Energy Barrier for an Enzymatic Reaction. *Phys. Rev. Lett.* **2005**, *94*, 138302.
- (130) Hu, L.; Söderhjelm, P.; Ryde, U. Accurate Reaction Energies in Proteins Obtained by Combining QM/MM and Large QM Calculations. *J. Chem. Theory Comput.* **2013**, *9*, 640–649.
- (131) Liao, R.-Z.; Thiel, W. Convergence in the QM-Only and QM/MM Modeling of Enzymatic Reactions: A Case Study for Acetylene Hydratase. *J. Comput. Chem.* **2013**, *34*, 2389–2397.
- (132) Tomasi, J.; Mennucci, B.; Cammi, R. Quantum Mechanical Continuum Solvation Models. *Chem. Rev.* **2005**, *105*, 2999–3094.
- (133) Cossi, M.; Tomasi, J.; Cammi, R. Analytical Expressions of the Free-energy Derivatives for Molecules in Solution – Application to the Geometry Optimization. *Int. J. Quantum Chem.* **1995**, *56*, 695–702.
- (134) Miertus, S.; Scrocco, E.; Tomasi, J. Electrostatic Interaction of a Solute with a Continuum. A Direct Utilization of Ab initio Molecular Potentials for the Prediction of Solvent Effects. *Chem. Phys.* **1981**, *55*, 117–129.
- (135) Klamt, A.; Schuurmann, G. COSMO: a New Approach to Dielectric Screening in Solvents with Explicit Expressions for the Screening Energy and Its Gradient. *J. Chem. Soc., Perkin Trans. 2* **1993**, 799–805.
- (136) Hoijsink, G. J.; de Boer, E.; Van der Meij, P. H.; Weijland, E. P. The Generalized Born Approach. *Recl Trav Pays-Bas* **1956**, *75*, 487–503.
- (137) Still, W. C.; Tempczyk, A.; Hawley, R. C.; Hendrickson, T. Semianalytical Treatment of Solvation for Molecular Mechanics and Dynamics. *J. Am. Chem. Soc.* **1990**, *112*, 6127–6129.
- (138) Warwicker, J.; Watson, H. C. Calculation of the Electric Potential in the Active Site Cleft Due to α -Helix Dipoles. *J. Mol. Biol.* **1982**, *157*, 671–679.
- (139) Sharp, K. A.; Honig, B. Salt Effects on Nucleic Acids. *Curr. Opin. Struct. Biol.* **1995**, *5*, 323–328.
- (140) Floris, F.; Tomasi, J. Evaluation of the Dispersion Contribution to the Solvation Energy. A Simple Computational Model in the Continuum Approximation. *J. Comput. Chem.* **1989**, *10*, 616–627.
- (141) Barone, V.; Cossi, M.; Tomasi, J. A New Definition of Cavities for the Computation of Solvation Free Energies by the Polarizable Continuum Model. *J. Chem. Phys.* **1997**, *107*, 3210–3221.
- (142) Marenich, A. V.; Cramer, C. J.; Truhlar, D. G. Universal Solvation Model Based on Solute Electron Density and A Continuum Model of the Solvent Defined by the Bulk Dielectric Constant and Atomic Surface Tensions. *J. Phys. Chem. B* **2009**, *113*, 6378–6396.
- (143) Klamt, A. Conductor-like Screening Model for Real Solvents: A New Approach to the Quantitative Calculation of Solvation Phenomena. *J. Phys. Chem.* **1995**, *99*, 2224–2235.
- (144) Eckert, F.; Klamt, A. Fast Solvent Screening via Quantum Chemistry: COSMO-RS Approach. *AIChE J.* **2002**, *48*, 369–385.
- (145) Riley, K. E.; Pitonák, M.; Jurecka, P.; Hobza, P. Stabilization and Structure Calculations for Noncovalent Interactions in Extended Molecular Systems Based on Wave Function and Density Functional Theories. *Chem. Rev.* **2010**, *110*, 5023–5063.
- (146) Hobza, P. Calculations on Noncovalent Interactions and Databases of Benchmark Interaction Energies. *Acc. Chem. Res.* **2012**, *45*, 663–672.
- (147) Li, A.; Muddana, H. S.; Gilson, M. K. Quantum Mechanical Calculation of Noncovalent Interactions: A Large-Scale Evaluation of PMx, DFT, and SAPT Approaches. *J. Chem. Theory Comput.* **2014**, *10*, 1563–1575.
- (148) Faver, J. C.; Benson, M. L.; He, X.; Roberts, B. P.; Wang, B.; Marshall, M. S.; Kennedy, M. R.; Sherrill, C. D.; Merz, K. M. Formal Estimation of Errors in Computed Absolute Interaction Energies of Protein–Ligand Complexes. *J. Chem. Theory Comput.* **2011**, *7*, 790–797.
- (149) Faver, J. C.; Benson, M. L.; He, X.; Roberts, B. P.; Wang, B.; Marshall, M. S.; Sherrill, C. D.; Merz, K. M. The Energy Computation Paradox and Ab Initio Protein Folding. *PLoS One* **2011**, *6*, e18868.

- (150) Yilmazer, N. D.; Korth, M. Comparison of Molecular Mechanics, Semi-Empirical Quantum Mechanical, and Density Functional Theory Methods for Scoring Protein–Ligand Interactions. *J. Phys. Chem. B* **2013**, *117*, 8075–8084.
- (151) Yilmazer, N. D.; Heitel, P.; Schwabe, T.; Korth, M. Benchmark of Electronic Structure Methods for Protein–Ligand Interactions Based on High-Level Reference Data. *J. Theor. Comput. Chem.* **2015**, *14*, 1540001.
- (152) Kruse, H.; Grimme, S. A Geometrical Correction for the Inter- and Intra-Molecular Basis Set Superposition Error in Hartree–Fock and Density Functional Theory Calculations for Large Systems. *J. Chem. Phys.* **2012**, *136*, 154101.
- (153) Kruse, H.; Goerigk, L.; Grimme, S. Why the Standard B3LYP/6-31G* Model Chemistry should not be Used in DFT Calculations of Molecular Thermochemistry: Understanding and Correcting the Problem. *J. Org. Chem.* **2012**, *77*, 10824–10834.
- (154) Sure, R.; Grimme, S. Corrected Small Basis Set Hartree–Fock Method for Large Systems. *J. Comput. Chem.* **2013**, *34*, 1672–1685.
- (155) Grimme, S.; Brandenburg, J. G.; Bannwarth, C.; Hansen, A. Consistent Structures and Interactions by Density Functional Theory with Small Atomic Orbital Basis Sets. *J. Chem. Phys.* **2015**, *143*, 054107.
- (156) Muddana, H. S.; Gilson, M. K. Calculation of Host–Guest Binding Affinities Using a Quantum-Mechanical Energy Model. *J. Chem. Theory Comput.* **2012**, *8*, 2023–2033.
- (157) Ucisik, M. N.; Zheng, Z.; Faver, J. C.; Merz, K. M. Bringing Clarity to the Prediction of Protein–Ligand Binding Energies Via “Blurring”. *J. Chem. Theory Comput.* **2014**, *10*, 1314–1325.
- (158) Åqvist, J.; Medina, C.; Samuelsson, J.-E. A New Method for Predicting Binding Affinity in Computer-Aided Drug Design. *Protein Eng., Des. Sel.* **1994**, *7*, 385–391.
- (159) Åqvist, J.; Hansson, T. On the Validity of Electrostatic Linear Response in Polar Solvents. *J. Phys. Chem.* **1996**, *100*, 9512–9521.
- (160) Almlöf, M.; Carlsson, J.; Åqvist, J. Improving the Accuracy of the Linear Interaction Energy Method for Solvation Free Energies. *J. Chem. Theory Comput.* **2007**, *3*, 2162–2175.
- (161) Carlsson, J.; Boukharta, L.; Åqvist, J. Combining Docking, Molecular Dynamics and the Linear Interaction Energy Method to Predict Binding Modes and Affinities for Non-Nucleoside Inhibitors to HIV-1 Reverse Transcriptase. *J. Med. Chem.* **2008**, *51*, 2648–2656.
- (162) Foloppe, N.; Hubbard, R. Towards Predictive Ligand Design with Free-Energy Based Computational Methods? *Curr. Med. Chem.* **2006**, *13*, 3583–3608.
- (163) Carlson, H. A.; Jorgensen, W. L. An Extended Linear Response Method for Determining Free Energies of Hydration. *J. Phys. Chem.* **1995**, *99*, 10667–10673.
- (164) Tominaga, Y.; Jorgensen, W. L. General Model for Estimation of the Inhibition of Protein Kinases using Monte Carlo Simulations. *J. Med. Chem.* **2004**, *47*, 2534–2549.
- (165) Huang, D.; Caffisch, A. Efficient Evaluation of Binding Free Energy Using Continuum Electrostatics Solvation. *J. Med. Chem.* **2004**, *47*, 5791–5797.
- (166) Srinivasan, J.; Cheatham, T. E.; Cieplak, P.; Kollman, P. A.; Case, D. A. Continuum Solvent Studies of the Stability of DNA, RNA, and Phosphoramidate–DNA Helices. *J. Am. Chem. Soc.* **1998**, *120*, 9401–9409.
- (167) Genheden, S.; Ryde, U. The MM/PBSA and MM/GBSA Methods to Estimate Ligand-binding Affinities. *Expert Opin. Drug Discovery* **2015**, *10*, 449–461.
- (168) Zwanzig, R. W. High-Temperature Equation of State by a Perturbation Method. I. Nonpolar Gases. *J. Chem. Phys.* **1954**, *22*, 1420–1427.
- (169) Kirkwood, J. G. Statistical Mechanics of Fluid Mixtures. *J. Chem. Phys.* **1935**, *3*, 300–313.
- (170) Bennett, C. H. Efficient Estimation of Free Energy Differences from Monte Carlo Data. *J. Comput. Phys.* **1976**, *22*, 245–268.
- (171) Shirts, M. R.; Pande, V. S. Comparison of Efficiency and Bias of Free Energies Computed by Exponential Averaging, the Bennett Acceptance Ratio, and Thermodynamic Integration. *J. Chem. Phys.* **2005**, *122*, 144107.
- (172) Shirts, M. R.; Chodera, J. D. Statistically Optimal Analysis of Samples From Multiple Equilibrium States. *J. Chem. Phys.* **2008**, *129*, 124105.
- (173) Boresch, S.; Tettinger, F.; Leitgeb, M.; Karplus, M. Absolute Binding Free Energies: A Quantitative Approach for Their Calculation. *J. Phys. Chem. B* **2003**, *107*, 9535–9551.
- (174) Deng, Y.; Roux, B. Calculation of Standard Binding Free Energies: Aromatic Molecules in the T4 Lysozyme L99A Mutant. *J. Chem. Theory Comput.* **2006**, *2*, 1255–1273.
- (175) Pearlman, D. A.; Charifson, P. S. Are Free Energy Calculations Useful in Practice? A Comparison with Rapid Scoring Functions for the p38 MAP Kinase Protein System. *J. Med. Chem.* **2001**, *44*, 3417–3423.
- (176) Mikulskis, P.; Genheden, S.; Rydberg, P.; Sandberg, L.; Olsen, L.; Ryde, U. Binding Affinities of the SAMPL3 Trypsin and Host-Guest Blind Tests Estimated with the MM/PBSA and LIE Methods. *J. Comput.-Aided Mol. Des.* **2012**, *26*, 527–541.
- (177) Genheden, S.; Ryde, U. How to Obtain Statistically Converged MM/GBSA Results. *J. Comput. Chem.* **2010**, *31*, 837–846.
- (178) Kolár, M.; Fanfrlík, J.; Hobza, P. Ligand Conformational and Solvation/Desolvation Free Energy in Protein–Ligand Complex Formation. *J. Phys. Chem. B* **2011**, *115*, 4718–4724.
- (179) Moghaddam, S.; Yang, C.; Rekharsky, M.; Ko, Y. H.; Kim, K.; Inoue, Y.; Gilson, M. K. New Ultrahigh Affinity Host-Guest Complexes of Cucurbit[7]uril with Bicyclo[2.2.2]octane and Adamantane Guests: Thermodynamic Analysis and Evaluation of M2 Affinity Calculations. *J. Am. Chem. Soc.* **2011**, *133*, 3570–3581.
- (180) Chen, W.; Chang, C.-E.; Gilson, M. K. Calculation of Cyclodextrin Binding Affinities: Energy, Entropy, and Implications for Drug Design. *Biophys. J.* **2004**, *87*, 3035–3049.
- (181) Zhou, H.-X.; Gilson, M. K. Theory of Free Energy and Entropy in Noncovalent Binding. *Chem. Rev.* **2009**, *109*, 4092–4107.
- (182) Liu, L.; Guo, Q.-X. Isokinetic Relationship, Isoequilibrium Relationship, and Enthalpy–Entropy Compensation. *Chem. Rev.* **2001**, *101*, 673–696.
- (183) Sharp, K. Entropy–Enthalpy Compensation: Fact or Artifact? *Protein Sci.* **2001**, *10*, 661–667.
- (184) Chodera, J. D.; Mobley, D. L. Entropy–Enthalpy Compensation: Role and Ramifications in Biomolecular Ligand Recognition and Design. *Annu. Rev. Biophys.* **2013**, *42*, 121–142.
- (185) Ryde, U. A Fundamental View of Enthalpy–Entropy Compensation. *MedChemComm* **2014**, *5*, 1324–1336.
- (186) Ryde, U.; Olsen, L.; Nilsson, K. Quantum Chemical Geometry Optimisations in Proteins Using Crystallographic Raw Data. *J. Comput. Chem.* **2002**, *23*, 1058–1070.
- (187) Peräkylä, M.; Pakkanen, T. A. Quantum Mechanical Model Assembly Study on the Energetics of Binding of Arabinose, Fucose, and Galactose to L-Arabinose-Binding Protein. *Proteins: Struct., Funct., Genet.* **1994**, *20*, 367–372.
- (188) Peräkylä, M.; Pakkanen, T. A. Model Assembly Study of the Ligand Binding by P-Hydroxybenzoate Hydroxylase: Correlation between the Calculated Binding Energies and the Experimental Dissociation Constants. *Proteins: Struct., Funct., Genet.* **1995**, *21*, 22–29.
- (189) Nikitina, E.; Sulimov, V.; Zayets, V.; Zaitseva, N. Semiempirical Calculations of Binding Enthalpy for Protein–Ligand Complexes. *Int. J. Quantum Chem.* **2004**, *97*, 747–763.
- (190) Nikitina, E.; Sulimov, V.; Grigoriev, F.; Kondakova, O.; Luschekina, S. Mixed Implicit/Explicit Solvation Models in Quantum Mechanical Calculations of Binding Enthalpy for Protein–Ligand Complexes. *Int. J. Quantum Chem.* **2006**, *106*, 1943–1963.
- (191) Villar, R.; Gil, M. J.; García, J. I.; Martínez-Merino, V. Are AM1 Ligand-Protein Binding Enthalpies Good Enough for Use in the Rational Design of New Drugs? *J. Comput. Chem.* **2005**, *26*, 1347–1358.
- (192) Rosso, L.; Gee, A. D.; Gould, I. R. Ab initio Computational Study of Positron Emission Tomography Ligands Interacting with Lipid Molecule for the Prediction of Nonspecific Binding. *J. Comput. Chem.* **2008**, *29*, 2397–2405.
- (193) Shi, J. Y.; Lu, Z. A.; Zhang, Q. L.; Wang, M. L.; Wong, C. F.; Liu, J. H. Supplementing the PBSA Approach with Quantum Mechanics to Study the Binding between CDK2 and N-2-substituted O-6-Cyclo-

hexylmethoxyguanine Inhibitors. *J. Theor. Comput. Chem.* **2010**, *9*, 543–559.

(194) Casini, A.; EDAFE, F.; Erlandsson, M.; Gonsalvi, L.; Cincetta, A.; Re, N.; Ienco, A.; Messori, L.; Peruzzini, M.; Dyson, P. J. Rationalization of the Inhibition Activity of Structurally Related Organometallic Compounds against the Drug Target Cathepsin B by DFT. *Dalton Trans.* **2010**, *39*, 5556–5563.

(195) Cincetta, A.; Genheden, S.; Ryde, U. A QM/MM Study of the Binding of RAPTA Ligands to Cathepsin B. *J. Comput.-Aided Mol. Des.* **2011**, *25*, 729–742.

(196) Saen-oon, S.; Kuno, M.; Hannongbua, S. Binding Energy Analysis for Wild-Type and Y181C Mutant HIV-1 RT/8-Cl TIBO Complex Structures: Quantum Chemical Calculations Based on the ONIOM Method. *Proteins: Struct., Funct., Genet.* **2005**, *61*, 859–469.

(197) Saparpakorn, P.; Kobayashi, M.; Hannongbua, S.; Nakai, H. Divide-and-Conquer-Based Quantum Chemical Study for Interaction between HIV-1 Reverse Transcriptase and MK-4965 Inhibitor. *Int. J. Quantum Chem.* **2013**, *113*, 510–517.

(198) DeChancie, J.; Houk, K. N. The Origins of Femtomolar Protein-Ligand Binding: Hydrogen-Bond Cooperativity and Desolvation Energetics in the Biotin-(Strept)Avidin Binding Site. *J. Am. Chem. Soc.* **2007**, *129*, 5419–5429.

(199) Poongavanam, V.; Steinmann, C.; Kongsted, J. Inhibitor Ranking through QM based Chelation Calculations for Virtual Screening of HIV-1 RNase H Inhibition. *PLoS One* **2014**, *9*, e98659.

(200) Friesner, R. A.; Murphy, R. B.; Repasky, M. P.; Frye, L. L.; Greenwood, J. R.; Halgren, T. A.; Sanschagrin, P. C.; Mainz, D. T. Extra Precision Glide: Docking and Scoring Incorporating a Model of Hydrophobic Enclosure for Protein-Ligand Complexes. *J. Med. Chem.* **2006**, *49*, 6177–6196.

(201) Roos, K.; Viklund, J.; Meuller, J.; Kaspersson, K.; Svensson, M. Potency Prediction of β -Secretase (BACE-1) Inhibitors Using Density-Functional Methods. *J. Chem. Inf. Model.* **2014**, *54*, 818–825.

(202) Antony, J.; Sure, R.; Grimme, S. Using Dispersion-Corrected Density-Functional Theory to Understand Supramolecular Binding Thermodynamics. *Chem. Commun.* **2015**, *51*, 1764–1774.

(203) Moghaddam, S.; Inoue, Y.; Gilson, M. K. Host–Guest Complexes with Protein–Ligand-Like Affinities: Computational Analysis and Design. *J. Am. Chem. Soc.* **2009**, *131*, 4012–4021.

(204) Houk, K. N.; Menzer, S.; Newton, S. P.; Raymo, F. M.; Stoddart, J. F.; Williams, D. J. [C–H \cdots O] Interactions As A Control Element in Supramolecular Complexes: Experimental and Theoretical Evaluation of Receptor Affinities for the Binding of Bipyridinium-Based Guests by Catenated Hosts. *J. Am. Chem. Soc.* **1999**, *121*, 1479–1487.

(205) Parac, M.; Etinski, M.; Peric, M.; Grimme, S. A Theoretical Investigation of the Geometries and Binding Energies of Molecular Tweezer and Clip Host–Guest Systems. *J. Chem. Theory Comput.* **2005**, *1*, 1110–1118.

(206) Benitez, D.; Tkatchouk, E.; Yoon, I.; Stoddart, J. F.; Goddard, W. A. Experimentally-Based Recommendations of Density Functionals for Predicting Properties in Mechanically Interlocked Molecules. *J. Am. Chem. Soc.* **2008**, *130*, 14928–14929.

(207) Zhao, Y.; Truhlar, D. G. Computational Characterization and Modeling of Buckyball Tweezers: Density Functional Study of Concave–Convex π – π Interactions. *Phys. Chem. Chem. Phys.* **2008**, *10*, 2813–2818.

(208) Ryde, U.; Mata, R. A.; Grimme, S. Does DFT-D Estimate Accurate Energies for the Binding of Ligands to Metal Complexes? *Dalton Trans.* **2011**, *40*, 11176–11183.

(209) Li, J.-L.; Mata, R. A.; Ryde, U. Large Density-Functional and Basis-Set Effects for the DMSO Reductase Catalyzed Oxo-Transfer Reaction. *J. Chem. Theory Comput.* **2013**, *9*, 1799–1807.

(210) Grimme, S. Supramolecular Binding Thermodynamics by Dispersion-Corrected Density Functional Theory. *Chem. - Eur. J.* **2012**, *18*, 9955–9964.

(211) Hesselmann, A.; Korona, T. Intermolecular Symmetry-Adapted Perturbation Theory Study of Large Organic Complexes. *J. Chem. Phys.* **2014**, *141*, 094107.

(212) Ambrosetti, A.; Alfe, D.; DiStasio, R. A.; Tkatchenko, A. Hard Numbers for Large Molecules: Toward Exact Energetics for Supramolecular Systems. *J. Phys. Chem. Lett.* **2014**, *5*, 849–855.

(213) Sure, R.; Grimme, S. Comprehensive Benchmark of Association (Free) Energies of Realistic Host–Guest Complexes. *J. Chem. Theory Comput.* **2015**, *11*, 3785–3801.

(214) Sure, R.; Antony, J.; Grimme, S. Blind Prediction of Binding Affinities for Charged Supramolecular Host–Guest Systems: Achievements and Shortcomings of DFT-D3. *J. Phys. Chem. B* **2014**, *118*, 3431–3440.

(215) Muddana, H. S.; Fenley, A. T.; Mobley, D. L.; Gilson, M. K. The SAMPL4 Host–Guest Blind Prediction Challenge: An Overview. *J. Comput.-Aided Mol. Des.* **2014**, *28*, 305–317.

(216) Mikulskis, P.; Cioloboc, D.; Andrejic, M.; Khare, S.; Brorsson, J.; Genheden, S.; Mata, R. A.; Söderhjelm, P.; Ryde, U. Free-Energy Perturbation and Quantum Mechanical Study of SAMPL4 Octa-Acid Host–Guest Binding Energies. *J. Comput.-Aided Mol. Des.* **2014**, *28*, 375–400.

(217) Bannwarth, C.; Hansen, A.; Grimme, S. The Association of Two “Frustrated” Lewis Pairs by State-of-the-Art Quantum Chemical Methods. *Isr. J. Chem.* **2015**, *55*, 235–242.

(218) Alex, A.; Finn, P. Fast and Accurate Predictions of Relative Binding Energies. *J. Mol. Struct.: THEOCHEM* **1997**, *398–399*, 551–554.

(219) Hensen, C.; Hermann, J. C.; Nam, K.; Ma, S.; Gao, J.; Hölte, H.-D. A Combined QM/MM Approach to Protein-Ligand Interactions: Polarization Effects of the HIV-1 Protease on Selected High Affinity Inhibitors. *J. Med. Chem.* **2004**, *47*, 6673–6680.

(220) Li, Y.; Yang, Y.; He, P.; Yang, Q. QM/MM Study of Epitope Peptides Binding to HLA-A*0201: The Roles of Anchor Residues and Water. *Chem. Biol. Drug Des.* **2009**, *74*, 611–618.

(221) Gleeson, M. P.; Burton, N. A.; Hillier, I. H. Prediction of the Potency of Inhibitors of Adenosine Deaminase by QM/MM Calculations. *Chem. Commun.* **2003**, 2180–2181.

(222) Morgado, C. A.; Hillier, I. H.; Burton, N. A.; McDouall, J. J. W. A QM/MM study of Fluoroaromatic Interactions at the Binding Site of Carbonic Anhydrase II, Using A DFT Method Corrected for Dispersive Interactions. *Phys. Chem. Chem. Phys.* **2008**, *10*, 2706–2714.

(223) Li, Q.; Gusarov, S.; Evoy, S.; Kovalenko, A. Electronic Structure, Binding Energy, and Solvation Structure of the Streptavidin-Biotin Supramolecular Complex: ONIOM and 3D-RISM Study. *J. Phys. Chem. B* **2009**, *113*, 9958–9967.

(224) Jia, R.; Yang, L.-J.; Yang, S.-Y. Binding Energy Contributions of the Conserved Bridging Water Molecules in CDK2-Inhibitor Complexes: A Combined QM/MM Study. *Chem. Phys. Lett.* **2008**, *460*, 300–305.

(225) Tripathi, S. K.; Singh, S. K. Insights into the Structural Basis of 3,5-Diaminindazoles As CDK2 Inhibitors: Prediction of Binding Modes and Potency by QM–MM Interaction, MESP and MD Simulation. *Mol. Biosyst.* **2014**, *10*, 2189–2201.

(226) Yoshida, T.; Hitaoka, S.; Mashima, A.; Sugimoto, T.; Matoba, H.; Chuman, H. Combined QM/MM (ONIOM) and QSAR Approach to the Study of Complex Formation of Matrix Metalloproteinase 9 with A Series of Biphenylsulfonamides-LERE-QSAR Analysis (V). *J. Phys. Chem. B* **2012**, *116*, 10283–10289.

(227) Zhou, P.; Zou, J.; Tian, F.; Shang, Z. Fluorine Bonding. How Does It Work in Protein-Ligand Interactions? *J. Chem. Inf. Model.* **2009**, *49*, 2344–2355.

(228) Wittayanarakul, K.; Aruksakunwong, O.; Saen-oon, S.; Chantratita, W.; Parasuk, W.; Sompornpisut, P.; Hannongbua, S. Insights into Saquinavir Resistance in the G48V HIV-1 Protease: Quantum Calculations and Molecular Dynamic Simulations. *Biophys. J.* **2005**, *88*, 867–879.

(229) Saen-oon, S.; Aruksakunwong, O.; Wittayanarakul, K.; Sompornpisut, P.; Hannongbua, S. Insight Into Analysis of Interactions of Saquinavir with HIV-1 Protease in Comparison between the Wild-Type and G48V and G48V/L90M Mutants Based on QM and QM/MM Calculations. *J. Mol. Graphics Modell.* **2007**, *26*, 720–727.

- (230) Beierlein, F.; Lanig, H.; Schürer, G.; Horn, A. H. C.; Clark, T. Quantum Mechanical/Molecular Mechanical (QM/MM) Docking: An Evaluation for Known Test Systems. *Mol. Phys.* **2003**, *101*, 2469–2480.
- (231) Chaskar, P.; Zoete, V.; Röhrig, U. F. Toward on-the-Fly Quantum Mechanical/Molecular Mechanical (QM/MM) Docking: Development and Benchmark of a Scoring Function. *J. Chem. Inf. Model.* **2014**, *54*, 3137–3152.
- (232) Parks, J. M.; Kondru, R. K.; Hu, H.; Beratan, D. N.; Yang, W. Hepatitis C Virus NS5B Polymerase: QM/MM Calculations Show the Important Role of the Internal Energy in Ligand Binding. *J. Phys. Chem. B* **2008**, *112*, 3168–3176.
- (233) Burger, S. K.; Thompson, D. C.; Ayers, P. W. Quantum Mechanics/Molecular Mechanics Strategies for Docking Pose Refinement: Distinguishing between Binders and Decoys in Cytochrome c Peroxidase. *J. Chem. Inf. Model.* **2011**, *51*, 93–101.
- (234) Gleeson, M. P.; Gleeson, D. QM/MM As a Tool in Fragment Based Drug Discovery. A Cross-Docking, Rescoring Study of Kinase Inhibitors. *J. Chem. Inf. Model.* **2009**, *49*, 1437–1448.
- (235) GOLD; Cambridge Crystallography Data Centre Software Ltd.: Cambridge, England, 2013.
- (236) Cho, A. E.; Chung, J. Y.; Kim, M.; Park, K. Quantum Mechanical Scoring for Protein Docking. *J. Chem. Phys.* **2009**, *131*, 134108.
- (237) Tian, F.; Yang, L.; Lv, F.; Luo, X.; Pan, Y. Why OppA Protein can Bind Sequence-independent Peptides? A Combination of QM/MM, PB/SA, and Structure-based QSAR Analyses. *Amino Acids* **2011**, *40*, 493–503.
- (238) Tian, F.; Lv, F.; Zhou, P.; Yang, L. Characterization of PDZ Domain–peptide Interactions using an Integrated Protocol of QM/MM, PB/SA, and CFEA Analyses. *J. Comput.-Aided Mol. Des.* **2011**, *25*, 947–958.
- (239) Guo, X.; He, D.; Huang, L.; Liu, L.; Liu, L.; Yang, H. Strain Energy in Enzyme–Substrate Binding: An Energetic Insight Into the Flexibility Versus Rigidity of Enzyme Active Site. *Comput. Theor. Chem.* **2012**, *995*, 17–23.
- (240) Guo, X.; He, D.; Liu, L.; Kuang, R.; Liu, L. Use of QM/MM Scheme to Reproduce Macromolecule–Small Molecule Noncovalent Binding Energy. *Comput. Theor. Chem.* **2012**, *991*, 134–140.
- (241) Wang, M.; Wong, C. F. Rank-ordering Protein–Ligand binding Affinity by a Quantum Mechanics/Molecular Mechanics/Poisson–Boltzmann-Surface Area Model. *J. Chem. Phys.* **2007**, *126*, 026101.
- (242) Ai, X.; Sun, Y.; Wang, H.; Lu, S. A Systematic Profile of Clinical Inhibitors Responsive to EGFR Somatic Amino Acid Mutations in Lung Cancer: Implication for the Molecular Mechanism of Drug Resistance and Sensitivity. *Amino Acids* **2014**, *46*, 1635–1648.
- (243) Yang, L.; Mo, X.; Yang, H.; Dai, H.; Tan, F. Testing the Sensitivities of Noncognate Inhibitors to Varicella Zoster Virus Thymidine Kinase: Implications for Postherpetic Neuralgia Therapy with Existing Agents. *J. Mol. Model.* **2014**, *20*, 2321.
- (244) Zhou, Z.-G.; Yao, Q.-Z.; Lei, D.; Zhang, Q.-Q.; Zhang, J. Investigations on the Mechanisms of Interactions between Matrix Metalloproteinase 9 and Its Flavonoid Inhibitors Using A Combination of Molecular Docking, Hybrid Quantum Mechanical/Molecular Mechanical Calculations, and Molecular Dynamics Simulations. *Can. J. Chem.* **2014**, *92*, 821–830.
- (245) Hayik, S. A.; Dunbrack, R.; Merz, K. M. Mixed Quantum Mechanics/Molecular Mechanics Scoring Function to Predict Protein–Ligand Binding affinity. *J. Chem. Theory Comput.* **2010**, *6*, 3079–3091.
- (246) Raha, K.; Merz, K. M. A Quantum Mechanics-Based Scoring Function: Study of Zinc Ion-Mediated Ligand Binding. *J. Am. Chem. Soc.* **2004**, *126*, 1020–1021.
- (247) Brahmshatriya, P. S.; Dobes, P.; Fanfrlik, J.; Rezac, J.; Paruch, K.; Bronowska, A.; Lepsik, M.; Hobza, P. Quantum Mechanical Scoring: Structural and Energetic Insights into Cyclin-Dependent Kinase 2 Inhibition by Pyrazolo[1,5-a]pyrimidines. *Curr. Comput.-Aided Drug Des.* **2013**, *9*, 118–131.
- (248) Fanfrlik, J.; Bronowska, A. K.; Rezac, J.; Prenosil, O.; Konvalinka, J.; Hobza, P. A Reliable Docking/Scoring Scheme Based on the Semiempirical Quantum Mechanical PM6-DH2Method Accurately Covering Dispersion and H-Bonding: HIV-1 Protease with 22 Ligands. *J. Phys. Chem. B* **2010**, *114*, 12666–12678.
- (249) Fanfrlik, J.; Kolár, M.; Kamlar, M.; Hurný, D.; Ruiz, F. X.; Cousido-Siah, A.; Mitschler, A.; Rezac, J.; Munusamy, E.; Lepsik, M.; Matejček, P.; Veselý, J.; Podjarný, A.; Hobza, P. Modulation of Aldose Reductase Inhibition by Halogen Bond Tuning. *ACS Chem. Biol.* **2013**, *8*, 2484–2492.
- (250) Fanfrlik, J.; Ruiz, F. X.; Kadlcíková, A.; Rezac, J.; Cousido-Siah, A.; Mitschler, A.; Haldar, S.; Lepsik, M.; Kolár, M.; Majer, P.; Podjarný, A.; Hobza, P. A. The Effect of Halogen-to-Hydrogen Bond Substitution on Human Aldose Reductase Inhibition. *ACS Chem. Biol.* **2015**, *10*, 1637–1642.
- (251) Morreale, A.; Maseras, F.; Iriepa, I.; Gálvez, E. Ligand-Receptor Interaction at the Neural Nicotinic Acetylcholine Binding Site: A Theoretical Model. *J. Mol. Graphics Modell.* **2002**, *21*, 111–118.
- (252) Gueto-Tettay, C.; Drosos, J. C.; Vivas-Reyes, R. Quantum Mechanics Study of the Hydroxyethylamines–BACE-1 Active Site Interaction Energies. *J. Comput.-Aided Mol. Des.* **2011**, *25*, 583–597.
- (253) Nowosielski, M.; Hoffmann, M.; Kuron, A.; Korycka-Machala, M.; Dziadek, J. The MM2QM Tool for Combining Docking, Molecular Dynamics, Molecular Mechanics, and Quantum Mechanics. *J. Comput. Chem.* **2013**, *34*, 750–756.
- (254) Nowosielski, M.; Hoffmann, M.; Wyrwicz, L. S.; Stepniak, P.; Plewczynski, D. M.; Lazniewski, M.; Ginalski, K.; Rychlewski, L. Detailed Mechanism of Squalene Epoxidase Inhibition by Terbinafine. *J. Chem. Inf. Model.* **2011**, *51*, 455–462.
- (255) Zhou, T.; Caffisch, A. High-Throughput Virtual Screening Using Quantum Mechanical Probes: Discovery of Selective Kinase Inhibitors. *Chem. ChemMedChem* **2010**, *5*, 1007–1014.
- (256) Rao, L.; Zhang, I. Y.; Guo, W.; Feng, L.; Meggers, E.; Xu, X. Nonfitting Protein–Ligand Interaction Scoring Function Based on First-Principles Theoretical Chemistry Methods: Development and Application on Kinase Inhibitors. *J. Comput. Chem.* **2013**, *34*, 1636–1646.
- (257) Guo, W. P.; Wu, A. A.; Xu, X. XO: An Extended ONIOM Method for Accurate and Efficient Geometry Optimization of Large Molecules. *Chem. Phys. Lett.* **2010**, *498*, 203–208.
- (258) Ucisik, M. N.; Dashti, D. S.; Faver, J. C.; Merz, K. M. Pairwise Additivity of Energy Components in Protein–Ligand Binding: The HIV II Protease Indinavir Case. *J. Chem. Phys.* **2011**, *135*, 085101.
- (259) Zhang, D. W.; Xiang, Y.; Zhang, J. Z. H. New Advance in Computational Chemistry: Full Quantum Mechanical ab Initio Computation of Streptavidin–Biotin Interaction Energy. *J. Phys. Chem. B* **2003**, *107*, 12039–12041.
- (260) Zhang, D. W.; Xiang, Y.; Gao, A. M.; Zhang, J. Z. H. Quantum Mechanical Map for Protein–ligand Binding with Application to β -trypsinO–benzamidine Complex. *J. Chem. Phys.* **2004**, *120*, 1145–1148.
- (261) Xiang, Y.; Zhang, D. W.; Zhang, J. Z. H. Fully Quantum Mechanical Energy Optimization for Protein–Ligand Structure. *J. Comput. Chem.* **2004**, *25*, 1431–1437.
- (262) Zhang, D. W.; Zhang, J. Z. H. Full Quantum Mechanical Study of Binding of HIV-1 Protease Drugs. *Int. J. Quantum Chem.* **2005**, *103*, 246–257.
- (263) Mei, Y.; He, X.; Xiang, Y.; Zhang, D. W.; Zhang, J. Z. H. Quantum Study of Mutational Effect in Binding of Efavirenz to HIV-1 RT. *Proteins: Struct., Funct., Genet.* **2005**, *59*, 489–495.
- (264) Bettens, R. P. A.; Lee, A. M. On the Accurate Reproduction of Ab Initio Interaction Energies between an Enzyme and Substrate. *Chem. Phys. Lett.* **2007**, *449*, 341–346.
- (265) Ding, Y.; Mei, Y.; Zhang, J. Z. H. Quantum Mechanical Studies of Residue-Specific Hydrophobic Interactions in P53-MDM2 Binding. *J. Phys. Chem. B* **2008**, *112*, 11396–11401.
- (266) da Costa, R. F.; Freire, V. N.; Bezerra, E. M.; Cavada, B. S.; Caetano, E. W. S.; De Lima Filho, J. L.; Albuquerque, E. L. Explaining Statin Inhibition Effectiveness of HMG-CoA Reductase by Quantum Biochemistry Computations. *Phys. Chem. Chem. Phys.* **2012**, *14*, 1389–1398.
- (267) Martins, A. C. V.; De Lima-Neto, P.; Barroso-Neto, I. L.; Cavada, B. S.; Freire, V. N.; Caetano, E. W. S. An ab initio Explanation of the

Activation and Antagonism Strength of an AMPA-Sensitive Glutamate Receptor. *RSC Adv.* **2013**, *3*, 14988–14992.

(268) Rodrigues, C. R. F.; Oliveira, J. I. N.; Fulco, U. L.; Albuquerque, E. L.; Moura, R. M.; Caetano, E. W. S.; Freire, V. N. Quantum Biochemistry Study of the T3–785 Tropocollagen Triple Helical Structure. *Chem. Phys. Lett.* **2013**, *559*, 88–93.

(269) da Silva Ribeiro, T. C.; da Costa, R. F.; Bezerra, E. M.; Freire, V. N.; Lyra, M. L.; Manzon, V. The Quantum Biophysics of the Isoniazid Adduct NADH Binding to Its Intra Reductase Target. *New J. Chem.* **2014**, *38*, 2946–2957.

(270) Zanatta, G.; Nunes, G.; Bezerra, E. M.; da Costa, R. F.; Martins, A.; Caetano, E. W. S.; Freire, V. N.; Gottfried, C. Antipsychotic Haloperidol Binding to the Human Dopamine D3 Receptor: Beyond Docking Through QM/MM Refinement Toward the Design of Improved Schizophrenia Medicines. *ACS Chem. Neurosci.* **2014**, *5*, 1041–1054.

(271) Dantas, D. S.; Oliveira, J. I. N.; Lima Neto, J. X.; da Costa, R. F.; Bezerra, E. M.; Freire, V. N.; Caetano, E. W. S.; Fulco, U. L.; Albuquerque, E. L. Quantum Molecular Modelling of Ibuprofen Bound to Human Serum Albumin. *RSC Adv.* **2015**, *5*, 49439–49450.

(272) Antony, J.; Grimme, S. Fully Ab Initio Protein–Ligand Interaction Energies with Dispersion Corrected Density-Functional Theory. *J. Comput. Chem.* **2012**, *33*, 1730–1739.

(273) Söderhjelm, P.; Aquilante, F.; Ryde, U. Calculation of Protein–Ligand Interaction Energies by a Fragmentation Approach Combining High-Level Quantum Chemistry with Classical Many-Body Effects. *J. Phys. Chem. B* **2009**, *113*, 11085–11094.

(274) Andrejic, M.; Ryde, U.; Mata, R.; Söderhjelm, P. Coupled-Cluster Interaction Energies for 200-Atom Host-Guest Systems. *ChemPhysChem* **2014**, *15*, 3270–3281.

(275) Fukuzawa, K.; Kitaura, K.; Uebayasi, M.; Nakata, K.; Kaminuma, T.; Nakano, T. Ab Initio Quantum Mechanical Study of the Binding Energies of Human Estrogen Receptor with Its Ligands: An Application of Fragment Molecular Orbital Method. *J. Comput. Chem.* **2005**, *26*, 1–10.

(276) Amari, S.; Aizawa, M.; Zhang, J.; Fukuzawa, K.; Mochizuki, Y.; Iwasawa, Y.; Nakata, K.; Chuman, H.; Nakano, T. VISCANA: Visualized Cluster Analysis of Protein–Ligand Interaction Based on the ab Initio Fragment Molecular Orbital Method for Virtual Ligand Screening. *J. Chem. Inf. Model.* **2006**, *46*, 221–230.

(277) Fukuzawa, K.; Mochizuki, Y.; Tanaka, S.; Kitaura, K.; Nakano, T. Molecular Interactions between Estrogen Receptor and Its Ligand Studied by the ab Initio Fragment Molecular Orbital Method. *J. Phys. Chem. B* **2006**, *110*, 16102–16110.

(278) Yamagishi, K.; Tokiwa, H.; Makishima, M.; Yamada, S. Interactions between 1 α ,25(OH) $_2$ D-3 and Residues in the Ligand-Binding Pocket of the Vitamin D Receptor: A Correlated Fragment Molecular Orbital Study. *J. Steroid Biochem. Mol. Biol.* **2010**, *121*, 63–67.

(279) Yamagishi, K.; Yamamoto, K.; Mochizuki, Y.; Nakano, T.; Yamada, S.; Tokiwa, H. Flexible Ligand Recognition of Peroxisome Proliferator-Activated Receptor-Gamma (PPAR Gamma). *Bioorg. Med. Chem. Lett.* **2010**, *20*, 3344–3347.

(280) Ito, M.; Fukuzawa, K.; Mochizuki, Y.; Nakano, T.; Tanaka, S. Ab Initio Fragment Molecular Orbital Study of Molecular Interactions between Liganded Retinoid X Receptor and Its Coactivator: Roles of Helix 12 in the Coactivator Binding Mechanism. *J. Phys. Chem. B* **2007**, *111*, 3525–3533.

(281) Fukuzawa, K.; Komeiji, Y.; Mochizuki, Y.; Kato, A.; Nakano, T.; Tanaka, S. Intra- and Intermolecular Interactions between Cyclic-AMP Receptor Protein and DNA: Ab Initio Fragment Molecular Orbital Study. *J. Comput. Chem.* **2006**, *27*, 948–960.

(282) Yoshioka, A.; Fukuzawa, K.; Mochizuki, Y.; Yamashita, K.; Nakano, T.; Okiyama, Y.; Nobusawa, E.; Nakajima, K.; Tanaka, S. Prediction of Probable Mutations in Influenza Virus Hemagglutinin Protein Based on Large-Scale Ab Initio Fragment Molecular Orbital Calculations. *J. Mol. Graphics Modell.* **2011**, *30*, 110–119.

(283) Koyama, T.; Ueno-Noto, K.; Takano, K. Interaction Analysis of HIV-1 Antibody 2G12 and Man9GlcNAc2 Ligand: Theoretical

Calculations by Fragment Molecular Orbital and MD Methods. *Chem. Phys. Lett.* **2013**, *578*, 144–149.

(284) Sawada, T.; Hashimoto, T.; Nakano, H.; Suzuki, T.; Suzuki, Y.; Kawaoka, Y.; Ishida, H.; Kiso, M. Influenza Viral Hemagglutinin Complicated Shape Is Advantageous to Its Binding Affinity for Sialosaccharide Receptor. *Biochem. Biophys. Res. Commun.* **2007**, *355*, 6–9.

(285) Nakanishi, I.; Fedorov, D. G.; Kitaura, K. Molecular Recognition Mechanism of FK506 Binding Protein: An All-Electron Fragment Molecular Orbital Study. *Proteins: Struct., Funct., Genet.* **2007**, *68*, 145–158.

(286) Sawada, T.; Fedorov, D. G.; Kitaura, K. Binding of Influenza A Virus Hemagglutinin to the Sialoside Receptor Is Not Controlled by the Homotropic Allosteric Effect. *J. Phys. Chem. B* **2010**, *114*, 15700–15705.

(287) Mazanetz, M. P.; Ichihara, O.; Law, R. J.; Whittaker, M. Prediction of Cyclin-Dependent Kinase 2 Inhibitor Potency Using the Fragment Molecular Orbital Method. *J. Cheminf.* **2011**, *3*, 2.

(288) Prato, G.; Silvestri, S.; Saka, S.; Lamberto, M.; Kosenkov, D. Thermodynamics of Binding of Di- and Tetrasubstituted Naphthalene Diimide Ligands to DNA G-Quadruplex. *J. Phys. Chem. B* **2015**, *119*, 3335–3347.

(289) Dedachi, K.; Hirakawa, T.; Fujita, S.; Khan, M. T. H.; Sylte, I.; Kurita, N. Specific Interactions and Binding Free Energies between Thermolysin and Dipeptides: Molecular Simulations Combined with Ab Initio Molecular Orbital and Classical Vibrational Analysis. *J. Comput. Chem.* **2011**, *32*, 3047–3057.

(290) Hirakawa, T.; Fujita, S.; Ohya, T.; Dedachi, K.; Khan, M. T. H.; Sylte, I.; Kurita, N. Specific Interactions and Binding Energies between Thermolysin and Potent Inhibitors: Molecular Simulations Based on Ab Initio Molecular Orbital Method. *J. Mol. Graphics Modell.* **2012**, *33*, 1–11.

(291) Murakawa, T.; Matsushita, Y.; Suzuki, T.; Khan, M. T. H.; Kurita, N. Ab Initio Molecular Simulations for Proposing Potent Inhibitors to Butyrylcholinesterases. *J. Mol. Graphics Modell.* **2014**, *54*, 54–61.

(292) Tsuji, S.; Kasumi, T.; Nagase, K.; Yoshikawa, E.; Kobayashi, H.; Kurita, N. The Effects of Amino-Acid Mutations on Specific Interactions between Urokinase-Type Plasminogen Activator and Its Receptor: Ab Initio Molecular Orbital Calculations. *J. Mol. Graphics Modell.* **2011**, *29*, 975–984.

(293) Koyama, Y.; Ueno-Noto, K.; Takano, K. Affinity of HIV-1 Antibody 2G12 with Monosaccharides: A Theoretical Study Based on Explicit and Implicit Water Models. *Comput. Biol. Chem.* **2014**, *49*, 36–44.

(294) Nagata, T.; Fedorov, D. G.; Sawada, T.; Kitaura, K. Analysis of Solute–Solvent Interactions in the Fragment Molecular Orbital Method Interfaced with Effective Fragment Potentials: Theory and Application to A Solvated Griffithsin–Carbohydrate Complex. *J. Phys. Chem. A* **2012**, *116*, 9088–9099.

(295) Okamoto, A.; Nomura, K.; Yano, A.; Higai, S.; Kondo, T.; Kamba, S.; Kurita, N. Proposal for an Inhibitor of Alzheimer's Disease Blocking Aggregation of Amyloid-B Peptides: Ab Initio Molecular Simulations. *J. Phys.: Conf. Ser.* **2013**, *433*, 012033.

(296) Asada, N.; Fedorov, D. G.; Kitaura, K.; Nakanishi, I.; Merz, K. M. An Efficient Method to Evaluate Intermolecular Interaction Energies in Large Systems Using Overlapping Multicenter ONIOM and the Fragment Molecular Orbital Method. *J. Phys. Chem. Lett.* **2012**, *3*, 2604–2610.

(297) Vasilyev, V.; Bliznyuk, A. Application of Semiempirical Quantum Chemical Methods As A Scoring Function in Docking. *Theor. Chem. Acc.* **2004**, *112*, 313–317.

(298) Pichiari, F. A Quantum Mechanical Study on Phosphotyrosyl Peptide Binding to the SH2 Domain of P56lck Tyrosine Kinase with Insights Into the Biochemistry of Intracellular Signal Transduction Events. *Biophys. Chem.* **2004**, *109*, 295–304.

(299) Ohno, K.; Wada, M.; Saito, S.; Inoue, Y.; Sakurai, M. Quantum Chemical Study on the Affinity Maturation of 48G7 Antibody. *J. Mol. Struct.: THEOCHEM* **2005**, *722*, 203–211.

- (300) Li, J.; Reynolds, C. H. A Quantum Mechanical Approach to Ligand Binding — Calculation of Ligand–Protein Binding Affinities for Stromelysin-1 (MMP-3) Inhibitors. *Can. J. Chem.* **2009**, *87*, 1480–1484.
- (301) Kamel, K.; Kolinski, A. Assessment of the Free Binding Energy of 1,25-Dihydroxyvitamin D3 and Its Analogs with the Human VDR Receptor Model. *Acta Biochim. Pol.* **2012**, *59*, 653–660.
- (302) Zhou, T.; Huang, D.; Caflisch, A. Is Quantum Mechanics Necessary for Predicting Binding Free Energy? *J. Med. Chem.* **2008**, *51*, 4280–4288.
- (303) Anikin, N. A.; Andreev, A. M.; Kuz'minskii, M. B.; Mendkovich, A. S. A Fast Method of Large-Scale Serial Semiempirical Calculations of Docking Complexes. *Russ. Chem. Bull.* **2008**, *57*, 1793–1798.
- (304) Anisimov, V. M.; Bugaenko, V. L. QM/QM Docking Method Based on the Variational Finite Localized Molecular Orbital Approximation. *J. Comput. Chem.* **2009**, *30*, 784–798.
- (305) Thiriot, E.; Monard, G. Combining A Genetic Algorithm with A Linear Scaling Semiempirical Method for Protein–Ligand Docking. *J. Mol. Struct.: THEOCHEM* **2009**, *898*, 31–41.
- (306) Barberot, C.; Boisson, J. C.; Gérard, S.; Khartabil, H.; Thiriot, E.; Monard, G.; Hénon, E. AlgoGen: A Tool Coupling A Linear-Scaling Quantum Method with A Genetic Algorithm for Exploring Non-Covalent Interactions. *Comput. Theor. Chem.* **2014**, *1028*, 7–18.
- (307) Raha, K.; Van der Vaart, A. J.; Riley, K. E.; Peters, M. B.; Westerhoff, L. M.; Kim, H.; Merz, K. M. Pairwise Decomposition of Residue Interaction Energies Using Semiempirical Quantum Mechanical Methods in Studies of Protein–Ligand Interaction. *J. Am. Chem. Soc.* **2005**, *127*, 6583–6594.
- (308) Raha, K.; Merz, K. M. Large-Scale Validation of A Quantum Mechanics Based Scoring Function: Predicting the Binding Affinity and the Binding Mode of A Diverse Set of Protein–Ligand Complexes. *J. Med. Chem.* **2005**, *48*, 4558–4575.
- (309) Zhang, X.; Gibbs, A. C.; Reynolds, C. H.; Peters, M. B.; Westerhoff, L. M. Quantum Mechanical Pairwise Decomposition Analysis of Protein Kinase B Inhibitors: Validating a New Tool for Guiding Drug Design. *J. Chem. Inf. Model.* **2010**, *50*, 651–661.
- (310) Benson, M. L.; Faver, J. C.; Ucisik, M. N.; Dashti, D. S.; Zheng, Z.; Merz, K. M. Prediction of Trypsin/Molecular Fragment Binding Affinities by Free Energy Decomposition and Empirical Scores. *J. Comput.-Aided Mol. Des.* **2012**, *26*, 647–659.
- (311) Dobes, P.; Fanfrlík, J.; Rezáč, J.; Otyepka, M.; Hobza, P. Transferable Scoring Function Based on Semiempirical Quantum Mechanical PM6-DH2Method: CDK2 with 15 Structurally Diverse Inhibitors. *J. Comput.-Aided Mol. Des.* **2011**, *25*, 223–235.
- (312) Dobes, P.; Rezáč, J.; Fanfrlík, J.; Otyepka, M.; Hobza, P. Semiempirical Quantum Mechanical Method PM6-DH2X Describes the Geometry and Energetics of CK2-Inhibitor Complexes Involving Halogen Bonds Well, While the Empirical Potential Fails. *J. Phys. Chem. B* **2011**, *115*, 8581–8589.
- (313) Fanfrlík, J.; Brahmshatriya, P. S.; Rezáč, J.; Jílková, A. M.; Horn, M.; Mares, M.; Hobza, P.; Lepsík, M. Quantum Mechanics-Based Scoring Rationalizes the Irreversible Inactivation of Parasitic Schistosoma Mansoni Cysteine Peptidase by Vinyl Sulfone Inhibitors. *J. Phys. Chem. B* **2013**, *117*, 14973–14982.
- (314) Ryde, U. On the Role of Covalent Strain in Protein Function. *Recent Research Developments in Protein Engineering*; Research Signpost: Trivandrum, India, 2002; Vol. 2, pp 65–91.
- (315) Boström, J.; Norrby, P.-O.; Liljefors, T. Conformational Energy Penalties of Protein-bound Ligands. *J. Comput.-Aided Mol. Des.* **1998**, *12*, 383–396.
- (316) Sitzmann, M.; Weidlich, I. E.; Filippov, I. V.; Liao, C.; Peach, M. L.; Ihlenfeldt, W.-D.; Karki, R. G.; Borodina, Y. V.; Cachau, R. E.; Nicklaus, M. C. PDB Ligand Conformational Energies Calculated Quantum-mechanically. *J. Chem. Inf. Model.* **2012**, *52*, 739–756.
- (317) Fu, Z.; Li, X.; Merz, K. M. Accurate Assessment of the Strain Energy in a Protein-bound Drug using QM/MM X-ray Refinement and Converged Quantum Chemistry. *J. Comput. Chem.* **2011**, *32*, 2587–2597.
- (318) Otsuka, T.; Okimoto, N.; Taiji, M.; Bowler, D. R.; Miyazaki, T. Structural Relaxation and Binding Energy Calculations of FK506 Binding Protein Complexes using the Large-scale DFT Code CONQUEST. *J. Phys.: Conf. Ser.* **2013**, *454*, 012057.
- (319) Gräter, F.; Schwarzl, S. M.; Dejaegere, A.; Fischer, S.; Smith, J. C. Protein/Ligand Binding Free Energies Calculated with Quantum Mechanics/Molecular Mechanics. *J. Phys. Chem. B* **2005**, *109*, 10474–10483.
- (320) Retegan, M.; Milet, A.; Jamet, H. Exploring the Binding of Inhibitors Derived from Tetrabromobenzimidazole to the CK2 Protein Using a QM/MM-PB/SA Approach. *J. Chem. Inf. Model.* **2009**, *49*, 963–971.
- (321) Ibrahim, M. A. A. Performance Assessment of Semiempirical Molecular Orbital Methods in Describing Halogen Bonding: Quantum Mechanical and Quantum Mechanical/Molecular Mechanical-Molecular Dynamics Study. *J. Chem. Inf. Model.* **2011**, *51*, 2549–2559.
- (322) Dubey, K. D.; Ojha, R. P. Binding Free Energy Calculation with QM/MM Hybrid methods for Abl-Kinase inhibitor. *J. Biol. Phys.* **2011**, *37*, 69–78.
- (323) Wang, Y.-T.; Chen, Y.-C. Insights from QM/MM Modeling the 3D Structure of the 2009 H1N1 Influenza A Virus Neuraminidase and Its Binding Interactions with Antiviral Drugs. *Mol. Inf.* **2014**, *33*, 240–249.
- (324) Barbault, F.; Maurel, F. Is Inhibition Process Better Described with MD(QM/MM) Simulations? The Case of Urokinase Type Plasminogen Activator Inhibitors. *J. Comput. Chem.* **2012**, *33*, 607–616.
- (325) Case, D. A.; Babin, V.; Berryman, J. T.; Betz, R. M.; Cai, Q.; Cerutti, D. S.; Cheatham, T. E.; Darden, T. A.; Duke, R. E.; Gohlke, H.; et al. *AMBER 14*; University of California: San Francisco, 2014.
- (326) Walker, R. C.; Crowley, M. F.; Case, D. A. The Implementation of A Fast and Accurate QM/MM Potential Method in Amber. *J. Comput. Chem.* **2008**, *29*, 1019–1031.
- (327) Wichapong, K.; Rohe, A.; Platzer, C.; Slynko, I.; Erdmann, F.; Schmidt, M.; Sippl, W. Application of Docking and QM/MM-GBSA Rescoring to Screen for Novel Myt1 Kinase Inhibitors. *J. Chem. Inf. Model.* **2014**, *54*, 881–893.
- (328) Kaukonen, M.; Söderhjelm, P.; Heimdal, J.; Ryde, U. A QM/MM-PBSA Method to Estimate Free Energies for Reactions in Proteins. *J. Phys. Chem. B* **2008**, *112*, 12537–12548.
- (329) Ryde, U. QM/MM calculations on proteins. *Methods Enzymol.* **2016**, in press.
- (330) Lu, H.; Goren, A. C.; Zhan, C.-G. Characterization of the Structures of Phosphodiesterase 10 Binding with Adenosine 3',5'-Monophosphate and Guanosine 3',5'-Monophosphate by Hybrid Quantum Mechanical/ Molecular Mechanical Calculations. *J. Phys. Chem. B* **2010**, *114*, 7022–7028.
- (331) Chen, X.; Zhao, X.; Xiong, Y.; Liu, J.; Zhan, C.-G. Fundamental Reaction Pathway and Free Energy Profile for Hydrolysis of Intracellular Second Messenger Adenosine 3',5'-Cyclic Monophosphate (cAMP) Catalyzed by Phosphodiesterase. *J. Phys. Chem. B* **2011**, *115*, 12208–12219.
- (332) Lu, H.; Huang, X.; AbdulHameed, M. D. M.; Zhan, C.-G. Binding Free Energies for Nicotine Analogs Inhibiting Cytochrome P450 2A6 by A Combined Use of Molecular Dynamics Simulations and QM/MM-PBSA Calculations. *Bioorg. Med. Chem.* **2014**, *22*, 2149–2156.
- (333) Manta, S.; Xipnitou, A.; Kiritsis, C.; Kantsadi, A. L.; Hayes, J. M.; Skamnaki, V. T.; Lamprakis, C.; Kontou, M.; Zoumpoulakis, P.; Zographos, S. E.; et al. 3'-Axial CH₂OH Substitution on Glucopyranose does not Increase Glycogen Phosphorylase Inhibitory Potency. QM/MM-PBSA Calculations Suggest Why. *Chem. Biol. Drug Des.* **2012**, *79*, 663–673.
- (334) Kantsadi, A. L.; Hayes, J. M.; Manta, S.; Skamnaki, V. T.; Kiritsis, C.; Psarra, A. M.; Koutsogiannis, Z.; Dimopoulou, A.; Theofanous, S.; Nikoleousakos, N.; et al. The Sigma-Hole Phenomenon of Halogen Atoms Forms the Structural Basis of the Strong Inhibitory Potency of C5 Halogen Substituted Glucopyranosyl Nucleosides Towards Glycogen Phosphorylase B. *ChemMedChem* **2012**, *7*, 722–732.
- (335) Tsitsanou, K. E.; Hayes, J. M.; Keramioti, M.; Mamais, M.; Oikonomakos, N. G.; Kato, A.; Leonidas, D. D.; Zographos, S. E. Sourcing the Affinity of Flavonoids for the Glycogen Phosphorylase

Inhibitor Site Via Crystallography, Kinetics and QM/MM-PBSA Binding Studies: Comparison of Chrysin and Flavopiridol. *Food Chem. Toxicol.* **2013**, *61*, 14–27.

(336) Söderhjelm, P.; Kongsted, J.; Ryde, U. Ligand Affinities Estimated by Quantum Chemical Calculations. *J. Chem. Theory Comput.* **2010**, *6*, 1726–1737.

(337) Genheden, S.; Kongsted, J.; Söderhjelm, P.; Ryde, U. Nonpolar Solvation Free Energies of Protein–Ligand Complexes. *J. Chem. Theory Comput.* **2010**, *6*, 3558–3568.

(338) Genheden, S.; Mikulskis, P.; Hu, L.; Kongsted, J.; Söderhjelm, P.; Ryde, U. Accurate Predictions of Non-Polar Solvation Free Energies Require Explicit Consideration of Binding Site Hydration. *J. Am. Chem. Soc.* **2011**, *133*, 13081–13092.

(339) Ishikawa, T.; Burri, R. R.; Kamatari, Y. O.; Sakuraba, S.; Matubayasi, N.; Kitao, A.; Kuwata, K. A Theoretical Study of the Two Binding Modes between Lysozyme and Tri-NAG with an Explicit Solvent Model Based on the Fragment Molecular Orbital Method. *Phys. Chem. Chem. Phys.* **2013**, *15*, 3646–3654.

(340) Shigemitsu, Y. Quantum Chemical Study on Molecular-Level Affinity of DJ-1 Binding Compounds. *Int. J. Quantum Chem.* **2013**, *113*, 574–579.

(341) Díaz, N.; Suárez, D.; Merz, K. M.; Sordo, T. L. Molecular dynamics simulations of the TEM-1 β -lactamase complexed with cephalothin. *J. Med. Chem.* **2005**, *48*, 780–791.

(342) Anisimov, V. M.; Civasotto, C. N. Quantum Mechanical Binding Free Energy Calculation for Phosphopeptide Inhibitors of the Lck SH2 domain. *J. Comput. Chem.* **2011**, *32*, 2254–2263.

(343) Anisimov, V. M.; Ziemys, A.; Kizhake, S.; Yuan, Z.; Natarajan, A.; Civasotto, C. N. Computational and Experimental Studies of the Interaction between Phospho-peptides and the C-terminal Domain of BRCA. *J. Comput.-Aided Mol. Des.* **2011**, *25*, 1071–1084.

(344) Mikulskis, P.; Genheden, S.; Wichmann, K.; Ryde, U. A Semiempirical Approach to Ligand-Binding Affinities: Dependence on the Hamiltonian and Corrections. *J. Comput. Chem.* **2012**, *33*, 1179–1189.

(345) Cole, D. J.; Skylaris, C.-K.; Rajendra, E.; Venkitaraman, A. R.; Payne, M. C. Protein-Protein Interactions From Linear-Scaling First-Principles Quantum-Mechanical Calculations. *EPL* **2010**, *91*, 37004.

(346) Fox, S.; Wallnofer, H. G.; Fox, T.; Tautermann, C. S.; Skylaris, C.-K. First Principles-Based Calculations of Free Energy of Binding: Application to Ligand Binding in a Self-Assembling Superstructure. *J. Chem. Theory Comput.* **2011**, *7*, 1102–1108.

(347) Fox, S. J.; Dziedzic, J.; Fox, T.; Tautermann, C. S.; Skylaris, C.-K. Density Functional Theory Calculations on Entire Proteins for Free Energies of Binding: Application to A Model Polar Binding Site. *Proteins: Struct., Funct., Genet.* **2014**, *82*, 3335–3346.

(348) Genheden, S.; Luchko, T.; Gusarov, S.; Kovalenko, A.; Ryde, U. An MM/3D-RISM Approach for Ligand-Binding Affinities. *J. Phys. Chem. B* **2010**, *114*, 8505–8516.

(349) Khandelwal, A.; Lukacova, V.; Comez, D.; Kroll, D. M.; Raha, S.; Balaz, S. A Combination of Docking, QM/MM Methods, and MD Simulation for Binding Affinity Estimation of Metalloprotein Ligands. *J. Med. Chem.* **2005**, *48*, 5437–5447.

(350) Khandelwal, A.; Balaz, S. Improved Estimation of Ligand–Macromolecule Binding Affinities by Linear Response Approach Using A Combination of Multi-Mode MD Simulation and QM/MM Methods. *J. Comput.-Aided Mol. Des.* **2007**, *21*, 131–137.

(351) Khandelwal, A.; Balaz, S. QM/MM Linear Response Method Distinguishes Ligand Affinities for Closely Related Metalloproteins. *Proteins: Struct., Funct., Genet.* **2007**, *69*, 326–339.

(352) Natesan, S.; Subramaniam, R.; Bergeron, C.; Balaz, S. Binding Affinity Prediction for Ligands and Receptors Forming Tautomers and Ionization Species: Inhibition of Mitogen-Activated Protein Kinase-Activated Protein Kinase 2 (MK2). *J. Med. Chem.* **2012**, *55*, 2035–2047.

(353) Alves, C. N.; Martí, S.; Castillo, R.; Andrés, J.; Moliner, V.; Tuñón, I.; Silla, E. A Quantum Mechanics/Molecular Mechanics Study of the Protein–Ligand Interaction for Inhibitors of HIV-1 Integrase. *Chem. - Eur. J.* **2007**, *13*, 7715–7724.

(354) Alves, C. N.; Martí, S.; Castillo, R.; Andrés, J.; Moliner, V.; Tuñón, I.; Silla, E. A Calculation of binding energy using BLYP/MM for the HIV-1 integrase complexed with the S-1360 and two analogues. *Bioorg. Med. Chem.* **2007**, *15*, 3818–3824.

(355) Alves, C. N.; Martí, S.; Castillo, R.; Andrés, J.; Moliner, V.; Tuñón, I.; Silla, E. A Quantum Mechanics/Molecular Mechanics Study of the Wild-Type and N155S Mutant HIV-1 Integrase Complexed with Diketo Acid. *Biophys. J.* **2008**, *94*, 2443–2451.

(356) Alzate-Morales, J. H.; Contreras, R.; Soriano, A.; Tuñón, I.; Silla, E. A Computational Study of the Protein-Ligand Interactions in CDK2 Inhibitors: Using Quantum Mechanics/Molecular Mechanics Interaction Energy as a Predictor of the Biological Activity. *Biophys. J.* **2007**, *92*, 430–439.

(357) Xiang, M.; Lin, Y.; He, G.; Chen, L.; Yang, M.; Yang, S.; Mo, Y. Correlation between Biological Activity and Binding Energy in Systems of Integrin with Cyclic RGD-Containing Binders: A QM/MM Molecular Dynamics Study. *J. Mol. Model.* **2012**, *18*, 4917–4927.

(358) Yoshida, T.; Yamagishi, K.; Chuman, H. QSAR Study of Cyclic Urea Type HIV-1PR Inhibitors Using Ab Initio MO Calculation of Their Complex Structures with HIV-1PR. *QSAR Comb. Sci.* **2008**, *27*, 694–703.

(359) Yoshida, T.; Munei, Y.; Hitaoka, S.; Chuman, H. Correlation Analyses on Binding Affinity of Substituted Benzenesulfonamides with Carbonic Anhydrase Using Ab Initio MO Calculations on Their Complex Structures. *J. Chem. Inf. Model.* **2010**, *50*, 850–860.

(360) Hitaoka, S.; Matoba, H.; Harada, M.; Yoshida, T.; Tsuji, D.; Hirokawa, T.; Itoh, K.; Chuman, H. Correlation Analyses on Binding Affinity of Sialic Acid Analogues and Anti-Influenza Drugs with Human Neuraminidase Using ab Initio MO Calculations on Their Complex Structures – LERE-QSAR Analysis (IV). *J. Chem. Inf. Model.* **2011**, *51*, 2706–2716.

(361) Muddana, H. S.; Yin, J.; Sapra, N. V.; Fenley, A. T.; Gilson, M. K. Blind Prediction of SAMPL4 Cucurbit-7-Uril Binding Affinities with the Mining Minima Method. *J. Comput.-Aided Mol. Des.* **2014**, *28*, 463–474.

(362) Reddy, M. R.; Erion, M. D. Relative Binding Affinities of Fructose-1,6-Bisphosphatase Inhibitors Calculated Using a Quantum Mechanics-Based Free Energy Perturbation Method. *J. Am. Chem. Soc.* **2007**, *129*, 9296–9297.

(363) Rathore, R. S.; Reddy, R. N.; Kondapi, A. K.; Reddanna, P.; Reddy, M. R. Use of Quantum Mechanics/molecular Mechanics-based FEP Method for Calculating Relative Binding Affinities of FBPase Inhibitors for Type-2 Diabetes. *Theor. Chem. Acc.* **2012**, *131*, 1096.

(364) Swiderek, K.; Martí, S.; Moliner, V. Theoretical studies of HIV-1 Reverse Transcriptase Inhibition. *Phys. Chem. Chem. Phys.* **2012**, *14*, 12614–12624.

(365) Luzhkov, V.; Warshel, A. Microscopic Models for Quantum Mechanical Calculations of Chemical Processes in Solutions: LD/AMPAC and SCAAS/AMPAC Calculations of Solvation Energies. *J. Comput. Chem.* **1992**, *13*, 199–213.

(366) Duarte, F.; Amrein, B. A.; Blaha-Nelson, D.; Kamerlin, S. C. L. Recent Advances in QM/MM Free Energy Calculations Using Reference Potentials. *Biochim. Biophys. Acta, Gen. Subj.* **2015**, *1850*, 954–965.

(367) König, G.; Boresch, S. Non-Boltzmann Sampling and Bennett's Acceptance Ratio Method: How to Profit from Bending the Rules. *J. Comput. Chem.* **2011**, *32*, 1082–1090.

(368) Hu, H.; Yang, W. Free Energies of Chemical Reactions in Solution and in Enzymes with Ab Initio Quantum Mechanics/Molecular Mechanics Methods. *Annu. Rev. Phys. Chem.* **2008**, *59*, 573–601.

(369) Heimdal, J.; Ryde, U. Convergence of QM/MM Free-Energy Perturbations Based on Molecular-Mechanics or Semiempirical Simulations. *Phys. Chem. Chem. Phys.* **2012**, *14*, 12592–12604.

(370) Woods, C. J.; Manby, F. R.; Mulholland, A. J. An Efficient Method for the Calculation of Quantum Mechanics/Molecular Mechanics Free Energies. *J. Chem. Phys.* **2008**, *128*, 014109.

(371) Fox, S. J.; Pittock, C.; Tautermann, C. S.; Fox, T.; Christ, C.; Malcolm, N. O. J.; Essex, J. W.; Skylaris, C.-K. Free Energies of Binding from Large-Scale First-Principles Quantum Mechanical Calculations:

Application to Ligand Hydration Energies. *J. Phys. Chem. B* **2013**, *117*, 9478–9485.

(372) Genheden, S.; Cabedo Martinez, A. I.; Criddle, M. P.; Essex, J. W. Extensive all-atom Monte Carlo Sampling and QM/MM Corrections in the SAMPL4 Hydration Free energy Challenge. *J. Comput.-Aided Mol. Des.* **2014**, *28*, 187–200.

(373) König, G.; Pickard, F. C.; Mei, Y.; Brooks, B. R. Predicting Hydration Free Energies with A Hybrid QM/MM Approach: An Evaluation of Implicit and Explicit Solvation Models in SAMPL4. *J. Comput.-Aided Mol. Des.* **2014**, *28*, 245–257.

(374) König, G.; Hudson, P. S.; Boresch, S.; Woodcock, H. L. Multiscale Free Energy Simulations: An Efficient Method for Connecting Classical MD Simulations to QM or QM/MM Free Energies Using Non-Boltzmann Bennett Reweighting Schemes. *J. Chem. Theory Comput.* **2014**, *10*, 1406–1419.

(375) Sampson, C.; Fox, T.; Tautermann, C. S.; Woods, C.; Skylaris, C.-K. A “Stepping Stone” Approach for Obtaining Quantum Free Energies of Hydration. *J. Phys. Chem. B* **2015**, *119*, 7030–7040.

(376) Beierlein, F. R.; Michel, J.; Essex, J. W. A Simple QM/MM Approach for Capturing Polarization Effects in Protein Ligand Binding Free Energy Calculations. *J. Phys. Chem. B* **2011**, *115*, 4911–4926.

(377) Woods, C. J.; Shaw, K. E.; Mulholland, A. J. Combined Quantum Mechanics/Molecular Mechanics (QM/MM) Simulations for Protein–Ligand Complexes: Free Energies of Binding of Water Molecules in Influenza Neuraminidase. *J. Phys. Chem. B* **2015**, *119*, 997–1001.

(378) Genheden, S.; Ryde, U.; Söderhjelm, P. Binding Affinities by Free-Energy Perturbation Using QM/MM with A Large QM System and Polarizable MM Model. *J. Comput. Chem.* **2015**, *36*, 2114–2124.

(379) Olsson, M. A.; Söderhjelm, P.; Ryde, U. Converging Ligand-Binding Free Energies Obtained with Free-Energy Perturbations at the Quantum Mechanical Level. *J. Comput. Chem.* **2016**, DOI: [10.1002/jcc.24375](https://doi.org/10.1002/jcc.24375).

(380) Cave-Ayland, C.; Skylaris, C.-K.; Essex, J. W. Direct Validation of the Single Step Classical to Quantum Free Energy Perturbation. *J. Phys. Chem. B* **2015**, *119*, 1017–1025.

(381) Hummer, G.; Szabo, A. Calculation of free-energy differences from computer simulations of initial and final states. *J. Chem. Phys.* **1996**, *105*, 2004–2012.

(382) Kästner, J.; Senn, H. M.; Thiel, S.; Otte, N.; Thiel, W. QM/MM Free-Energy Perturbation Compared to Thermodynamic Integration and Umbrella Sampling: Application to an Enzymatic Reaction. *J. Chem. Theory Comput.* **2006**, *2*, 452–461.

(383) Jansík, B.; Høst, S.; Johansson, M. P.; Olsen, J.; Jørgensen, P.; Helgaker, T. Robust and Reliable Multilevel Minimization of the Kohn-Sham Energy. *J. Chem. Theory Comput.* **2009**, *5*, 1027–1032.

(384) Jakobsen, S.; Kristensen, K.; Jensen, F. Electrostatic Potential of Insulin: Exploring the Limitations of Density Functional Theory and Force Field Methods. *J. Chem. Theory Comput.* **2013**, *9*, 3978–3985.

(385) Smith, R. Peer Review: A Flawed Process at the Heart of Science and Journals. *J. R. Soc. Med.* **2006**, *99*, 178–182.

(386) Emerson, G. B.; Warme, W. J.; Wolf, F. M.; Heckman, J. D.; Brand, R. A.; Leopold, S. S. Testing for the Presence of Positive-Outcome Bias in Peer Review. A Randomized Controlled Trial. *Arch. Intern. Med.* **2010**, *170*, 1934–1939.

(387) Christ, C.; Fox, T. Accuracy Assessment and Automation of Free Energy Calculations for Drug Design. *J. Chem. Inf. Model.* **2014**, *54*, 108–120.

(388) Mikulskis, P.; Genheden, S.; Ryde, U. A Large-Scale Test of Free-Energy Simulation Estimates of Protein-Ligand Binding Affinities. *J. Chem. Inf. Model.* **2014**, *54*, 2794–2806.

(389) Wang, L.; Wu, Y.; Deng, Y.; Kim, B.; Pierce, L.; Krilov, G.; Lupyan, D.; Robinson, S.; Dahlgren, M. K.; Greenwood, J.; et al. Accurate and Reliable Prediction of Relative Ligand Binding Potency in Prospective Drug Discovery by Way of a Modern Free-Energy Calculation Protocol and Force Field. *J. Am. Chem. Soc.* **2015**, *137*, 2695–2703.